sfa
EURATOM-MESCS

Slovenska Fuzijska Asociacija
Slovenian Fusion Association

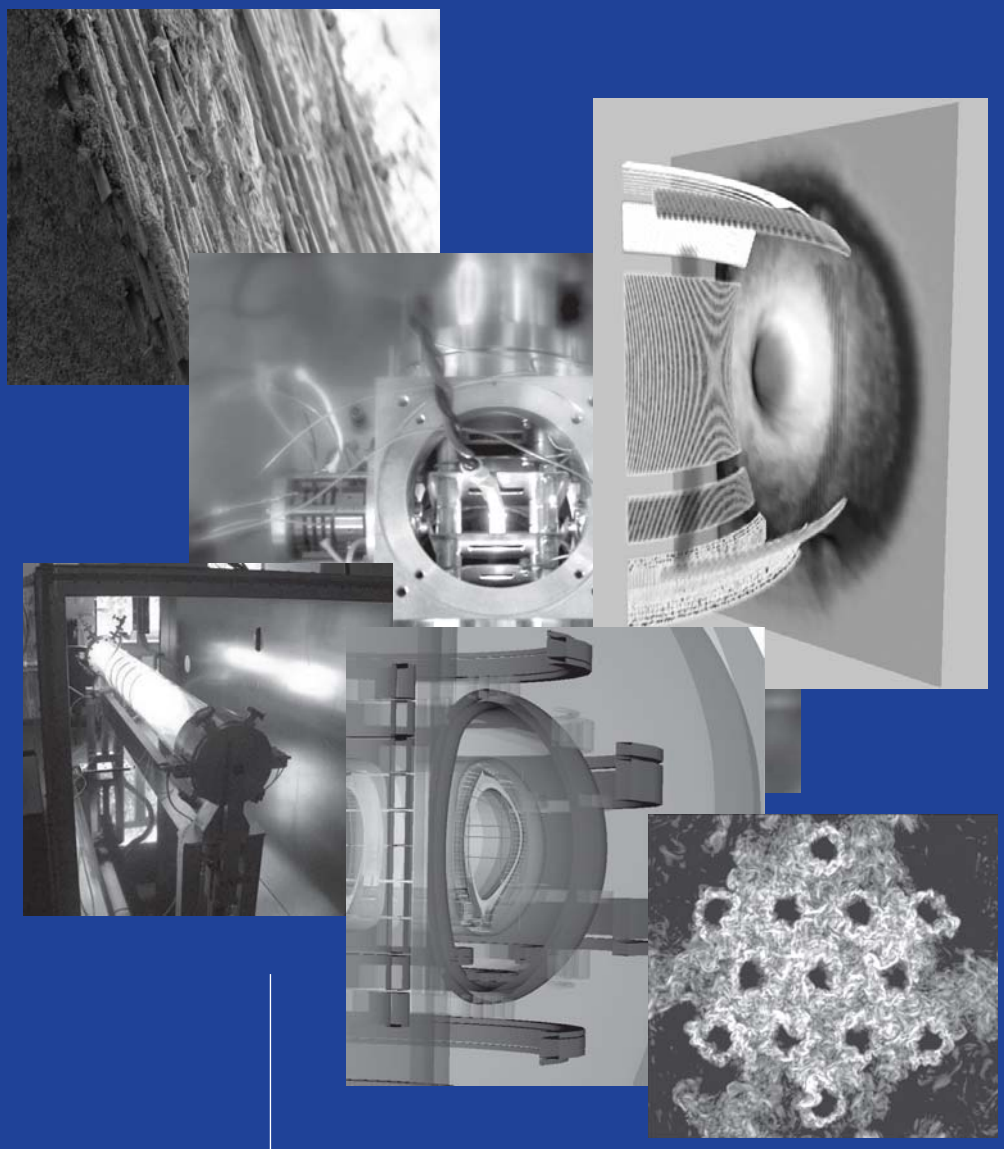

Association EURATOM – MESCS
FINAL REPORT 2007-2013

Ljubljana, November 2014

EURATOM-MESCS

Slovenska Fuzijska Asociacija
Slovenian Fusion Association

Association EURATOM – MESCS
FINAL REPORT 2007-2013

Final Report 2007-2013
of the Association EURATOM-MESCS
covers the period from 2007 to 2013.

Compiled by Boštjan Končar and Bojan Žefran

This work, supported by the European Communities under the contract of Association between EURATOM and MESCS (former MHEST), was carried out within the framework of the European Fusion Development Agreement (EFDA). The views and opinions expressed herein do not necessarily reflect those of the European Commission.

Association EURATOM-MESCS

Jožef Stefan Institute
Jamova cesta 39
SI-1000 Ljubljana
Tel. +386 1 5885 450
http://www.sfa-fuzija.si

Ljubljana, November 2014

Figures on the front cover are from SFA annual reports 2008-2013.

Association EURATOM-MESCS
FINAL REPORT 2007-2013

Slovenska fuzijska asociacija
Slovenian fusion association EURATOM-MESCS

ISSN 1855-2072

Ljubljana, 2014

CONTENTS

FOREWORD

At the time of the 7th framework program EURATOM, some important steps towards the realization of fusion energy have been made. The ITER construction was put forward as the key facility for development of fusion as an energy source. In 2007, the year when FP7 was launched, the ITER organisation was officially established and the preparation works for the ITER site started in Cadarache. In the same year Fusion for Energy (F4E), a joint European undertaking was established in Barcelona with the main objective to provide EU contribution to ITER. An important milestone for European fusion research was adoption of the "EFDA Fusion Roadmap" in 2012, which laid down the strategy and identified clear research priorities leading towards producing of electricity from demonstration fusion power plant by 2040. By the end of 2013 the fusion research driven by national associations and coordinated by EFDA formally ceased to exist. The spirit of EFDA however continues in Horizon 2020 within the new "EUROfusion" Consortium, which integrates national research units with firm commitment to the realisation of "Roadmap" goals. Thanks to the successful work in FP7 – strongly aligned with EFDA priorities, the Slovenian Fusion Association - SFA (EURATOM-MESCS) responded well to the EUROfusion Calls in 2014 and adapted to the newly established Consortium programme which will also direct our research activities in coming years.

The Slovenian Research Unit, called Slovenian Fusion Association- SFA was founded in 2005 by the contract of association with EURATOM and was signed by the Ministry for Higher Education, Science and Sport. SFA is composed of several research groups from leading Slovenian research institutions and universities: Jožef Stefan Institute, University of Ljubljana and University of Nova Gorica. Eventually the SFA research activities have evolved in a focused programme well incorporated into the common EU fusion programme led by EFDA. This report summarises the main activities and achievements of SFA, over the entire 7-year period of FP7 EURATOM, in the following fields:

- In ITER Physics program our researchers were strongly involved in the Plasma Wall Interaction (PWI) Task Force, encompassing studies of various plasma surface processes like particle removal, deposition and retention, as well as improving of the edge plasma diagnostics. Within the Integrated Tokamak Modelling (ITM) Task Force visualization tools for common ITM platform were developed.
- The research related to the JET program encompasses the development of fusion reactor neutron diagnostics focusing on the neutron detection and modelling. Our researchers have also actively participated in JET experimental campaigns.
- In Emerging Technologies program, later carried out within the EFDA department Power Plant Physics and Technology (PPPT), the work was divided between dedicated DEMO tasks (helium cooled divertor design,

neutronic studies, blanket test case) and more general tasks related to development of high-heat flux ceramic based materials for application in fusion power plants.

- The Public information program emerged as one of our stronger activities, as SFA did not only service domestic needs for education and information on thermonuclear fusion, but also successfully run the international Fusion Expo itinerant exhibition for more than five years.

More details can be of course found in annual reports.

Though I was already strongly involved in running the Slovenian Fusion Association in the last months of 2013, I have formally took over the leadership in turbulent year 2014 helping to establish and integrate the Slovenian research activities under EUROfusion Consortium. So all the credit for the success of Association under EFDA program goes to former Heads of SFA, dr. Milan Čerček (founder and a long-time Head) and dr. Andrej Trkov (Head in the years 2012-2013). Last but not least, I would like to express my sincere thanks to all SFA researchers for their excellent and dedicated work in fusion physics and technology and to the institutions in Slovenia and EU that have supported us since the very establishment of the Association.

Dr. Boštjan Končar
Head of research Unit

IMPROVEMENT OF DIAGNOSTICS IN PLASMAS OF FUSION DEVICES*

Tomaž Gyergyek[1,2], Jernej Kovačič[1], Milan Čerček[1]

[1] Jožef Stefan Institute
[2] University of Ljubljana, Faculty of Electrical Engineering
tomaz.gyergyek@ijs.si

1 INTRODUCTION

Probe diagnostics remain the only reliable source of measuring the plasma parameters with a good temporal and spatial resolution, yet their use is limited to SOL or just a bit beyond and will likely become obsolete with bigger fusion devices. Nonetheless, the methods for probe measurements and even the tools itself are constantly improved, since they keep providing relevant new results. The work of our probe diagnostics group from the Reactor Physics Department was until 2009 under the tasks "Interaction of vibrationally excited hydrogen molecules with fusion relevant material" and "Hydrogen-deuterium molecule wall interaction". These tasks were PWI related, and the group collaborated in the experimental part of the work. In 2010 we switched to the dedicated field of "Improvement of diagnostics in plasmas of fusion devices", which was mostly related to transport tasks. Our work therefore, became oriented in providing a better understanding of the behavior of various probes, with emphasis being put on the Langmuir probe and the emissive probe in order to correctly evaluate the data related to transport studies. In this time we have provided improved theoretical modeling and computer simulation of Langmuir and emissive probes, support in data evaluation of probe measurements and worked on the theory of the potential formation in front of electrodes. In general, our work was carried out in accordance with the submitted proposals, more so, we had established firm research relationships in the fusion community and we hope to continue to make advances in our field.

2 WORK PERFORMED IN 2010 - 2013

The work performed in years 2007-2009 is described in this report under the aforementioned tasks. Here, an overview of the work in the research field "Improvement of diagnostics in plasmas of fusion devices" is made.

2.1. Electrical probe measurements

Emissive probe

The motivation behind emissive probe measurements in tokamak plasmas is that of obtaining reliable results for plasma potential measurements. As it can be shown with a basic theoretical approach, the floating potential of the emissive probe becomes equal to plasma potential for high enough values of electron emission from its surface. This emission is thermionic and the heating can be provided either externally, from current flowing through the probe or laser heating, or by plasma itself, thus becoming self-emissive.

Our work was mostly oriented in modeling of the floating potential behavior and occurrence of various potential structures in front of the probe for different plasma parameters, which could then be used in evaluation of the measurement data. The research had become a part of the Priority supported tasks in 2012-2013 (WP12-IPH-A08-2-12/PS-017MHEST and WP13-IPH-A06-P1-02/MESCS/PS), since quick and reliable plasma potential measurements are still very important. Unfortunately besides the modeling and simulation of emissive surfaces, an actual emissive probe had not yet been installed in a tokamak up until now. We have however contributed to the design of the emissive probe head, which is led by the ÖAW group. Mobility funds were therefore used on a few occasions to strengthen our collaboration.

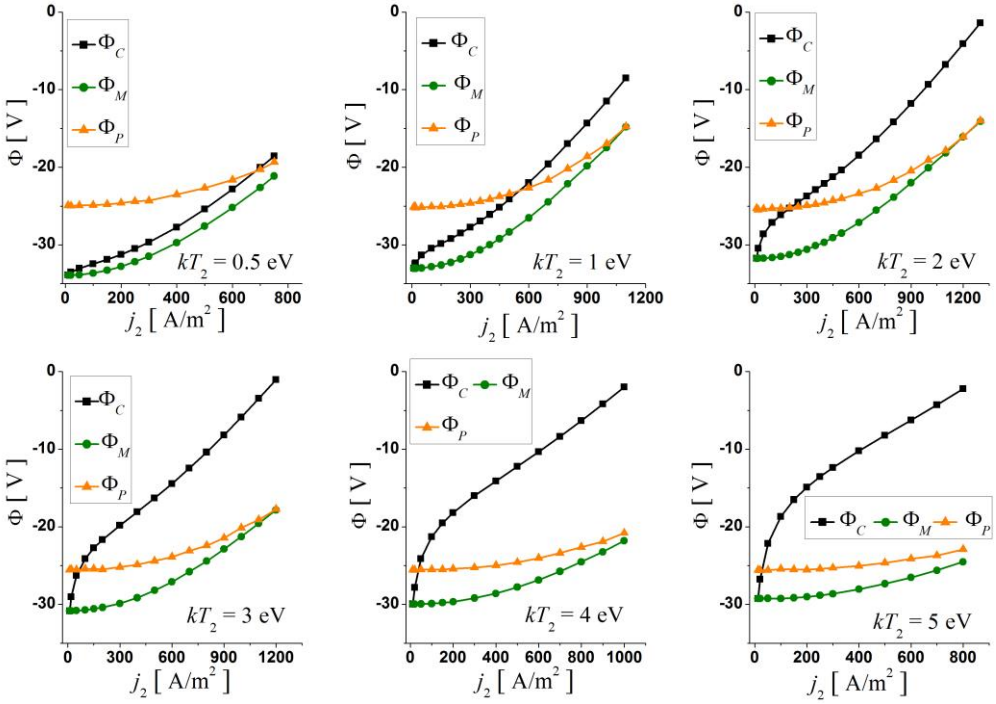

Figure 2: potentials Φ_C, Φ_M, Φ_P are plotted versus emissive current j_2 for six different temperatures of the emitted electrons. The electron temperature is kT_1=20 eV and the emitted electrons temperature are kT_2=0.5 eV, 1 eV, 2 eV, 3 eV, 4 eV and 5 eV, respectively.

In our modeling and simulation we have taken in account most of the relevant physics. It was shown using different approaches, that the floating potential of the highly emissive probe will saturate at 1.7-1.8 kT_e below the plasma potential, as

calculated in detailed simulation [1] in collaboration with ÖAW. The simulations were very time consuming, requiring more than 10^6 CPUh, mostly on HPC-FF (High-Performance-Computer – For Fusion). The floating potential saturation was shown to be due to the inhibited transport of emitted electrons through the sheath due to the negative space-charge accumulation in front of the surface. Additionally, the simulation model was used to calculate the effects of the secondary electron emission on the heat load to the wall. It was shown, that in the case of the critical emission, the heat load is $Q_{e,heat}\left(\Gamma_{em} = \Gamma_{em,crit}\right) = 2.7 Q_{e,heat}\left(\Gamma_{em} = 0\right)$. Models were constructed, which allow for a calculation of the transition point between the temperature limited regime and the space-charge limited regime [2-5], also for the case of non-Maxwellian plasmas (also in next subsection) due to additional population of fast electrons.

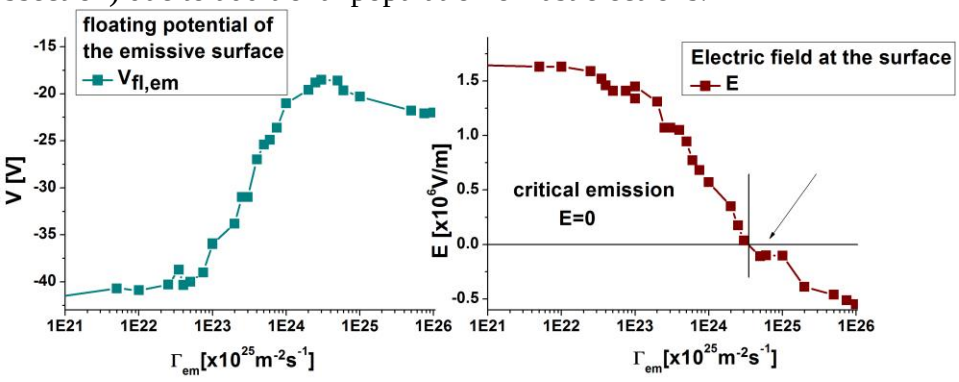

Figure 1: Floating potential of and electric field at an emissive surface with dependence on the electron emission flux from the wall.

It was determined, that the main cause of the saturation lies in the temperature ratio between the bulk electrons and the emitted electrons. This ratio unfortunately cannot be altered, since thermionic emission occurs at temperatures around 0.2 eV.

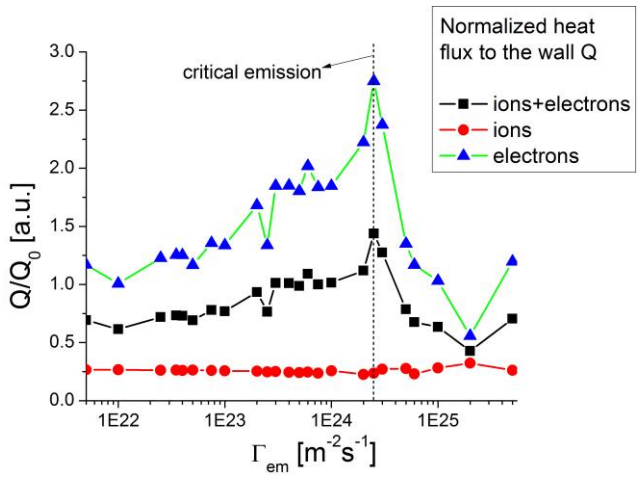

Figure 1: Electron (blue), ion (red) and total heat flux with dependence on the electron emission flux from the wall. The dashed line designates the point of critical emission.

Langmuir probe

In 2010 we began a fruitful collaboration with Bulgarian fusion association INRNE.BG and University of St. Kliment Ohridsky in Sofia regarding probe measurements in non-Maxwellian plasmas. Non-Maxwellian plasmas are a common occurrence in plasma fusion devices, however they are often not acknowledged, mostly due to incapability of measuring methods to define them properly. Our collaborators from INRNE.BG have developed a method for a more precise measurement of electron energy distribution function, which we have later used successfully in tokamaks and stellarators [6, 7].

The First Derivative Probe Technique (FDPT) the non-Maxwellian distribution in SOL of tokamaks by assuming a bi-Maxwellian distribution, individually modeling bulk electrons and the high energy tail, also taking into account the suppression of the electron part of the I-V characteristic due to magnetic field. The method was refined also with measurements in our Linear Magnetized Plasma Device, where we made measurements in plasmas with additional group of fast electrons or an additional group of slow negative ions [8]. Measurements proved the method to be very accurate for measurements of particle species' densities, temperatures and the plasma potential.

We have also helped in evaluating the COMPASS measurements using this technique for simultaneous measurements using horizontal, vertical and divertor probes [6, 7]. It was shown, that there is indeed a radial influx of electrons in SOL which slow down through collisions (preferably ionization) and thus forming a rather distinct bi-Maxwellian distribution of thermal and sub-thermal groups. Mobility funding scheme was again put to great use for this joint endeavor.

We have also performed detailed fully-kinetic PIC simulation of probe I-V characteristic inside LMPD and compared it with actual EEDF measurements [9], which provided good foundations for the more elaborate simulations described just below.

Through the aforementioned priority task WP12-IPH-A06-2-05/PS-01/MHEST we have also made fully-kinetic PIC simulations of COMPASS SOL to study the relaxation of the thermal electrons to sub-thermal. The simulations results obtained point to the fact, that purely parallel transport does not provide enough "distortion" for such a deviation from Maxwellian plasma. For these simulations a computer project was again obtained at HPC-FF.

Ball-pen probe

In 2010 we have collaborated with IPP.CR and Charles University of Prague on the ball-pen probe measurements. Dedicated measurements [10, 11] with the ball-pen probe were performed in our Linear magnetized plasma device for different ratios of characteristic parameters, i.e. the degree of particle species' magnetization.

2.2. Boundary conditions in magnetized edge plasma

In close connection to the probe theory are also the boundary conditions in front of electrodes in general. In tokamak modeling the fluid approach to modeling is much more favorable than kinetic approach, albeit the latter being able to deal with e.g. plasmas outside of thermodynamic equilibrium (plasma sheath). It has recently been discovered, that unlike in the classical approach, the polytropic coefficient γ used as a closure of the system of fluid equations (e.g. Braginskii equations) is not a constant, but rather a space and time dependent variable. The results obtained with coupled fluid model are then in complete agreement with the kinetic model. Polytropic coefficient function is however highly dependent on the ratios of characteristic lengths in the system. We have studied the effects of the ratios between the Debye length, ion Larmor radius and ionization length of the system with emphasis on the sheath entrance values [12,13]. The research again employed theoretical work and use of fully-kinetic PIC (particle-in-cell) code BIT1. A simple theoretical model predicts a cosinusoidal dependence of the polytropic coefficient on the angle of the applied magnetic field, which was confirmed via simulation. The dependence on the level of magnetization is however significantly smaller.

The results can be used to improve the accuracy of the fluid models by taking into account finite ratios between characteristic system lengths. We have partly included this research under WP12-IPH-A06-2-05/PS-01/MHEST, where probe measurements were employed for analyzing SOL transport.

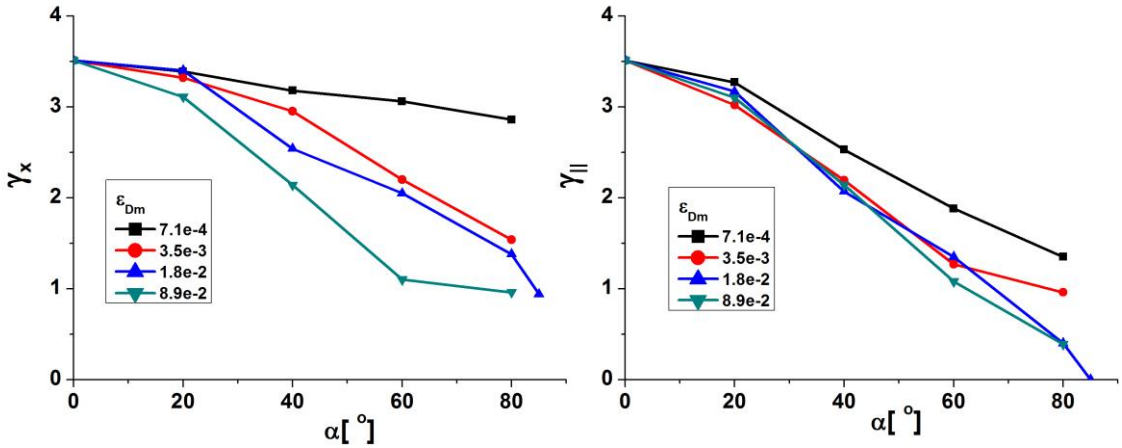

Figure 4:Values of the ion polytropic function (normal γ_x (left) and parallel $\gamma_{\|}$ (right))at the entrance to the space-charge region depending on the magnetization parameter and the angle of magnetic field.

3 CONCLUSIONS AND OUTLOOK FOR FURTHER WORK

In the past three years we have been included in various tasks regarding the probe measurements. Mainly, we had provided theoretical and simulation support and helped with the evaluation of the data. However, we were also involved in measuring campaigns on our LMPD machine and others. During this time we have made many new connections in this field and we are continuing our research in the framework of EUROfusion. We are again involved in a task regarding the use of emissive probe in a stellarator, as well as a task regarding the development of a 2d3v fully-kinetic particle-in-cell code. We are also continuing our collaboration with INRNE.BG on the advanced

Langmuir probe techniques for measuring the plasma potential, albeit currently not under EUROfusion flag.

4 REFERENCES

1 J. Kovačič, T. Gyergyek, Simulation of a planar emissive probe in a mid-sized tokamak plasma, Contrib. plasma phys., 51 (2011), 962-970.
2 T. Gyergyek, J. Kovačič, M. Čerček, Potential formation in front of an electron emitting electrode immersed in a plasma that contains a monoenergetic electron beam, Phys. plasmas, 17 (2010), 1-16.
3 C. Ionita, M. Čerček, T. Gyergyek, J. Kovačič et al., The use of emissive probes in laboratory and tokamak plasmas, Contrib. plasma phys., 51 (2011), 264-270.
4 T. Gyergyek, J. Kovačič, Saturation of a floating potential of an electron emitting electrode with increased electron emission: a one-dimensional kinetic model and particle-simulation, Phys. Plasmas, 19 (2012), 1-16.
5 T. Gyergyek, J. Kovačič, Potential formation in a bounded plasma system which is terminated by an electron emitting floating collector studied by a particle-in-cell simulation, Contrib. plasma phys., 53 (2013), 189-201.
6 Tsv. K. Popov, M. Dimitrova, P. Ivanova, J. Kovačič et al., Langmuir probe evaluation of the plasma potential in tokamak edge plasma for non-Maxwellian EEDF, Contrib. plasma phys., 54 (2014), 267-272.
7 M. Dimitrova, R. Dejarnac, Tsv. K. Popov, J. Kovačič et al., Plasma parameters in the COMPASS divertor during ohmic plasmas, Contrib. plasma phys., 54 (2014), 255-260.
8 Tsv. K. Popov, M. Mitov, A. Bankova, J. Kovačič, T. Gyergyek, M. Čerček et al., Contrib. plasma phys., 53 (2013), 51-56
9 J. Gruenwald, D. Tskhakaya, J. Kovačič, M. Čerček, T. Gyergyek, C. Ionita, R. Schrittwieser, Comparison of measured and simulated electron energy distribution function in low-pressure helium plasmas, Plasma sour., sci. & technol., 22 (2013), 1-7.
10 J. Adamek, M. Peterka, T. Gyergyek, P. Kudrna, M. Tichy, Diagnostics of low temperature plasma by ball-pen probe, Nukleonika, 57 (2012), 297-300.
11 J. Adamek, M. Peterka, T. Gyergyek, P. Kudrna, P. Ramisch, U. Stroth, J. Cavalier, M. Tichy, Application of the ball-pen probe in two low-temperature magnetized plasma devices and in torsatron TJ-K, Contrib. plasma phys., 53 (2013), 39-44.
12 J. Kovačič, T. Gyergyek, M. Čerček, Pre-sheath formation in an oblique magnetic field: fluid model and PIC simulation, Eur. phys. jour. D, atomic, molecular and optical physics, 54 (2009), 383-389.
13 J. Kovačič, Study of the potential formation in front of a negative electrode for fusion relevant plasmas, PhD thesis, (2013)

PROCESSES WITH NEUTRAL HYDROGEN ATOMS AND MOLECULES

Iztok Čadež[1], Sabina Markelj[1], Primož Pelicon[1], Zdravko Rupnik[1], Anže Založnik[1], Zvone Grabnar, Milan Čerček[2a], Tomaž Rudman[2a], Tomaž Gyergyek[3a], Vida Žigman[4]

[1]Department for Low and Medium Energy Physics, "Jožef Stefan" Institute, Jamova cesta 39, SI-1000 Ljubljana
[2]Reactor Physics Department, "Jožef Stefan" Institute, Jamova cesta 39, SI-1000 Ljubljana
[3]Faculty of Electrical Engineering, University of Ljubljana, Ljubljana, Slovenia
[4]University of Nova Gorica, Vipavska 13, SI-5000 Nova Gorica
e-mail: iztok.cadez@ijs.si (2007-2012); sabina.markelj@ijs.si (2013)

1 INTRODUCTION

The main goal of the project "Processes with neutral hydrogen atoms and molecules" (1.4.1) during 2007 to 2013 period was to contribute to understanding and to providing quantitative data for processes with neutral hydrogen atoms and molecules which are relevant for the current efforts in EU towards developing the magnetically confined fusion. Processes on the surface and in the bulk of fusion relevant materials as well as A/M collision processes in the gas phase of importance to edge plasma were our concern. Work program was from year to year more and more specific and focused to the problems recommended by EFDA to be of higher relevance. The title of the program changed twice during this period of time: it was "Interaction of vibrationally excited hydrogen molecules with fusion relevant material" in 2007, "Hydrogen-deuterium molecule wall interaction" in 2008-2009 and finally "Processes with neutral hydrogen atoms and molecules" since 2010. Collaborators of Plasma group from Reactor Physics Department of "Jožef Stefan" Institute participated in the Project until 2009.

Initial main subject of the Project were processes in which vibrationally excited molecules of hydrogen isotopologues (mainly H_2 and D_2) are involved. The experimental studies were based on specific, original vibrational spectrometer for hydrogen molecules, Ion Beam Analytical (IBA) methods at 2 MV tandem accelerator for surface characterization, and Linear Magnetized Plasma devise of the Plasma group. By the time work was more and more directed towards hydrogen/deuterium retention and global release from fusion relevant materials and the main experimental technique became the *in situ* exposure of fusion relevant materials to hydrogen (H or D) atomic

[a] Participant in the Project until 2009

beam. Coordination of the annual work programs with EFDA was assured by active collaboration in the EU Task Force for Plasma-Wall Interaction.

2 WORK PERFORMED IN 2007 - 2013

All the activities which were undertaken within our project are mentioned and shortly commented in present report even if they did not result in journal publications but only in contributions presented at conference. Particular annual project reports are not included in the reference list but if needed they are denoted in the text by abbreviation AR followed by the year. Activities are listed according to the respective start time within reported period.

2.1. Production of vibrationally excited hydrogen molecules by atom recombination on surfaces

The motive for this activity was high vibrational temperature of neutral hydrogen molecules observed by the analyses of Fulcher-band emission from edge plasmas. It was initially the main activity of the project [1] and it was based on the use of an original vibrational spectrometer for hydrogen molecules employing the properties of dissociative electron attachment. The yield of low energy H^-/D^- ions as a function of energy of an initial electron beam provides data for determination of vibrational population of target hydrogen molecules. The spectrometer itself was developed and used in variety of applications throughout the duration of the project. Its performances were presented in detail in [2] and [3]. A special test source coupled to the vibrational spectrometer was used in the study of vibrational distribution of molecules produced by atom recombination on surfaces. Vibrationally hot molecules in this source are produced by atom recombination on the cooled sample surface exposed to hydrogen gas partially dissociated by means of an incandescent tungsten filament.

Special effort was devoted to the study of H and D recombination on tungsten as fusion relevant material and Cu as a benchmark comparison case. The vibrational population of H_2 and D_2 molecules produced by atom (H or D) recombination on tungsten and copper material were analyzed and measured. The obtained vibrational populations shown in Figure 1 for H_2 and Figure 2 for D_2 could be well described by the Boltzmannian distribution, with specific vibrational temperatures for each material. The experimentally obtained vibrational populations for copper approximately agreed with the theoretical predictions, whereas the experimentally obtained vibrational temperature for tungsten was higher and thus showing a considerable overpopulation of highly excited vibrational states than predicted. We proposed that the origin of this higher excitation is related to the existence of high hydrogen surface coverage on tungsten, where hydrogen is occupying binding sites with different desorption energies. In order to obtain an insight into the recombination mechanism with more than one binding site per unit cell, a Monte Carlo simulation was performed, where it was assumed that the main production of molecules proceeds through the hot atom recombination with an adsorbed atom. The results show that the recombination proceeds mainly through the weak binding sites, once they are occupied. A detailed description of results including a kinetic modelling was presented in [3] and [4].

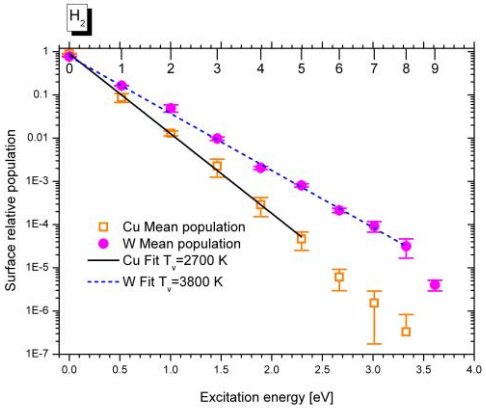

Figure1: The H2 mean relative populations for Cu and W sample. The lines are the fit of the data with the Boltzmann distribution, with vibrational temperature Tv = 2700 K for Cu and 3800 K for W.

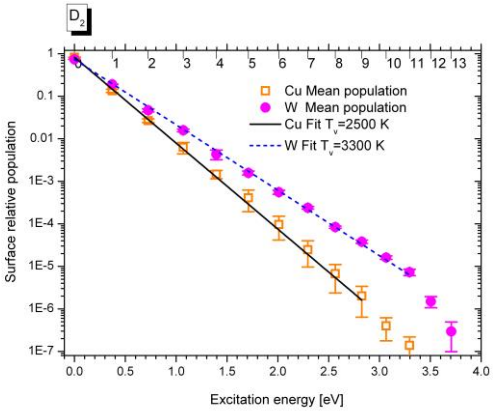

Figure2: The mean relative populations for D2 produced by atom recombination on Cu and W samples. The lines are the fit of the data with Boltzmann distribution, with vibrational temperature Tv = 2500 K for Cu and 3300 K for W.

2.2. Other experiments involving vibrationally excited hydrogen molecules

Due to the availability of unique vibrational spectrometer for hydrogen molecules some other pilot studies were undertaken within the project.

A small, compact source of vibrationally excited molecules, named ISPEC, based on the same principle as above mentioned test source was constructed and employed in some of these studies. It was used in an attempt to observe role of vibrationally excited molecules in chemical erosion of hydrogenated carbon films. Such a role could not be detected due to the presence of dominating contribution of atoms in the gas beam from the source. Discussion on this work and detailed characteristics of ISPEC were presented at the conference [5]. However, even the role of hot molecules in erosion could not be observed we did observe in this experiment for the first time deposition of impurity layer on the cold surface subjected to the atom beam [AR2008], a process which was studied in more detail in another experiment later.

Another pilot study was vibrational spectroscopy of hydrogen molecules produced by recombination of atoms at the low pressure side of a permeation membrane (77%Pd+23%Ag alloy). Only weak excitation could be observed at 515 K [AR2007].

A study of vibrational distribution of hydrogen molecules from a commercial hydrogen atom source, HABS was performed, which was acquired in 2007 and later extensively used in experiments.

2.3. In situ studies of hydrogen – metal interaction by Ion Beam Analytical methods

We started in situ studies of hydrogen interaction with metals using Ion Beam Analytical methods since the very beginning of our involvement in the fusion program. First studies [6] were performed using a special cell similar to those used as a source for vibrationally excited molecules containing incandescent tungsten filament providing

hydrogen atoms for exposure of the surface. H and D concentration in material was measured by Elastic Recoil Detection Analysis (ERDA) with ^{7}Li incident ion beam. Such studies got special momentum since 2008 when atomic beam source using hot tungsten capillary was acquired as it allowed precise exposure characterization. As the time was evolving such studies became a dominant part of our activities and by the end of reported period almost all others are marginal and only part of our voluntary activity. Particular activities within this domain are presented in following subsections.

2.3.1. In situ study of erosion and deposition of amorphous hydrogenated carbon films

We have performed first dual-beam experiment employing a hydrogen atom beam for sample exposure and an ion beam for analysis, enabling *in-situ* real-time studies of hydrogen atom interaction with materials by Elastic Recoil Detection Analysis (ERDA) [7]. The experimental set up is shown in Figure 3. The erosion of an amorphous hydrogenated carbon (a-C:H) layer by deuterium atoms at 580 K sample temperature was studied and the uptake of deuterium during the erosion process was measured. Formation of a polymer-like deposit on an a-C:H layer held at room temperature and subjected to the deuterium atom beam was observed and also studied *in-situ*. For both erosion and deposition studies an a-^{13}C:H layer on top of an Si substrate was used as a sample, making the experiments isotopically fully specified and thereby differentiating the deposited from the original layer and the interacting D atoms from H atoms present in the layer and in the residual vacuum. From the deposition study it was shown that carbon in the deposited layer originates from carbon-carrying species in the background vacuum that interact with hydrogen atoms. The cross section for ^{7}Li on D at 4.3 MeV Li ion energy and at a recoil angle of 30^{o} was also determined to be $(236\pm16)\times10^{-27}$ cm^{2}/sr. This is a factor of 360 times higher than the Rutherford elastic cross section.

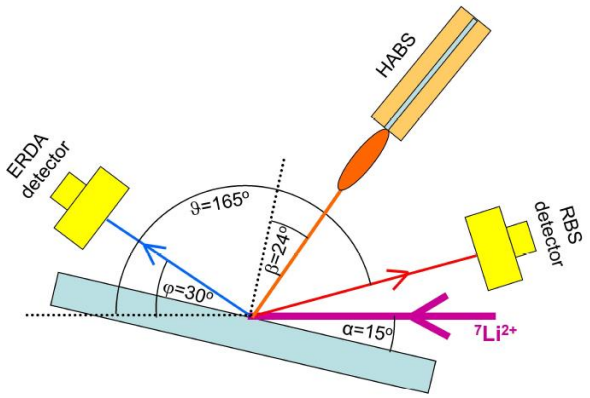

Figure 3: Dual-beam experimental configuration for the in situ studies of hydrogen atom interaction with materilas by ion beam methods ERDA and RBS. The hydrogen atom beam is produced by a hot capilary source HABS.

2.3.2. Study of thermal hydrogen atom interaction with undamaged and self-damaged tungsten by in situ ERDA and NRA

Study of hydrogen retention in tungsten modified by radiation damage has been initiated in collaboration with IPP. A study with undamaged samples was done as a reference and appropriate model developed and applied [8]. There, thermal deuterium atom adsorption on polycrystalline tungsten was studied *in-situ* by ERDA. New procedure named "thermoadsorption" was used so that concentration of adsorbed deuterium was measured during sample cooling while it was continuously exposed to D atom beam. Both, D and H concentrations on the surface and bellow it were simultaneously followed by ERDA. It was observed that deuterium surface areal density was increasing stepwise, identifying three individual binding states for the studied polycrystalline tungsten. Surface areal density as a function of temperature and time were modelled according to specific experimental procedure and binding energies for desorption/adsorption were derived. The isotope exchange at fixed sample temperature of 485 K was also measured and modelled. From the measured data an estimate of the reflection coefficient for 0.2 eV hydrogen atoms on polycrystalline W was obtained.

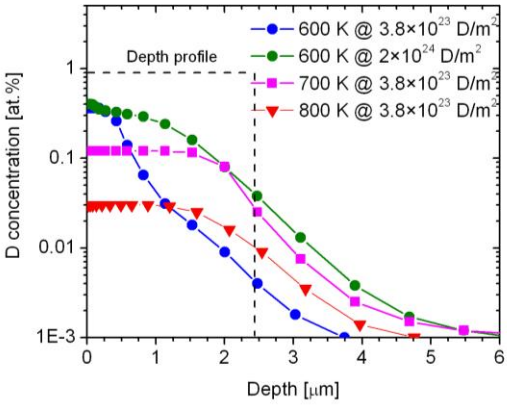

Figure 4 : *D depth profile in damaged W at 600 K for two different D fluences and at 700 K and 800 K. The damage profile is shown by dashed line*.

First retention study in damaged polycrystalline tungsten exposed to thermal D beam was performed between 370 K and 500 K as a function of D fluence [9]. Damaged samples were produced by W ion irradiation with damage concentration up to 0.89 displacements per atom (dpa). ERDA was used to follow near-surface H and D areal densities *in situ* during the exposure and the D depth profiles down to 6 μm were extracted *ex situ* by Nuclear Reaction Analysis (NRA) performed at IPP. The NRA method uses nuclear reaction $D(^3He,p)^4He$ for determination of D concentration and allows depth profile analysis much deeper and with better sensitivity compared to the ERDA method. Both methods gave the same D concentration within the first 400 nm. We have shown for the first time that D is retained in undamaged and damaged W exposed to thermal (0.2 eV) atoms. Retention in damaged W was found to be higher than in undamaged due to additional traps created by heavy W ion pre-irradiation. Isotope exchange at the surface and in bulk of damaged W was also investigated *in situ* by ERDA at different sample temperatures. Following this study, several exposures of

self-damaged tungsten to hydrogen atom beam and *ex situ* ^{3}He NRA at IPP were performed at different sample temperatures, to study the temperature effect on retention. Deuterium depth profile in damaged W exposed to D atom to different fluences and sample temperatures are shown together with the damage profile in Figure 4. This work was conducted within EFDA PWI WP12-IPH-A03-1-13/PS&BS-01/MHEST entitled: "Atomic and low-energy hydrogenic plasma interaction with damaged tungsten" in collaboration with IPP, Garching.

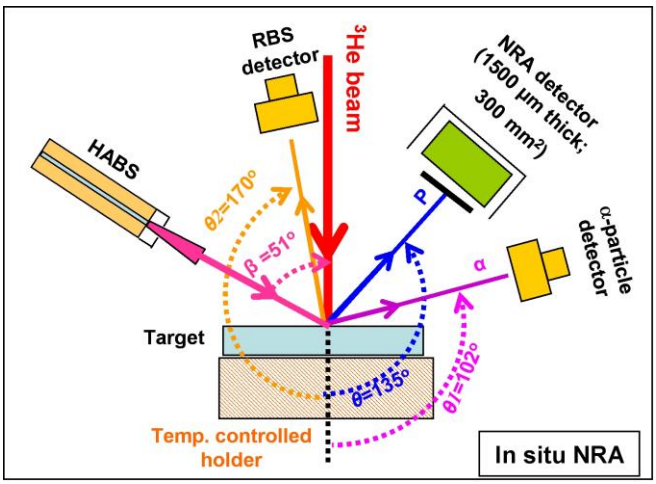

Figure 5 : *The set up for in situ NRA measurements. The incident 3He beam is perpendicular to the sample surface. Hydrogen atom beam source (HABS) is also shown in the figure.*

We have performed first study of D retention in undamaged and damaged W exposed to D atoms by *in situ* NRA, where depth profile was measured during the exposure (paper accepted for publication in Physica Scripta [10]). The NRA set up for in situ measurements is shown in Figure 5. The deuterium depth profile in the sample is obtained by analyzing the energy distribution of protons and alpha particles created by D(^{3}He,p)^{4}He nuclear reaction. One example of the results of the present *in situ* NRA measurements on damaged W exposed to D atoms at 590 K is presented in Figure 6. *In situ* measurements gave direct information about the dynamics of D migration in W. The *in situ* measurements of terminal D concentration after stop of exposure are in good agreement with *ex situ* measurements on equivalently damaged W. The *in situ* NRA during D atom exposure on undamaged W gave higher retention compared to *ex situ* measurements. The results of these measurements appear to be due to simultaneous effect of dynamic retention and D decoration of damage produced by the analyzing He beam. Further studies are needed in order to analyze the influence of the probing He beam, since this is crucial for further *in situ* NRA studies and to clearly distinguish the contribution of the probing beam irradiation and dynamic retention for undamaged W. The isotope exchange in damaged W was also studied for the first time by *in situ* NRA. Complete isotope exchange was achieved for 590 K sample temperature what was not for the case for 500 K, with D atom exposure performed at 700 K. Further studies are needed in order to see the efficiency of isotope exchange at other sample temperatures and to separate the deuterium bulk decrease due to the thermal desorption versus isotope exchange. This work was conducted within EFDA PWI WP13-IPH-A03-P1-

01/PS/MESCS entitled: "Atomic and low-energy hydrogenic plasma interaction with damaged tungsten" in close collaboration with IPP, Garching.

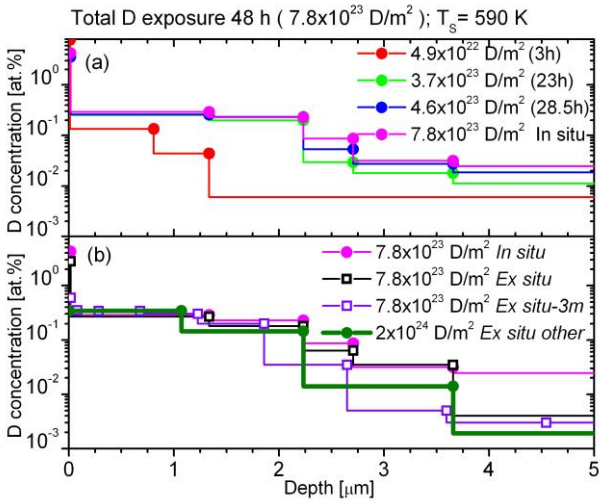

Figure 6: a) D depth profile obtained by in situ NRA during the exposure. b) NRA measured after stop of the exposure and ex situ 5 days and 3 months after exposure on the same sample. For comparison the depth profile of the previous ex situ NRA study is shown ("Ex situ other"). D atom flux density at the probing beam position is 4.5×10^{18} D/m^{2}s.

2.4. Deuterium thermal desorption from tungsten exposed to deuterium ion beam under well-defined surface and exposure conditions

The main goal of this part was to study thermal desorption (TD) of deuterium from W exposed to well defined deuterium ion beam or plasma. The purpose of this is to developing a well-controlled step-by-step procedure aimed to facilitate in-depth understanding of adsorption, diffusion and desorption of D at/in/from W and the formation of defects by D removal techniques and their impacts on the re-adsorption. The work has been partly performed at PIIM laboratory, University Aix-Marseille, within the postdoctoral visit of Sabina Markelj from JSI (9 month EURATOM mobility scheme). This was priority supported task in 2012 and 2013 entitled: "D re-adsorption/re-saturation of W surfaces subjected to helium RF-discharge as a fuel removal technique" - PWI WP12-IPH-A03-2-06/PS&BS-01/MHEST, WP12-IPH-A03-P2-01/PS/MESCS. The exposure and the TD spectroscopy were to be made at the PIIM laboratory and the depth profiling of D in the exposed samples was to be preformed by NRA at JSI. In the first year we have obtained and quantified first data on D retention by TD on W sample with controlled submonolayer oxygen contamination and NRA&RBS setup at the broad ion beam experimental station has been completed, tested and detectors calibrated. In second year a detailed study of thermal desorption of D from W subjected to different ion fluences was performed and results compared to available data from other experiments. For the first time an extension to very low exposure fluences was made (10^{18} D/m^2) as compared to other retention studies for W. A detailed study of the influence of the storage time in vacuum on decrease of the amount of retained deuterium was performed, showing that the dynamic retention is

very large. The NRA study on samples exposed to 5 keV and 500 eV D_2^+ ions was performed; showing that the deuterium was retained mainly at the surface for the long storage time, whereas increased concentration up to 1 μm below the surface was observed for short storage time. Further studies are needed in order to quantify the impact of exposure of D-containing samples to air on the amount of retained deuterium and to study the discrepancy between NRA and TD results of D concentration measurements.

2.5. Study of cross sections for dissociative electron attachment

Dissociative electron attachment (DEA) in hydrogen is a basic process for hydrogen molecule vibrational spectroscopy which we are using and therefore we had interest to providing some new data on this process. DEA is taken into account in detailed modelling of hydrogen plasma and has special importance in volume sources of negative hydrogen ions. Cross section for DEA in D_2 is strongly decreased with respect to H_2 due to isotope effect so that not many results exist in the literature for this case. We have provided new values for the ratio of DEA in two molecules [1]. It was especially important that we drove attention on the important contribution of background leading to the wrong values for the 14 eV DEA in hydrogen usually used in the literature. New measurements were jointly undertaken in another laboratory and corrected cross sections provided [11]. Besides this we did measurements of low energy H^- production by DEA in some small hydrocarbons (CH_4, C_2H_2, C_2H_4, C_2H_6, C_3H_8) [12].

2.6. Processes with hydrocarbons

Some activities were devoted to hydrocarbons due to its rich chemistry with hydrogen and consequently high fusion fuel retention and material migration. Even the carbon is presently not considered as a fusion relevant material the work with carbon containing molecules is still interesting due to their potential presence as impurity in fusion plasmas, as there is much complementary data available in the literature and as such studies provide insight in processes which might occur with other elements as well. A pilot study of the influence of methane on hydrogen vibrational excitation was performed using ISPEC [13]. Through this study we also measured vibrational distribution of H_2 molecules which are created by thermal decomposition of C_2H_4 and C_2H_6 on hot tungsten filament. Such processes are relevant to the tungsten divertors where high surface temperature also occur.

2.7. Modelling of neutral hydrogen in a cell

Variety of processes occur in a cold wall metallic cell containing hot tungsten filament when neutral hydrogen gas is let to flow through it at low pressure. If the filament temperature is high enough (1600 K to 2200 K) neutral hydrogen molecules can dissociate or get ro-vibrationally excited. Atoms can subsequently recombine on the cold wall creating vibrationally excited molecules. Besides this, excited molecules can be de-excited by the collisions on the wall and also different inelastic collisions can occur in the volume. In collaboration with the University of Nova Gorica we have

worked on development of numeric model for such gas cells as we were using for production of vibrationally excited molecules as described above but also for some in situ IBA studies [6]. Modelling was simplified by assuming low gas pressure so that volume collisions could be neglected with respect to the surface collisions. Both equilibrium and non-equilibrium kinetic and Monte Carlo models were considered taking into account restricted number of particle species [14] and finally a simple but complete kinetic model was developed [15] taking into account 16 types of particles: ground and 14 vibrationally excited states of molecule and atom.

2.8. Hydrogen plasma

Activities in the field of plasma research conducted on the Linear Magnetized Plasma device while being a part of the present project was twofold. Main activity was devoted to the plasma theory and plasma diagnostics which later evolved in the separate, new SFA project (e.g. [16], [17], [AR2009]). Characteristics of the hydrogen plasma were studied by Langmuir probe and also by optical emission spectroscopy [18]. For this studies a dual channel fibre-optical spectrometer was used which was specially acquired for this purpose. A dedicated experiment was performed using source of vibrationally excited hydrogen molecules ISPEC in order to identify possible contribution of surface created molecules to the Fulcher band emission but no effect could be observed [AR2009].

3 CONCLUSIONS AND OUTLOOK FOR FURTHER WORK

Past work on the project was innovative but rather scattered at the beginning and became very focussed on just few issues, mainly deuterium retention in damaged tungsten and development of tungsten cleaning procedures by isotope exchange in plasma, by the end of this period. These two activities were chosen and stimulated by EFDA as appropriate priority supported tasks. Although not explicitly supported by EFDA we did continue steady development of our method for hydrogen vibrational spectroscopy as we find it very suitable and unique tool for some studies, some of them were already tested and described above. Further work will be conducted within the framework of new EUROfusion consortium mainly on the two above mentioned subjects. Some of our previous voluntary activities were proposed for support to the Enabling Research call of Consortium but were not accepted.

4 REFERENCES

1 I. Čadež, S. Markelj, Z. Rupnik and P. Pelicon, Processes with neutral hydrogen and deuterium molecules relevant to edge plasma in tokamaks, J. of Physics: Conf. Series, 133 (2008) 012029, 10pages.
2 S. Markelj, Z. Rupnik and I. Čadež, An extraction system for low-energy hydrogen ions formed by electron impact, International Journal of Mass Spectrometry, 275 (2008) 64-74.
3 S. Markelj, Interaction and production of vibrationally excited hydrogen molecules on surfaces, Ph.D. thesis, University of Ljubljana, (2010) 195 pages.
4 S. Markelj, I. Čadež, Production of vibrationally excited hydrogen molecules by atom recombination on Cu and W materials, The Journal of chemical physics, 134 (2011) 124707-1-123707-17.

5 S. Markelj, I. Čadež, Th. Schwarz-Selinger, Chemical erosion of carbon by vibrationally hot hydrogen molecules. V: 18th International Conference on Plasma Surface Interactions, Toledo, Spain, May 26-30, 2008 Program and book of abstracts, page 110.
6 S. Markelj, I. Čadež, P. Pelicon, Z. Rupnik, Studying process of hydrogen interaction with metallic surfaces in situ and real-time by ERDA. Nuclear instruments & methods in physics research. Section B, Beam interactions with materials and atoms, 259 (2007) 989-996. (also for Project 1.4.3.)
7 S. Markelj, P. Pelicon, I. Čadež, T. Schwarz-Selinger and W. Jacob, In situ study of erosion and deposition of amorphous hydrogenated carbon films by exposure to a hydrogen atom beam, J.Vac. Sci. Tech. A 30 (2012) 041601-1.
8 S. Markelj, O. V. Ogorodnikova, P. Pelicon, Th. Schwarz-Selinger, I. Čadež, Temperature dependence of D atom adsorption on polycrystalline tungsten, Appl. Surf. Sci., 282 (2013) 478-486.
9 S. Markelj, O. V. Ogorodnikova, T. Schwarz-Sellinger, P. Pelicon, K. Sugyama and I. Čadež, Study of thermal hydrogen atom interaction with undamaged and self-damaged tungsten, J. Nucl. Mater., 438 (2013) S1027-S1031.
10 S. Markelj, O.V. Ogorodnikova, P. Pelicon, T. Schwarz-Selinger, P. Vavpetič, G. Kukec and I. Čadež, In-situ NRA analysis of D retention in undamaged and self-damaged tungsten under atomic D exposure, 14th PFMC conference, May 2013, Juelich, Germany; accepted in Physica Scripta.
11 E. Krishnakumar, S. Denifl, I. Čadež, S. Markelj, N. J. Mason, Dissociative electron attachment cross sections for H_2 and D_2, Physical review letters, 106 (2011) 243201-1-243201-4.
12 I. Čadež, S. Markelj and Z. Rupnik, Low energy H^- production by dissociative electron attachement to small hydrocarbons. The European physical journal. D, Atomic, molecular and optical physics, (2012) 66: 73, 7pages.
13 I. Čadež, S. Markelj, A. R. Milosavljević, Influence of hydrocarbons on vibrational excitation of H_2 molecules. Nuclear Engineering and Design, 241 (2011) 1267-1271.
14 V. Žigman, Non-equilibrium kinetic versus Monte Carlo modelling of hydrogen–surface interactions, Nuclear Engineering and Design 241 (2011) 1272–1276.
15 A. Založnik, I. Čadež, S. Markelj and V. Žigman, Modelling hydrogen-metal surface interactions : the integral study, 22nd International Conference Nuclear Energy for New Europe - NENE 2013, Bled, September 9-12. Eds. L. Cizelj, M. Leskovar, M. Uršič, Proceedings. Ljubljana: Nuclear Society of Slovenia (2013) paper 1406, 7pages.
16 T. Gyergyek, B. Jurčič-Zlobec, and M. Čerček, Potential formation in a one-dimensional bounded plasma system containing a two-electron temperature plasma: Kinetic model and PIC simulation, Physics of Plasmas 15 (2008) 063501-1-28.
17 T Gyergyek, B Jurčič-Zlobec, M. Čerček and J. Kovačič, Sheath structure in front of an electron emitting electrode immersed in a two-electron temperature plasma: a fluid model and numerical solutions of the Poisson equation, Plasma Sources Sci. Technol. 18 (2009) 035001 (18pp).
18 M. Čerček, T. Gyeryek, B. Fonda, C. Ionita, R. Schrittwieser, Electric and spectroscopic characterization of magnetized hydrogen and helium hot cathode discharge plasma, Journal of plasma and fusion research series, 8 (2009) 381-384.

REMOVAL OF DEPOSITS BY NEUTRAL OXYGEN AND NITROGEN ATOMS

Miran Mozetič, Alenka Vesel, Aleksander Drenik, Tatjana Filipič, Borut Praček, Janez Trtnik, Rok Zaplotnik, Gregor Primc

Jožef Stefan Institute, Jamova 39, SI-1000 Ljubljana, Slovenia
miran.mozetic@ijs.si

1 INTRODUCTION

Although plasma wall interaction in fusion devices is dominated by bombardment by energetic ions, the surface processes in areas that are not in direct contact with the plasma are mainly influenced by neutral species with low kinetic energies. The research activities within our project were focused on surface reactions of atomic species that could have an important effect on the operation of ITER. Until 2013, the list of materials for the ITER divertor included carbon-fibe-composite (CFC) tiles. In fusion devices with carbon-based plasma facing components (PFCs), neutral hydrogen atoms can contribute to chemical erosion of the wall material and the subsequent formation of amorphous hydrogenated carbon (a-C:H) deposits[1]. This is a very efficient mechanism of in-vessel fuel retention and can present serious operational and safety issues. Due to the relatively large surface are of CFC PFCs, and the long plasma pulse duration, the tritium inventory was expected to build up above allowed levels as soon as in one month of operation[2]. To be able to reliably asses the scale of a-C:H production, all contributions should be known, including the erosion by atomic hydrogen. As the erosion rates are strongly influenced by the density of atomic species, measurements of the densities are thus essential.

At the same time, neutral atomic species could be used to mitigate the problem of a-C:H buildup. Atomic oxygen has been shown to be efficient in erosion of carbo-hydrates, which could be efficiently applied to removal of a-C:H[3]. Compared to molecular oxygen, atomic oxygen is significantly more chemically reactive while at the same time, due to the electric neutrality, shares the same ability to penetrate into plasma-shaded areas that are out of reach to glow discharge based cleaning methods.

Following promising results of a full-metal first wall from ASDEX-U and JET, it was decided in 2013 that ITER would start with a full tungsten divertor. However, the full-metal wall results indicate that another surface reaction of neutral atomic species could present as an important safety and operational issue. In order to replace carbon as intrinsic radiative species whose presence reduces the heat load on the PFCs, nitrogen is being seeded into the plasma to promote radiation[4]. Nitrogen then reacts with hydrogen species to form ammonia[5]. With a DT fuel mixture, formation of ammonia would, as in the case of a-C:H, mean a mechanism of in-vessel tritium retention.

Current laboratory results indicate that the formation of ammonia is a surface reaction[6], however, the role of the surface itself is not yet sufficiently well known, and further laboratory experiments are needed to address this issue.

2 WORK PERFORMED IN 2007 - 2013

From the beginning of the project, the main focus have mostly been laboratory experiments of erosion of carbon deposits. However, development and characterisation of atom sources was represented just as strongly. Mostly in the context of support activities of a-C:H removal studies, though sometimes as independent research topics, such as the adaptation of laboratory characterisation methods to use in fusion devices. Sometimes, independent research topics branched out from a-C:H related research, as is the case of our dusty plasma research. While performing experiments to asses dust production during oxidation of a-C:H layers, we also explored a novel method of dusty plasma characterisation which could provide a simple way of identifying the dust population in the plasma volume. As it became apparent that carbon was not likely to be present in the first wall of ITER, our focus has began to shift accordingly, so in 2012, we began our studies of ammonia production in $H_2 – N_2$ plasmas.

While a significant part of our work has been performed in the collaboration with major European fusion research centres, the fuel removal experiments were still performed in laboratory set-ups, with laboratory produced a-C:H samples. However, in 2012, we performed fuel removal studies on samples from a COMPASS graphite limiter tile, and developed an atomic oxygen source for use at the COMPASS tokamak. Beside our laboratory experiments on ammonia production, we have been taking part in ammonia production studies at JET since late 2011.

2.1. Removal of carbon deposits

In the first stages of the project, the carbon deposit removal experiments were performed at the solar facility MESOX of the PROMES – CNRS Laboratory in Font-Romeu, France. This unique experimental facility features a microwave plasma reactor which allows for heating of samples with 6 KW/m^2, obtained by concentrated sunlight from a 12.5 m^2 parabolic mirror. Sample surfaces can thus be heated to temperatures around 2500 K independent of plasma operation. The microwave plasma reactor is capable of achieving densities of neutral atoms up to 10^{22}m^{-3} while maintaining low densities and kinetic energies of ionic species[7-9].

In the initial experiments, samples of bulk graphite were exposed to fluxes of neutral atomic oxygen, produced in the microwave discharge, heated to temperatures of 1200 K. The erosion rates were determined by weight-loss measurements, and were found to be 31 mg/min for graphite discs of 2.5 cm diameter[10].

To study the removal efficiency of atomic oxygen of carbon layers from mixed deposits, mixed W/C deposits were exposed neutral atomic oxygen with the density of $9\cdot10^{21}$m^{-3} and heated up to 850 K. Subsequent analyses by Auger electron spectroscopy depth profiling and X-ray photoelectron spectroscopy revealed that the carbon was efficiently removed in the treatment, however the treatment also resulted in the formation of a surface layer of WO_3[11].

As the formation of oxides is an unwanted side-effect of the cleaning procedure, the possibility of reduction of oxide layers by hydrogen plasma species was studied in the same reactor. Samples of 160 nm thick WO_3 were exposed to atomic hydrogen with the density of $2.5 \cdot 10^{21}/m^3$. After 10 seconds of such treatment, the oxide layers were found to be completely removed from the surface[12-17].

In parallel to the experiments at PROMES CNRS Font-Romeu, removal of a-C:H by neutral species was being researched in our home laboratories at the JSI. These experiments, and some support activities, were performed also in the framework of EFDA ITER Physics Support Tasks: WP09-PWI-02-05/MHEST/BS, WP09-PWI-02-05/MHEST/PS, WP11-PWI-02-02-02/MHEST/BS and WP11-PWI-02-04-01/MHEST/PS.

Samples of laboratory-prepared a-C:H deposits were exposed to different densities of oxygen atoms, from two different plasma sources, namely an inductively coupled plasma system powered by a 1 kW RF generator, and a 300 W MW-powered plasma system. The samples were mounted on a temperature controlled sample holder, heated by a resistive heating element, allowing for temperatures up to 620 K. The erosion process was monitored in-situ with a pyrometer. The erosion rates, shown in Fig. 1, were found to increase exponentially with surface temperature and linearly with atomic oxygen density. The highest measured erosion rate was 50 nm/s[18-21]. The linear dependence on the atomic oxygen density suggests that the saturation regime was not reached and that higher densities would result in even higher erosion rates.

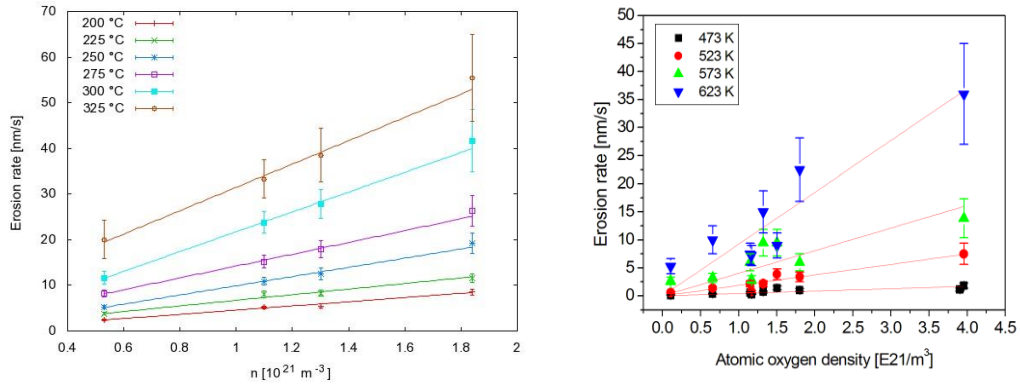

Fig. 1: Erosion rates versus atomic oxygen density, measured in the RF system (left) and in the MW system (right).

As the use of atomic species is associated with the concern of oxidation of plasma facing and structural components and their subsequent degradation, alternative fuel removal methods were researched. Collaborating with CIEMAT, Madrid, we performed research of the scavenger effect, also within the scope of the EFDA ITER Physics Support tasks WP09-PWI-02-02/MHEST/BS, WP09-PWI-02-02/MHEST/PS, WP10-PWI-02-02-04/MHST/BS, WP10-PWI-02-02-04/MHST/PS and WP11-PWI-02-02-01/MHEST/BS. The idea behind the scavenger effect is that nitrogen species react with C_xH_y complexes, form volatile products and thus prevent the formation of a-C:H on the surface. During the initial experiments, it became apparent that NH_3 plasma radicals were also quite effective at removing pre-existing a-C:H deposits. After performing erosion experiments in the plasma volume, we studied erosion in the

afterglow region. While less effective than atomic oxygen, neutral radicals of NH_3 plasma were shown to remove a-C:H deposits without the aid of charge particles, and the maximum achieved erosion rate was 7 nm/s.

These methods of a-C:H removal were applied to samples of the surface from the COMPASS tokamak limiter graphite tile. Unlike laboratory-prepared samples used in our experiments, the COMPASS samples featured a thick B-rich layer, produced during the boronisation of the machine. While the topmost pure a-C:H layers was removed successfully, the underlying B layer was still present despite relatively long treatment times, indicating that the B-C layer is chemically significantly more resistive than pure a-C:H.

2.2. Development and characterisation of remote atom sources

As the laboratory a-C:H removal experiments have shown, the efficiency of removal depends on the density of active species. In order to achieve densities comparable to laboratory conditions in fusion devices, a suitably powerful source of atomic species is needed.

In response to the need for a powerful atom source, we developed a large-scale inductively coupled plasma reactor. The reactor is built around a quartz vacuum chamber with the dimensions of 2 m in length and 20 cm of outer diameter and is powered by a 8 kW radiofrequency generator, operating at the frequency of 27.12 MHz. The densities of oxygen atoms in the reactor vessel exceeded the detection range of our measuring methods (fiber optic catalytic probes), from which we conclude that the degree of dissociation was close to unity. To test the efficiency of the atom source, it was connected to a mid-sized glass-walled vacuum chamber by a 1.1 m long glass tube with two sharp bends, simulating a non-optimal transport of atomic oxygen. The neutral oxygen atom densities in the chamber were measured at $10^{20}m^{-3}$[21-23], depending on the gas flow rate and output power of the RF generator.

In 2012, we started developing an atom source for use at the COMPASS tokamak. This time, we took a different approach, using a smaller source which would be located much closer to the reactor. By eliminating the long transfer path, we managed to achieve similar densities as with the large RF reactor. The atom source is powered by 300 W microwave power supply, coupled to the plasma through a surfatron. The atom source is mounted on a specially fabricated flange for fitting to the COMPASS reactor vessel. Beside the atom source, the flange allows for the simultaneous mounting of two catalytic probes for measuring the atomic oxygen density. While the atom source is yet to be tested at COMPASS, it was tested at our laboratory, connected to a mid-sized stainless steel vacuum chamber, and found to deliver atomic oxygen at densities up to $10^{20}m^{-3}$. However, compared to the large atom source, these high densities were found to be localized in the vicinity of the atom source and were found to decrease by an order of magnitude through the volume of the vacuum chamber.

2.3. Recombination of neutral atoms on carbon-covered surfaces

At a given efficiency of the atom source, the density of neutral atoms in a reactor vessel depends on the rate of loss of atoms on the enclosing surfaces (reactor

vessel walls). Beside erosion, the most important loss mechanism for neutral atomic species is recombination in which neutral atoms form molecules. For a given type of recombination reaction, the reaction rate depends chiefly on the surface material. It is known to vary by orders of magnitude, depending on the surface material. Coverage of the reactor vessel walls by a-C:H could significantly influence the density distribution of the oxygen atoms, and thus the efficiency of the cleaning method.

The recombination probability was determined for oxygen atoms on two different types of amorphous carbon deposits, and fine-grain graphite EK98 with three different grades of surface roughness. The source of oxygen atoms was a laboratory plasma reactor, powered by an inductively coupled radiofrequency generator. The recombination probability was determined using the Smith diffusion method which is based on measuring the spatial profile of atomic species in a closed part of the vessel, whose walls, or a part thereof, are lined with the investigated material.

The measured values for "hard" a-C deposits and "soft" a-C:H deposits was $1.7 \cdot 10^{-3}$ and $0.9 \cdot 10^{-3}$ respectively[19-20, 24]. These are relatively low values, especially compared to PFC and structural materials. Therefore, it is expected that the coverage of the inner vessel walls with carbon deposits would not hinder the delivery of oxygen atoms. The recombination probability of fine-grain graphite ranged from $4 \cdot 10^{-3}$ to $7 \cdot 10^{-3}$ and was found to depend strongly on the surface roughness[20, 25].

2.4. Adaptation of catalytic probes for the environment of a fusion device

In the characterisation of our laboratory plasma sources and reactors, we frequently use catalytic probes. Compared to modern day spectroscopy-based techniques of neutral atom detection, the catalytic probe may seem as a very basic instrument, however they feature very attractive advantages: low cost, ease of construction and use and a relatively simple interpretation of the signal which yields absolute atom densities without the need for a calibration. The catalytic probe relies on the exothermic nature of the recombination of neutral atomic species. As the atoms recombine into molecules on the surface of the catalytic probe tip, the released energy is absorbed by the probe tip. By observing the temperature of the catalytic tip, it is possible to determine the density of neutral atoms in its vicinity. Collaborating with FZJ and CIEMAT, Madrid, we developed adaptations of the catalytic probe for the environment of the fusion device, with the aim of providing measurements of atomic atoms species in areas and/or conditions where spectroscopic methods are not applicable.

In 2006, we developed a catalytic probe design for use in the TEXTOR tokamak. Due to the strong magnetic field in the reactor vessel, the probe design had to rely on non-magnetic materials. The probe tip was made out of gold, and its temperature was measured with a type C thermocouple (tungsten/rhenium). The housing of the probe was compatible with the TEXTOR limiter lock system. The probe was at first used mostly during glow discharge wall conditioning, however the interpretation of the signal proved to be inconclusive because of the issue of background heating. To obtain data about the background (probe housing) temperature, a second thermocouple was fitted to the probe housing. However, in subsequent experiments, the probe was destroyed due to overheating. A modified probe design was developed for mounting in the TEXTOR periscope mirror system in early 2008, however during the plasma

discharges, there was no change in the probe signal, indicating that the densities of H atoms were below the level of detection ($10^{18}m^{-3}$).

2.5. Dusty plasma studies

In the past years, it has become apparent that the production of dust in fusion devices will present serious problems, both from the point of view of operation as well as safety, since dust particles may carry – and release – significant amounts of fuel. While dust may be formed by many processes in a tokamak, it is especially important that further production of dust by fuel-removal methods is avoided.

During cleaning by neutral oxygen atoms, dust would most likely be produced by flaking of the deposit, or by mobilization of hard grains, embedded in the deposit. Collaborating with CNRS LAPLACE, Toulouse, and in the scope of the EFDA ITER Physics Support Tasks WP12-IPH-A03-2-MESCS-BS and WP13-IPH-A03-P2-02-MESCS-BS, we developed a method of deposition of a large-scale model dusty deposit (MDD). The deposition was performed with dusty plasma, created in an electron cyclotron resonance plasma reactor, in pure acetylene. The dust population in the plasma volume consisted of graphite-like carbon grains of various dimensions, some of them visually observable[26]. With this method, the deposition resulted in a reactor-wide coverage with a thin film, composed of a soft a-C:H matrix and hard, graphite like grains. Moreover, the film exhibited poor adhesion to the substrate surface, indicating that it was prone to peeling and cracking. Thus, the deposit met both dust-producing criteria.

The MDD was then exposed to an oxygen discharge in the same reactor. No dust was observed in the plasma volume during the cleaning procedure, nor in the post-mortem inspection of the reactor surface. This indicates that the dust particles were being removed along with the matrix, and that despite the poor adhesion to the surface, the deposit did not crack or peel during cleaning.

During the deposition of the MDD, we monitored the frequency spectrum of the floating potential of the discharge and identified a broad peak at approximately 20 MHz that corresponded with the appearance of dust in the plasma volume. In 2013, we performed additional experiments to further study the behaviour of the peak in frequency spectrum in the floating potential, in the scope of the EFDA ITER Physics Support Task WP13-IPH-A03-P2-02-MESCS-BS. Initial data analysis indicates that the peak could be associated to oscillations of dust particles in the magnetic field[27]. More data analyses are currently underway, and additional experiments are planned in the following years. However, if the broad peak is indeed linked to the oscillations of dust particles, the spectral analysis of the floating potential could provide information about the density and charge-to-mass ratio of the dust particles, and could thus be developed into a simple and effective method of dust detection in magnetized plasmas.

2.6. Ammonia production

In the second half of 2012, we began the laboratory research of ammonia production in collaboration with CIEMAT, Madrid. A dedicated experimental set-up was constructed, consisting of the 1 kW inductively coupled radio frequency plasma reactor and a mass spectrometer used to analyse the reaction products formed in the

plasma. The experimental system allows for the insertion of a temperature-controlled sample holder, to study the role of surface parameters on the ammonia production, however, thus far only the preliminary experiments, without any inserted samples, were performed. The plasma was created in a mixture of N_2 and H_2 with variable ratios, at a constant pressure of 50 Pa. The partial pressure of NH_3 produced in the plasma system was found to vary with nitrogen concentration, with the maximum occurring at 10 vol. % of N_2. In all cases, the partial pressure of NH_3 was two orders of magnitude lower than that of N_2 and H_2. This indicates that on quartz glass, the probability of recombination into N_2 and H_2 for N and H atoms is far more likely than into NH_3 molecules, and that the "background" NH_3 production of the system is relatively low, so it should not cause much difficulties in separating the production due to the inserted sample surfaces.

In addition to laboratory experiments, since late 2011 we have been involved in the research of NH_3 production also in the framework of the C28-30 (Ex. – 1.1.9)[28] and C31-32 (T13-15, M13-27) experimental campaigns at JET. Formation of ammonia was studied under designated Task: T13-15: Application of Residual Gas Analysis for nitrogen seeding and Experiment M13-27: Quantification of N retention and ammonia production in nitrogen seeded discharges, however other experiments with nitrogen seeded discharges also provided data.

The main instruments in these studies were residual gas analysers (RGAs) that are operating in the JET subdivertor region and in the pump ducts. However, while the RGAs have been installed and operating at JET for a while, they were not included in the automatic data acquisition system prior to the start of the experimental campaigns. Thus, a considerable effort was exerted in integrating the existing RGAs into the automatic data acquisition system. While this task is still not yet completely finished, the automated data acquisition is now operational and RGA data is available through the standard methods of data display at JET.

Because JET operates with a D-H gas mixture with a high D concentration, the identification of the ammonia molecule in the mass spectra is difficult as the masses of the molecular fragments overlap with the masses of methane and water fragments. To interpret the RGA data, a method of de-convolution of the mass spectra was developed, based on a least-squares fit of candidate molecules to the recorded mass spectra. The full data analysis is still underway and is expected to be finished in 2015.

3 REFERENCES

1 A. Kirschner, Erosion and Deposition Mechanisms in Fusion Plasmas, Fusion Sci. Technol., 57 (2010), 2T, 277-292.

2 G. Counsell; P. Coad; C. Grisola, et al., Tritium retention in next step devices and the requirements for mitigation and removal techniques, Plasma Phys. Control. Fusion, 48 (2006), 12B, B189-B199.

3 M. Mozetic, Controlled oxidation of organic compounds in oxygen plasma, Vacuum, 71 (2003), 1-2, 237-240.

4 C. Giroud; G. P. Maddison; S. Jachmich, et al., Impact of nitrogen seeding on confinement and power load control of a high-triangularity JET ELMy H-mode plasma with a metal wall, Nuclear Fusion, 53 (2013), 11.

5 D. Neuwirth; V. Rohde; T. Schwarz-Selinger, et al., Formation of ammonia during nitrogen-seeded discharges at ASDEX Upgrade, Plasma Phys. Control. Fusion, 54 (2012), 8.

6 J. H. van Helden; W. Wagemans; G. Yagci, et al., Detailed study of the plasma-activated catalytic generation of ammonia in N-2-H-2 plasmas, J. Appl. Phys.**,** 101 (2007), 4.
7 A. Vesel; A. Drenik; M. Mozetic, et al., Hydrogen atom density in a solar plasma reactor, Vacuum**,** 84 (2010), 7, 969-974.
8 A. Vesel; M. Mozetic; M. Balat-Pichelin, Oxygen atom density in microwave oxygen plasma, Vacuum**,** 81 (2007), 9, 1088-1093.
9 A. Drenik; A. Tomeljak; M. Mozetic, et al., Behaviour of neutral hydrogen atom density in the presence of a sample holder in a plasma reactor, Vacuum**,** 84 (2009), 1, 90-93.
10 R. Zaplotnik; A. Vesel; A. Drenik, et al. In *Interaction of Air Plasma with Graphite at Elevated Temperature*, International Conference Nuclear Energy for New Europe, 14-17 September; 2009.
11 A. Vesel; M. Mozetic; P. Panjan, et al., Etching of carbon-tungsten composite with oxygen plasma, Surface & Coatings Technology**,** 204 (2010), 9-10, 1503-1508.
12 A. Vesel; A. Drenik; R. Zaplotnik, et al., Reduction of thin oxide films on tungsten substrate with highly reactive cold hydrogen plasma, Surface and Interface Analysis**,** 42 (2010), 6-7, 1168-1171.
13 A. Vesel; M. Mozetic; M. Balat-Pichelin, Interaction of highly dissociated low pressure hydrogen plasma with W-C thin film deposits, Thin Solid Films**,** 520 (2012), 7, 2916-2921.
14 A. Vesel; M. Mozetic; P. Panjan, et al., Interaction of hydrogen plasma with carbon-tungsten composite layer, Nuclear Engineering and Design**,** 241 (2011), 4, 1255-1260.
15 A. Vesel; R. Zaplotnik; M. Mozetic, Inductively coupled oxygen plasma in H mode for removal of carbon from mixed a-C:H, W films, Nuclear Engineering and Design**,** 261 (2013), 275-278.
16 Z. Kregar; M. Biscan; S. Milosevic, et al., OPTICAL EMISSION CHARACTERIZATION OF EXTREMELY REACTIVE OXYGEN PLASMA DURING TREATMENT OF GRAPHITE SAMPLES, Materiali in Tehnologije**,** 46 (2012), 1, 25-30.
17 A. Drenik; L. Salamon; R. Zaplotnik, et al., Erosion of amorphous carbon layers in the afterglow of oxygen microwave plasma, Vacuum**,** (2013), 0.
18 A. Drenik; A. Vesel; M. Mozetic, Controlled carbon deposit removal by oxygen radicals, J. Nucl. Mater.**,** 386 (2009), 893-895.
19 A. Drenik; A. Vesel; M. Mozetič, et al., Recombination of atomic oxygen and hydrogen on amorphous carbon, J. Nucl. Mater.**,** 442 (2013), 1–3, Supplement 1, S751-S754.
20 A. Drenik. Verjetnost za heterogeno rekombinacijo vodikovih in kisikovih atomov na površinah fuzijsko relevantnih materialov. Mednarodna podiplomska šola Jožefa Stefana, Ljubljana, 2009.
21 R. Zaplotnik. Optimizacija sklopa med visokofrekvenčnim generatorjem in nizkotlačno plazmo. Mednarodna podiplomska šola Jožefa Stefana, Ljubljana, 2012.
22 R. Zaplotnik; A. Vesel, RADIOFREQUENCY INDUCED PLASMA IN LARGE-SCALE PLASMA REACTOR, Materiali in Tehnologije**,** 45 (2011), 3, 227-231.
23 R. Zaplotnik; A. Vesel; M. Mozetic, A Powerful Remote Source of O Atoms for the Removal of Hydrogenated Carbon Deposits, Journal of Fusion Energy**,** (2013), 1-10.
24 A. Drenik; K. Elersic; M. Modic, et al., Probability of Recombiantion and Oxidation of O Atoms on a-C:H Surface, Materiali in Tehnologije**,** 45 (2011), 3, 281-285.
25 A. Drenik; A. Vesel; A. Kreter, et al., Recombination of hydrogen atoms on fine-grain graphite, Appl. Surf. Sci.**,** 257 (2011), 13, 5820-5825.
26 A. Drenik; P. Yuryev; R. Clergereaux, Trajectories of Dust Particles in Low-Pressure Magnetized Plasma, IEEE Trans. Plasma Sci.**,** 39 (2011), 11, 2734-2735.
27 A. Drenik; P. Yuryev; A. Vesel, et al., Observation of plasma instabilities related to dust particle growth mechanisms in electron cyclotron resonance plasmas, Phys. Plasmas**,** 20 (2013), 10.
28 M. Oberkofler; D. Douai; S. Brezinsek, et al., First nitrogen-seeding experiments in JET with the ITER-like Wall, J. Nucl. Mater.**,** (2013), 0.

APPLICATION OF ION BEAM ANALYTICAL METHODS TO THE STUDIES OF PLASMA-WALL INTERACTION IN TOKAMAKS (IBAF)

Primož Pelicon, Iztok Čadež, Zdravko Rupnik, Primož Vavpetič, Sabina Markelj, Matjaž Kavčič, Zvone Grabnar, Mirko Ribič, Anže Založnik

Department for Low and Medium Energy Physics,
Jožef Stefan Institute, Jamova cesta 39, P.O.B. 3000, SI-1000 Ljubljana
e-mail: Primoz.Pelicon@ijs.si

1 INTRODUCTION

The goal of the Project was two-fold: to continuously upgrade the Ion Beam Analytical (IBA) methods available at 2MV tandem accelerator at Jožef Stefan Institute (JSI) and to perform measurements on specific samples of interest to the EU fusion program. During this continuous process we have developed and then systematically used ^{7}Li ion beam-Elastic Recoil Detection Analyses (Li-ERDA) for H and D depth profiling in fusion relevant material and also Nuclear Reaction Analysis (NRA) with ^{3}He ion beam for deuterium depth profiling by D(^{3}He,p)^{4}He nuclear reaction. NRA was first used at the micro-beam experimental beam-line (probing beam diameter of the order of 5 μm) and was later implemented also in the ERDA/RBS experimental chamber with broad beam (beam diameter of 1 or 2 mm) where real time in situ studies of absorption/desorption of D were performed besides standard static measurements. Particle Induced X-ray Emission (PIXE) and/or Rutherford Back Scattering (RBS) are used in parallel to extract auxiliary information on the sample when needed.

2 WORK PERFORMED IN 2007 - 2013

After an overview of the facility development the individual actions within the Project are describe in short following the time order when they were performed. More detailed information can be found in respective publications or annual reports (quoted as [ARyear] in the text). A substantial user of the developed IBA methods was another project within our Association, 1.4.1. »Processes with neutral hydrogen atoms and molecules« and results of this Project are presented in its own Report.

2.1. Facility upgrading

The overall layout of the current status (end of 2013) of 2MV tandem accelerator (HVEE Tandetron) at Jožef Stefan Institute (JSI) is shown in fig. 1 [1]. All fusion development related studies were performed on micro-beam and ERDA/RBS

experimental stations at +10° and -10° beam lines. The following main upgrades of the installation largely also motivated by enhancing capabilities for fusion material studies are the following:

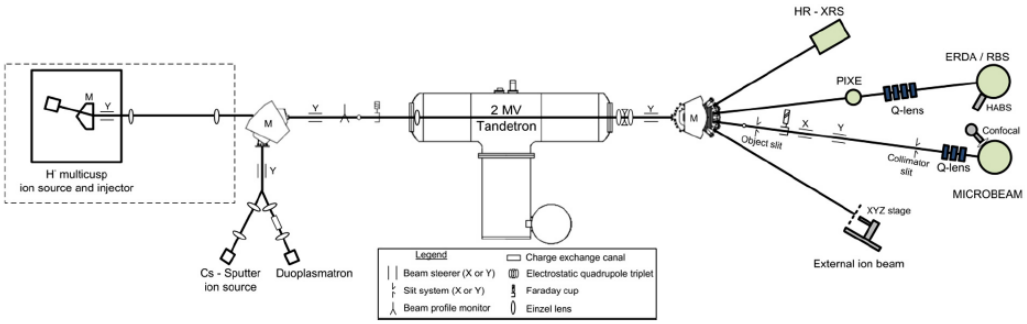

Figure 1: Schematic overview of the accelerator facility at Jožef Stefan Institute [1].

Ion sources: Two ion sources were initially available at the injection side of the accelerator: duoplasmatron source for H and He ions and sputtering ion source for majority of other ion beams, in our case mainly ^{7}Li. Having single ion source for both H and He had a dissuasive effect on the application of He beams because most other applications on accelerators are routinely using protons. Therefore, in order to configure ion source for He meant that p-beam is not available for substantial time. The major improvement was achieved when alternative, high intensity multi cusp H^- source was acquired in 2011 and made fully operational in 2012. This allowed duoplasmatron ion source to be permanently configured for He beam. Very convenient gas handling system was also conceived and realised so that ^{4}He can be used for beam tuning and only for NRA measurements gas can be switched to ^{3}He or ^{4}He-^{3}He mixture in order to provide ^{3}He ion beam. This drastically reduced consumption of ^{3}He gas and altogether made D depth profiling by NRA to be almost on stand-by.

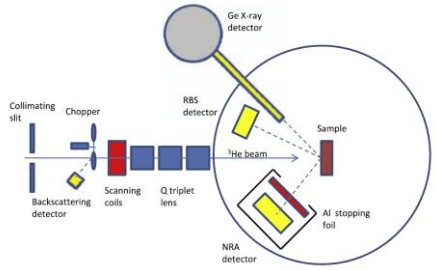

Figure 2: Detailed schematics of micro-beam experimental station equipped with micro-NRA detection setup and auxiliary detectors [pel2011].

Li exchange channel: This element is needed in ion injection line for He beam and during reported period we had to purchase a new one due to the failure of original device. This was also of high importance for availability of NRA to be used as design of the new Li exchange channel was much improved and requires less frequent maintenance. This improvement of the beam line was supported by EFDA PWI task PWI-08-TA-06/MHEST/PS/01.

Micro-beam experimental station (fig. 2) [2], [3]: This is the most sophisticated experimental station and is constantly upgraded. The probing beam is here focused to micrometre size by means of a powerful triplet magnetic quadrupole lens. Various detectors (for PIXE, RBS, NRA, SE,…) are located in the chamber what allows generation of 2D elemental composition maps of studied sample by scanning beam over the sample while simultaneously detecting the signal. The analysing area of about 2mm x 2mm is accessible by beam sweeping without displacing sample. Appropriate list-mode data acquisition system has been developed which allows saving the complete experimental data (individual events) for later off-line analysis.

Exposure dose monitors: For absolute measurements by IBA methods one needs precise measurement of the ion dose on the sample. For this purpose we are using and constantly upgrading rotating beam chopper on micro-beam and mesh integrator on ERDA/RBS/NRA station.

^{3}He NRA: Development and application of Nuclear Reaction Analysis (NRA) with ^{3}He ion beam for deuterium depth profiling using D(^{3}He,p)^{4}He nuclear reaction was a permanent activity on the Project during reported period. Besides providing ion beam it also required introduction of new detectors, calibration and data analyses.

Calibration: To calibrate ERDA method for the quantified H analysis a polyamide foil was used [4], [5], but for calibrating D analyses by ERDA and NRA a amorphous deuterated carbon films (a-C:D) produced, quantified and provided by Thomas Schwartz-Selinger, Max-Planck-Institut für Plasmaphysik, Garching, were used as a standard.

Material damaging by high energy ions: The upgrading of the beam line for NRA/RBS/ERDA experimental chamber was initiated in order to enable homogeneous sample irradiation by high energy ions to allow studies of synergic effects of tungsten or helium ion irradiation on the hydrogen retention in tungsten foreseen for the next period.

2.2. D concentrations in carbon fibre composites exposed to a deuterium plasma

Three carbon-based materials – the carbon fibre composite (CFC) NB31 from Snecma, the CFC DMS780 from Dunlop and fine-grain graphite Ringsdorff EK98 – were mounted in the form of stripes on a roof-like test limiter in the TEXTOR tokamak at FZJ. They were exposed to the deuterium rich plasma in the erosion-dominated zone of the scrape-off layer under well-defined conditions. By a post mortem analysis using NRA at JSI the integral D-yield from the three samples was measured using 2 MeV $^3He^+$ broad probing beam. This energy assured that integral signal corresponded to the total depth of about 8 μm what is the expected depth range for most of absorbed deuterium. It was shown that the similar amount of D was present in CFC NB31 and fine-grain EK98 and about 10% lower in CFC DMS780 [6].

The sample of CFC NB31 from this experiment was later cleaved in order to check for the possible long-range deuterium penetration in the material. An area of the cleavage, 0.5x0.5 mm^2, was analysed by μ-NRA with a raster step of 7.8 μm. Energy of ^{3}He beam was set to 0.65 MeV to enhance sensitivity to surface D. Deuterium was detected as deep as 80 micrometres below the exposed surface. The 2-dimensional map showed a pronounced inhomogeneity of the D distribution in both the depth and the lateral directions. It was attributed to the non-uniformly porous structure of the CFC

material, with higher D amounts accumulated inside the inner cavities. The depth profile, summed up over 0.5 mm along the surface, showed the decay of the amount of D with a characteristic length of about 30–40 μm [6]. This work was supported by Preferential Support project WP11-PWI-01-01-01.

2.3. In situ Li-ERDA study of hydrogen permeation

A pilot study of hydrogen permeation through a membrane using Li-ERDA method was performed. A 100 μm pure palladium membrane was used in this study. Successive energy spectra of recoiled hydrogen (simultaneously, both isotopes H and D) ejected by 4.2 MeV ^{7}Li were recorded in order to follow permeation *in situ*. The membrane was exposed to H_2 or D_2 gas at 1bar driving pressure. Time evolution of concentration depth profiles of H and D while membrane temperature was varied were obtained. Comparing the permeation properties of the two isotopes we observed that stable conditions were achieved faster in the case of H_2 than in the case of D_2. Temperature where permeation becomes diffusion limited was found to be around 380 K and 420 K in the case of D and H, respectively [7].

2.4. Hydrogen concentration profiles in the carbon-based PVD thin films by RBS/Li-ERDA

Li-ERDA together with RBS was used for the characterization of the thin layers of amorphous hydrogenated carbon through collaboration with Department for Thin Films and Surface, JSI, Project »Synthesis and characterization of hydrogenated carbon deposits« [8], [9]. We performed analysis of C:H thin films produced by CVD process and carbon-based a-C:H thin films produced by sputtering of the graphite target in argon atmosphere. In addition to argon, several other gases can be used, such as Ar+H_2 mixture or Ar+C_2H_2 mixture. It could be anticipated, that films produced without hydrogen or hydrogen-containing gas are hydrogen-free. However, the ERDA results revealed, that even in this case the concentration of hydrogen is no negligible but around 20 at. %. The source of hydrogen is in residual atmosphere which contains mainly water vapour. Hydrogen concentration in films prepared in presence of H_2 or C_2H_2 was around 40 %. A brief conclusion was that hydrogen concentration in PVD carbon-based films is always in the range 20-40 at. %. Sample with interlaced W and Cr layer was also studied [AR2008]. Li-ERDA was also used for characterization of hydrogen content in the amorphous hydrogenated carbon layers produce by linear anode layer discharge with acetylene as a working gas. It was shown that hydrogen content did not vary with discharge voltage, being between 21.2% and 23.5% [8].

2.5. Surface lateral distribution of the retained deuterium and retained deuterium distribution in the castellation gaps - CFC tiles exposed to the deuterium plasma in DITS experiment

We did some post mortem analyses of deuterium in selected tile samples through the DITS project (Deuterium Inventory in Tore Supra). Fresh CFC tiles had been exposed to deuterium under well recorded plasma conditions and after

experimental campaign samples were distributed to various laboratories for ex situ analyses. The JSI measurements were performed at micro-beam station of our tandem accelerator. For the sample characterisation, four detection systems were used simultaneously: NRA PIPS detector, RBS PIPS detector, HPGe X-ray detector for ^{3}He-induced X-ray emission (3HIXE) and PIPS detector for detection of ions scattered from beam chopper providing beam dose normalisation. 2D elemental maps of D, Cr, Fe, Ni deposited in the CFC sample were obtained.

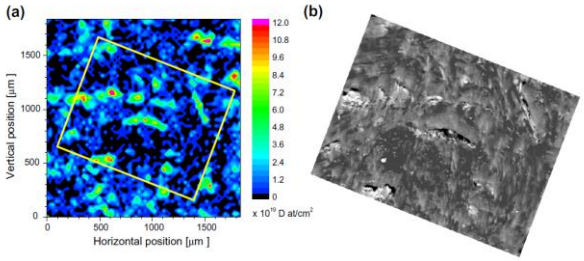

Figure 3: (a) Quantitative deuterium distribution on the front exposed surface of a Tore Supra tile. (b) A SEM picture of the thin deposit zone, indicated by a rectangular frame in Fig. 3a. Voids in the surface correlate with the areas of high deuterium concentration [3].

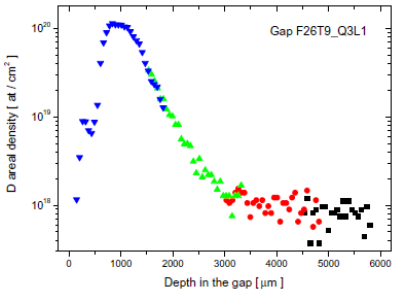

Figure 4: P Deuterium distribution measured by micro-NRA along the depth axis of the castellation gap located in the erosion zone (Tore Supra DITS experiment; depth zero – gap position close to the exposed surface, depth 6000μm - bottom of the gap [3].

Enhanced local deuterium concentration was correlated to the observed structures in the material (fig. 3). To evaluating the total D-retention in tokamak chamber it is important to estimate the amount of fuel in the castellation gaps of the tiles as well. We performed a detailed survey of the gaps oriented differently with respect to the magnetic field by making series of 2D micro-beam scans. On this way the whole 6 mm gap depth was mapped. We showed that earlier in literature reported increase of deuterium concentration at the bottom of the gap was instrumental artefact due to the beam size in the conventional NRA. The deuterium concentration in the deep parts of the castellation was shown to be approximately two orders of magnitude lower than in the area close to the exposed surface (fig. 4) [AR2009], [10], [11].

2.6. Deuterium depth profiles in mixed layers and multilayers and temperature dependence of deuterium retention in mixed thin layers relevant for ITER operation

By the end of the reported period work was dedicated to the study of deuterium retention in mixed material layers relevant to ITER. All mixed material samples were provided by MEdC. This work was supported by EFDA through preferentially supported task »Analyses of the deuterium trapping in mixed materials«, WP13-IPH-A01-P3-01/MESCS/PS. By this work we did first characterization of Be containing samples in our laboratory.

We have developed experimental procedures for studies of deuterium release from mixed material samples using *in situ* NRA-thermal desorption technique. On this way we have studied release of deuterium from layers with co-deposited D: C:W(D)/Si, C:W:Al(D)/Si, Be(D)/C, Be(D)/Si in order to evaluate the influence of layer

composition to deuterium retention. In addition the D-uptake by initially D-free mixed layers (C:W/C, Al:W/Si, Al:W(N_2)/Si, Be:W(N_2)/Si) was studied by *in situ* NRA during layer exposure to D-atom beam and subsequent thermal desorption. Pronounced influence of nitrogen impurity on D-uptake was observed [AR2013], [12].

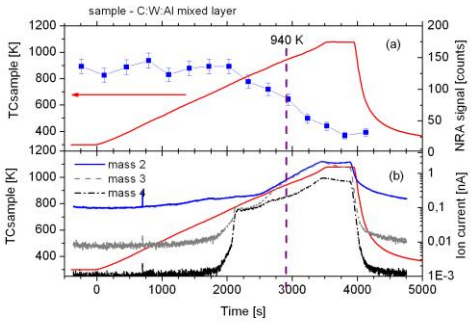

Figure 5: Heating of the C:W:Al mixed layer. a) Integrated NRA signal at 2.5 MeV ^{3}He beam energy and b) ion signal of masses 2, 3 and 4 are shown as a function of time. On both graphs sample temperature is also shown, heating rate 13K/min [12].

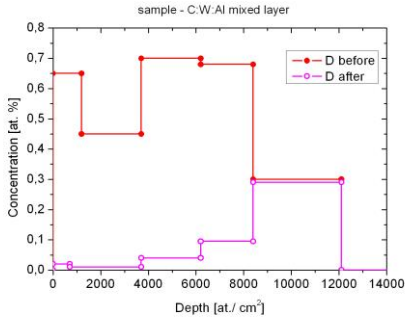

Figure 6: Deuterium depth profile measured by NRA in C:W:Al mixed layer before and after the linear heating[12] .

An example of such study is shown in figures 5 and 6 [12]. Mass spectrum in the background vacuum is also followed during thermal desorption stage by a quadrupole residual gas analyser.

An interesting effect was observed by monitoring hydrogen release from hydrogenated carbon deposit on tungsten in one specific experiment [13]. Abrupt desorption of hydrogen atoms was detected at the temperature where carbide formation occur what might be more general process in mixed material layers.

2.7. Application of Micro-NRA for the analysis of deuterium in the deuterated flakes/dust

NRA method based on the D(^{3}He,p)^{4}He nuclear reaction was at micro-beam experimental station was also applied for study of deuterium content in small particles and flakes. Deuterium concentration on tungsten micro-particles deuterated in plasma reactor Casimir at CEA was measured using 4.5 MeV incident beam energy. Image of the tungsten distribution in studied particle is obtained by detecting characteristic W Lα X-rays induced by ^{3}He ion impact – (3HIXE technique). Such image provided information on overall shape of the studied sample which was dominantly W. Due to the extremely low D content only integral NRA spectrum could be recorded simultaneously with 3HIXE image recording and total D content on the particle was quantified by comparison to the scan of the standard a-C:D target [AR2013]. Some activity during the work on the project was also devoted to the studies of nuclear reactions pertinent to our activities [14].

3 CONCLUSIONS AND OUTLOOK FOR FURTHER WORK

In previous years we have done substantial progress on development of experimental techniques based on IBA methods enabling efficient studies of material properties related to fusion research. Particularly important qualitative breakthrough was done in 2012 when system upgrades provided highly efficient use of ^{3}He beam for NRA, reducing the associated costs connected to the price of ^{3}He gas to sustainable level. This is the reason that in 2013 a high fraction of total accelerator beam-time was dedicated to the fusion-related studies. These were mainly performed on the broad beam NRA/RBS/ERDA experimental station also described in report on the project 1.4.1. What concerns new development of the accelerator facility for future studies, we have undertaken modification of the broad-beam beam-line in order to allow dual beam irradiation of the sample. This is needed for studies of the influence of ion induced damage of materials and hydrogenic retention.

We plan to extend *in situ* NRA D-retention studies of deuterium thermal desorption and deuterium uptake methods applied for the first time in 2013. Extension of such studies on isotope exchange is very promising. Systematic studies on standardized sets of mixed material layers relevant for fusion experiments deposited with or without presence of seeding impurities are planned to be performed in 2014. This work will be continued within the new framework of EUROfusion program.

4 REFERENCES

1 P. Pelicon, N. C. Podaru, P. Vavpetič, L. Jeromel, N. Ogrinc, S. Ondracka, A. Gottdang and D.J.M. Mous, A high brightness proton injector for the Tandetron accelerator at Jožef Stefan Institute, Nuclear Instruments and Methods in Physics Research B, (2014) DOI: 10.1016/j.nimb.2014.02.067 in press

2 P. Pelicon, J. Simčič, M. Jakšić, Z. Medunić, F. Naab and F. D. McDaniel, Spherical chamber – effective solution for multipurpose nuclear microprobe, Nucl. Instrum. Methods Phys. Res., Sect. B 231 (2005) 53–59.

3 P. Pelicon, P. Vavpetič, N. Grlj, I. Čadež, S. Markelj, S. Brezinsek, A. Kreter, T. Dittmar, E. Tsitrone, B. Pegourie, P. Languille, M. Rubel, T. Schwarz-Selinger, Fuel retention study in fusion reactor walls by micro-NRA deuterium mapping, Nucl.Instr.Meth. B 269 (2011) 2317-2321.

4 P. Pelicon, A. Razpet, S. Markelj, I. Čadež, M. Budnar, Elastic recoil detection analysis of hydrogen with ^{7}Li ions using a polyimide foil as a thick hydrogen reference, Nuclear Instruments and Methods in Physics Research B 227 (2005) 591–596.

5 S. Markelj, I. Čadež, P. Pelicon, Z. Rupnik, Studying processes of hydrogen interaction with metallic surfaces in situ and in real-time by ERDA, Nuclear Instruments and Methods in Physics Research B 259 (2007) 989–996. (also for Project 1.4.1.)

6 A. Kreter, S. Brezinsek, M. Rubel, B. Emmoth, M. Freisinger, P. Pelicon, V. Philipps, O. Schmitz, P. Sundelin, G. Sergienko and TEXTOR team, Journal of Physics: Conf. Series 100 (2008) 062024.

7 S. Markelj, P. Pelicon, J. Simčič, Z. Rupnik, I. Čadež, Studying permeation of hydrogen (H and D) through Palladium membrane dynamically with ERDA method, Nuclear Instruments and Methods in Physics Research B 261 (2007) 498–503.

8 M. Kahn, S. Paskvale, M. Čekada, T. Schöberl, W. Waldhauser, C. Mitterer, P. Pelicon, E. Brandstätter, The relationship between structure and mechanical properties of hydrogenated amorphous carbon films, Diamond and Related Materials 19 (2010), 1245.

9 M. Čekada, M. Kahn, P. Pelicon, Z. Siketić, I. Bogdanović Radović, W. Waldhauser, S.Paskvale, Analysis of nitrogen-doped ion-beam-deposited hydrogenated diamond-like

carbon films using ERDA/RBS, TOF-ERDA and Raman spectroscopy, Surface and Coatings Technology 211 (2012) 72 - 75.

10 T. Dittmar, E. Tsitrone, B. Pégourié, I. Čadež, P. Pelicon, E. Gauthier, P. Languille, J. Likonen, A. Litnovsky, S. Markelj, C. Martin, M. Mayer, J.-Y. Pascal, C. Pardanaud, V. Philipps, J. Roth, P. Roubin, P. Vavpetič, Deuterium Inventory in Tore Supra (DITS): 2nd post-mortem analysis campaign and fuel retention in the gaps, Journal of Nuclear Materials 415 (2011) S757.

11 B. Pégourié, S. Panayotis, P. Languille, C. Martin, T. Dittmar, l, E. Gauthier, J.-C. Hatchressian, J.-Y. Pascal, P. Roubin, R. Ruffe, E. Tsitrone, S. Vartanian, H. Wang, m, A. Beauté, J. Bouvet, C. Brosset, J. Bucalossi, M. Cabié, E. Caprin, X. Courtois, R. Dachicourt, E. Delchambre, C. Dominici, D. Douai, A. Ekedahl, J.P. Gunn, A. Hakola, W. Jacob, H. Khodja, J. Likonen, F. Linez, A. Litnovsky, Y. Marandet, S. Markelj, A. Martinez, M. Mayer, O. Meyer, P. Monier-Garbet, P. Moreau, V. Negrier, P. Oddon, C. Pardanaud, B. Pasquet, P. Pelicon, P. Petersson, V. Philipps, G. Possnert, D. Reiter, J. Roth, I. Roure, M. Rubel, F. Saint-Laurent, F. Samaille, P. Vavpetič, Deuterium inventory in Tore Supra: Coupled carbon–deuterium balance, J. Nucl. Mater., 438 (2013) S120-S125.

12 S. Markelj, I. Čadež, P. Pelicon, P. Vavpetič, C. Porosnicu, C. Lungu, Deuterium Thermal Desorption From Mixed Layers Relevant for ITER, 22nd International Conference Nuclear Energy for New Europe - NENE 2013, Bled, September 9-12. Eds. L. Cizelj, M. Leskovar, M. Uršič, Proceedings. Ljubljana: Nuclear Society of Slovenia (2013) paper 1405, 9pages.

13 I. Čadež and S. Markelj, Hydrogen Desorption from Hydrogenated Carbon on Tungsten, 21st International Conference Nuclear Energy for New Europe - NENE 2012, Ljubljana, September 5-7. Eds. T. Žagar and S. Fürst, Proceedings. Ljubljana: Nuclear Society of Slovenia (2012) paper 1113, 7pages.

14 M. Lipoglavšek, I. Čadež, S. Markelj, P. Pelicon, P. Vavpetič, Electron screening in the $^{1}H(^{7}Li,\alpha)^{4}He$ reaction. The European physical journal. A, Hadrons and nuclei, 44 (2010) 71-75

PERMEATION AND OUTGASSING MEASUREMENTS OF BE, W AND MIXED BE/W LAYERS DEPOSITED ON EUROFER BY VARIOUS METHODS

Vincenc Nemanič, Marko Žumer, Bojan Zajec

Jožef Stefan Institute, Jamova 39, 1000 Ljubljana, Slovenia
e-mail: *vincenc.nemanic@ijs.si*

1 INTRODUCTION

Beryllium and tungsten will be used for the first wall of ITER. Thermal load and ion impact will induce tritium retention in mixed deposits of tungsten and beryllium. So far, as follows from a literature survey, a few reported data on investigation of such mixed layers exist, [1, 2]. Mixed materials were also investigated as Be films on W substrate, but they have rarely been investigated as mixed layers as may be formed in ITER during the operation. The missing knowledge of their possible interaction with hydrogen isotopes is thus searched by using various experimental techniques.

Hydrogen in metals represents a complex two element interaction system as the lattice may have any form extending from a well-structured mono-crystal to nano-crystalline metal. Accordingly, hydrogen (H/D/T) may occupy a single-energy-type interstitial site of the mono-crystal or any type of defects which represent sites for a single H atom with different binding energy. Beside single occupation interstitial or defect-induced sites, metal vacancies may be present in the disordered lattice. Each may be occupied by several H atoms and the term super-abundant vacancy (SAV) was launched in theory. Their role influencing metal properties has also been calculated recently. Grouping of vacancies into clusters was also predicted which further complicates experimental evidence of SAV. In general, sophisticated experimental techniques are needed to determine contribution of defects and SAV on observed hydrogen mobility. Classic permeability measurement of gaseous hydrogen through bulk specimens is a suitable complementary method to determine its mobility. Unfortunately, macroscopic sizes and thicknesses of samples with low hydrogen diffusivity result in extremely low permeability which is beyond the detection limit of present day experimental technique. The same technique using a “duplex membrane” simplifies the experiments as thin W or Be/W films with desired micro-structure can be prepared on a highly permeable substrate much easier than bulk W samples [3,4]. Fortunately, Be/W deposits will be formed as thin and disordered layers which makes our data even more relevant, initially mainly for JET as well as later on also for ITER. In exceptional cases, stable tungsten beryllides Be_2W, $Be_{12}W$, $Be_{22}W$ can be formed, but generally non-stoichiometric alloy is supposed to be formed in fusion reactors.

2 EXPERIMENTS PERFORMED IN 2007 - 2013

It the period 2007 - 2013, precise hydrogen permeability measurements combined with long term outgassing rate measurements were performed starting with building and testing the UHV setup for extremely low permeation rate measurements, [5]. Highly impermeable ceramic films with the lowest reported permeability were tested as a good starting platform for evaluation of Be, W and Be/W films, [6, 7]. All films were deposited in various laboratories participating in EURATOM. We have formal and non-formal cooperation with these groups enabled a fruitful exchange of knowledge. The first experiments were with pure Be films deposited by thermionic vacuum arc (TVA) in the laboratory of dr. Cristian Lungu, at National Institute for Laser, Plasma and Radiation Physics, NILPRP, Romania, were tested. The same experimental approach continued with pure tungsten deposited by four different methods: a) pulsed laser deposition (PLD) method by M. Passoni at Politechnico di Milano, Italy b) by combined magnetron sputtering and ion implantation (CMSII) by dr. Cristian Ruset (NILPRP), Romania c) by TVA dr. Cristian Lungu and d) by magnetron sputtering in two different laboratories (S Deambrosis, Institute for Energetics and Interphases (IENI) Padova and E. Vassalo, Instituto di Fisica del Plasma, Milano). Each deposition method gives a specific film microstructure and morphology which was characterized by various techniques, AFM, SEM, XPS and XRD. Most of experimental data points for permeation measurements which lasted at least 24 hours were obtained at 400 °C. Magnetron sputtered W films were found to be transparent for hydrogen due to nano-channels protruded through the film from the substrate.

Be/W films were studied in 2012 and 2013, all deposited by TVA by dr. Cristian Lungu.

The correlation between permeation flux and film morphology was searched. Film surface was characterized by various surface sensitive techniques SEM, XPS, XRD, AFM while the XRD was applied for determination of average grain size. Our investigation included study of 4 samples with TVA deposited pure W films and 8 samples with Be/W films. As the complex and mutual dependence of film nanostructure and additionally beryllium high chemical activity on overall observed permeation properties, all samples were deposited with the same thickness of 8 μm and in atomic ratio Be:W = 3:1.

2.1. Experimental

Substrate preparation and film deposition procedures

The base substrate material on which we applied the coating was the reduced-activation tempered martensitic steel Eurofer with the chemical composition (wt. %): 0.11 C, 8.7 Cr, 1.0 W, 0.10 Ta, 0.19 V, 0.44 Mn and 0.004 S, balance Fe. The steel was supplied in the form of a 100-mm diameter bar by Forschungszentrum Karlsruhe GmbH, Karlsruhe, Germany, in the normalized plus tempered condition, i.e., 980 °C/110 min plus tempering at 740 °C/220 min/air-cooled. The reason for selecting this special grade of steel are: a) it is well characterized in the last few year for interaction with hydrogen and b) it has extremely high permeability for hydrogen at elevated

temperature and c) good mechanical properties which enabled simple machining as smooth substrates had to be prepared for this study.

Permeation / outgassing rate measurements

Membranes were sealed in the permeation cell by two Au 0.6 mm thick O-rings. The resulting hydrogen exposed area was 8.4 cm^2. The film was oriented into the upstream chamber. The setup is assembled from all-metal UHV components applying gas accumulation technique described elsewhere [3]. Accumulated gases were analyzed by the QMS in the separate chamber each time just before they were pumped out. Hydrogen represented the main species with traces of CO and CO_2. In addition, transients of hydrogen kinetics at the downstream side after upstream pressure changes were followed directly by the QMS.

For all measuring campaigns with coated membranes, the time to reach a steady permeation flux was substantially longer than 6.5 s, which is the characteristic time of bare membranes [3]. For most experiments, the hydrogen permeation flux was recorded for 24 h while keeping the upstream pressure at 1 bar and 400 °C when films had been stabilized. After hydrogen removal, the membrane was pumped on both sides for 1 h, the valves were closed and pressure dependence of the permeation flux was recorded.

The response of the permeation rate to the step change of the upstream pressure may give some additional data about the mechanism of hydrogen transport through the film. This information is important since the formalism to apply experimental data assumes that the diffusion is the rate limiting process of the permeation.

W film deposition

The W films were prepared by means of PLD, using a nanosecond laser (λ =532 nm, pulse duration 5–7 ns, repetition rate 10 Hz), focused on a 2 inch Tungsten target (sintered with purity 99.9%). Films have been deposited in vacuum and in presence of a He atmosphere (pressure 60 Pa, 99.9995 grade, less than 1 ppm of hydrogen.

The next W film type was coated at National Institute for Laser, Plasma and Radiation Physics (NILPRP) by CMSII technique. This technique involves simultaneous magnetron sputtering and high energy ion bombardment. In the deposition process, three low pressure electrical discharges are superposed. Typical parameters for the high voltage pulse discharge are: U=30-50 kV, t=20 ms, f=25 Hz. The DC bias up to -900 V is applied between pulses. Periodical ion bombardment increases the surface mobility of the deposited atoms resulting in a high densification of the coating. An extremely dense and pore free nano-structure is produced by this technique.

Most of other films, both pure W and Be/W were prepared by means of the thermionic vacuum arc TVA method. The anode tungsten target is heated by a focused electron gun, which leads to the tungsten evaporation and succeeding ionization. The ionization initiates plasma discharge in pure tungsten vapors, and the tungsten deposited layer is then formed on the substrate, located at the opposite side of the anode target. The chosen deposition parameters were: anode – cathode voltage: 1400V, anode – cathode current: 1.90 A, substrate temperature: 400 ^oC, and substrate bias related to the ground; -400 V. For deposition of Be/W films additional Be source was running in parallel.

2.2. Results

Results of XPS, AFM and SEM on pure W and pure Be surface

Morphology of the W-coating deposited on the Eurofer substrate, characterized by FM and SEM show similar features. Corresponding sample image of W film deposited by CMSII is shown in Figure 1. The surface is uniformly composed of small plate-like crystallites of triangular shapes. The SEM of cross section of nano-porous W film deposited by PLD is presented in Figure 2. Nanoporosity and vacancy abundance resulted in the PRF which was 1000 higher compared to CMSII films.

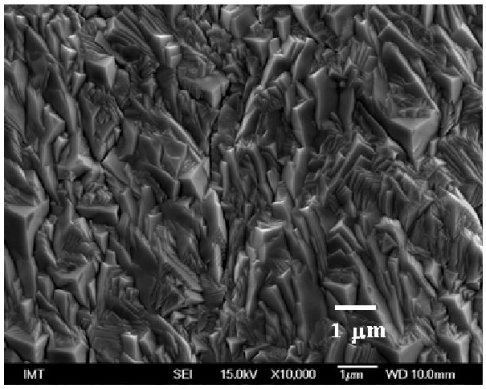

Figure. 1: SEM image of the surface of W layer deposited on the Eurofer substrate by CMSII

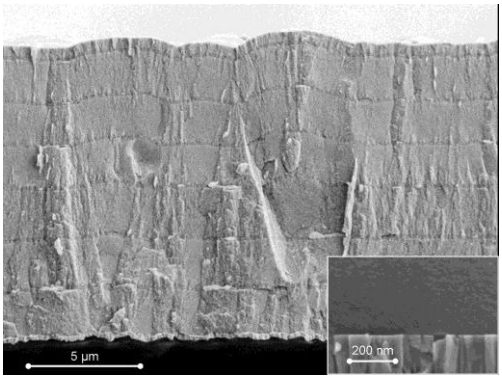

Figure. 2: SEM cross section of an amorphous-like 10 µm thick film deposited by PLD.

Results on permeation measurements on pure Be and pure W films

Detailed report on W films deposited by PLD was reported in Ref. 8. Their main characteristics is very low permeability since the initial permeation reduction factor (PRF) exceeded value of 1000. Besides this unexpected property, extremely high content of trapped hydrogen, absorbed during the deposition in He atmosphere. Its content was as high as H/W ~0.1. Results on W films deposited by CMSII technique have been published in Ref. 3. These films are well permeable due to permeation assisted by shallow traps. Results on permeation of H through Be films were reported in Ref.9 and Ref.10. They reveal the importance of reactivity of Be with impurities in hydrogen. As BeO may be formed during the permeation of purified hydrogen, data are very difficult to be attributed to bulk Be versus surface BeO. Identical bare 0.5 mm thick Eurofer membranes applied as substrates in next experiments have been formerly investigated since a good reference for evaluation of W, Be and Be/W films was needed. The high diffusivity and permeability of clean bare membranes is manifested in fast response to hydrogen exposure; high steady flux ~1.12×10^{-5} mol H_2/m^2s is established at 400 °C at 1 bar. This value allows evaluation of the PRF of all coated samples. Time–lag for bare substrate was ≈6.4 s. Both these data were recorded after the sealed membrane had been outgassing for some hours at 400 °C.

Results on permeation measurements on Be/W films

Be/W films with stated composition (75 at.% Be, 25 at.% W) exhibit even less predictable behavior after hydrogen exposure compared to pure W films deposited by TVA method. The actual nanostructure of the film is always influenced by slight modification of true deposition parameters which are not fully controlled. An important parameter was substrate temperature which influenced coalescence of grain. Unless the temperature was increased to 400 °C, Be/W films, films were not dense enough to enable measurements. Another problem was high Be affinity to water as it could result in BeO formation during deposition as well as during the permeation rate measurements. We realized that hydrogen purity is extremely important in experiments with Be, but a few ppb level purity, trusted to be maintained in present experiments, might not be enough [6,7]. It seems that water desorption from hot surfaces of the cell contribute the uncontrolled conditions. Moreover, the role of BeO layer grown on pure Be has not been reported to influence hydrogen permeability, except our report [7]. Even its bulk solubility and diffusivity for hydrogen is lower than in Be and it may not suppress the permeation flux as it may have porous structure like FeO which also does not influence permeation rate through Fe. In 2013 better controlled experimental parameters enabled us to obtain more reliable and stable values in permeation rate measurements. At present, we have no explanation for the difference on two simultaneously deposited samples, Sample 10 and Sample 11. They both were very stable, but the difference is almost tenfold. Our prime goal, to distinguish between two parameters: film nanostructure and Be/W ratio on permeability and hydrogen retention has not been realized completely.

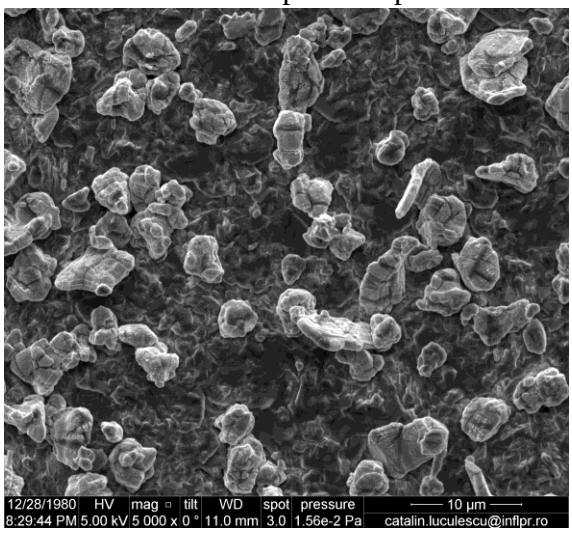

Figure 3: Be/W surface exhibits different morphology than pure W in Fig. 2. The contrast on grains is related to poor sample conductivity and does not express different grain composition.

3 CONCLUSIONS

Knowledge of the properties of hydrogen diffusion, permeability, solubility and trapping in pure Be and W and Be/W alloys is rather incomplete today and our research contributes a noticeable complementary part. Since both pure W and Be films were rarely measured in relation to fusion, we have an advantage that we have our own experimental data on both material in form of films relevant to ITER. We may claim that most of our results could be used for better forecast of tritium retention of films formed inside future fusion reactors.

In the first stage of the project, we achieved extremely high sensitivity of new setup both for outgassing as well as for permeation rate. Test were done on highly

impermeable ceramic films on Eurofer. Such films made of TiAlN and SiN may be relevant as tritium permeation barriers for DEMO as achieved permeation reductuion factor was among the lowest reported in the literature.

In all metal films, made of Be, W and Be/W alloys with different Be/W ratio, it was important to determine parameters that govern the permeation process at known film structure and composition. This enables understanding of the influence of material morphology, structure and high temperature loads on H/D/T retention.

Besides this knowledge, our data may contribute complementary data to predict the upper limit for D/T accumulation in Be/W deposits or dust formed in JET or ITER. Permeation properties of nano-crystalline W films on Eurofer, produced by different techniques, exhibit substantial differences which can be attributed to the size of crystal grains and their orientation. Our technique is unique in this sense as formerly published data on W rely on bulk material and very high temperature. We have determined the permeation properties W films deposited by the TVA which enabled direct comparison to Be/W films. Unfortunately, the influence of crystal size in pure W seems to compete Be reactivity with traces of water at the upstream side may result in BeO formation. This detail requires some improvements of the experimental setup, particularly cryo-cooling of tubes delivering hydrogen to the upstream side….. As these improvements have been tested, even more relevant data will be extracted from experimental data in 2014.

The final remark of this report is that the program was realized successfully and besides this report, the scientific output is almost prepared for two papers in fusion related journals. The total output from 2008 is 8 scientific papers cited in references, all published in relevant journals. Results were also presented in reports and presented at conferences related to nuclear fusion.

4 REFERENCES

1 Skinner CH et al, Fus. Sci. & Technol., 54 (2008) 891-945
2 Doerner RP, Baldwin MJ, Causey RA, J Nucl. Mater., 342 (2005) 63–67
3 Zajec B, Nemanič V and Ruset C, J. Nucl. Mater. 412 (2011) 116 – 122.
4 Zajec B Int. J. of Hydrogen Energy 36 (2011), 7353–7361.
5 Nemanič V, Zajec B, Žumer M, J Vac Sci Technol, 28 (2010) 578-582
6 Nemanič V, McGuiness P, Daneu N, Zajec B, Siketić Z, Waldhauser W J of Alloys Comp., 539 (2012), 184-189,
7 McGuiness , Čekada M, Nemanič V, Zajec Bojan Rečnik A, Surface & Coatings technol, 205 (2011) 2709-2713
8 Nemanič V, Zajec B, Dellasega D, Passoni, J. Nucl. Mater., 429 (2012) 92-98
9 Nemanič V, Zajec B, Žumer M, Porosnicu C, Lungu C, Fusion Eng. Des., 86, (2011) 2421-2424
10 Zajec B, Nemanič V, Žumer M, Porosnicu C, Lungu C, JNM, 443 (2013) 185-194

PLASMA DEPOSITION OF H:C-METAL COATINGS

Peter Panjan, Miha Čekada, Matjaž Panjan, Darinka Kek Merl, Damjan Matelič

Jožef Stefan Institute, Department for Thin Films and Surfaces, Jamova 39, 1000 Ljubljana, Slovenia
peter.panjan@ijs.si

1 INTRODUCTION

The background of our involvement in the project is the fact that any plasma-facing component in a tokamak is exposed to a flux of energetic ions. Upon reaching the component surface these ions cause sputtering of the surface material, which in time degrades the component structure, integrity and functionality. Yet another problem relates to the question, where does this sputtered material deposit. With increasing operation time, the density of these deposits increases too, and in this way there is a decrease of the quality and functionality of the surfaces, covered by these deposits. To regain the original clean surface, the deposits have to be cleaned periodically which is performed by plasma etching using different working gases. The etching parameters have to be adapted for optimal cleaning, i.e. enable a quick and steady removal of the deposits while leaving the base substrate intact.

This tuning of etching parameters can only be succesfull if appropriate deposits are available to the group which deals with plasma etching. The deposit samples can be delivered directly from an operational tokamak where such sputtering and deposition took place. This has the advantage on working on real deposits, however, it turns out these deposits are in short supply and difficult to obtain in reasonable quantities. A far better way is to produce these deposits artificially, i.e in a non-fusion environment, which can be done at low cost and in large quantities, and perform the etching experiments on these samples.

Our primary task has been to deposit various thin films as substitutes for deposits in tokamaks. The group entered the consortium in 2008.

2 WORK PERFORMED IN 2007 - 2013

We have worked on three types of fusion-relevant deposits. The first one is based on amorphous carbon, originating in carbon fibre reinforced composites – a common type of structural materials in tokamaks. Amorphous carbon comes in many forms. It can be hydrogenated (a-C:H) or not (a-C), predominantely sp^2-bound, also known as "soft" (a-C), or predominantely sp^3-bound i.e. "hard" (ta-C). It can be alloyed with additional non-metallic elements (a-C:N) or metals (a-C:W). The bulk of our work

has been performed on this type of deposits, using three different deposition procedures (see below).

In a minor extent, we have also worked on two other types of deposits. The first type contains tungsten, another fusion-relevant structural material. The other is beryllium, however, due to its high toxicity we cannot perform sputtering experiments. We have neither the equipment nor the certification. Nevertheless, chemical similarity between beryllium and magnesium can be used to apply magnesium-containing deposits (which are not toxic) to study beryllium deposits indirectly. Some experiments were thus performed using magnesium.

2.1. Deposition of amorphous carbon by triode sputtering

For lab-scale experiments we primarily used the Balzers Sputron apparatus, which works using the principle of triode sputtering (Fig. 1). The plasma arc is ignited between a hot filament (cathode) and an anode at 50 V / 50 A. An additional voltage is applied on the target (1800 V / 0.6 A), which causes sputtering of the target material. The sputtered atoms are deposited on the substrates, while nonmetallic elements (such as carbon) can be supplied in gaseous form. The amorphous carbon coatings were deposited using a graphite target in two different modes: either in pure argon plasma (a-C films), or in an Ar-C_2H_2 mixture (a-C:H films).

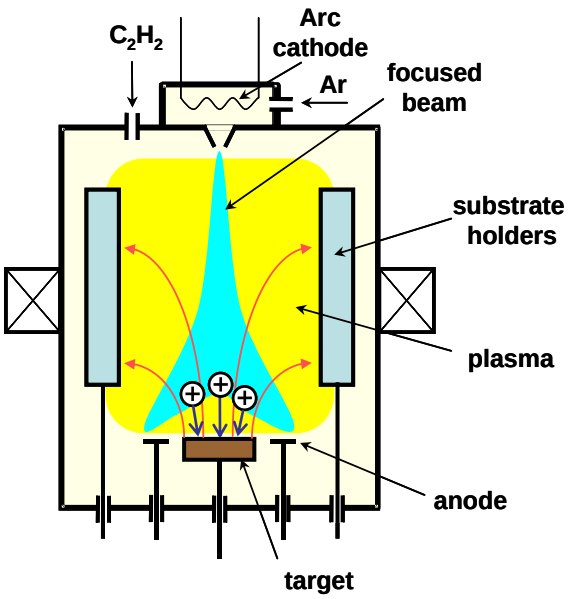

Figure 1: Scheme of the Balzers Sputron triode sputtering apparatus

A major draw-back in depositing amorphous carbon films is their poor adhesion to the substrate. In non-fusion applications, this problem is typically addressed by applying several interlayers. In the strategy we applied the idea is to have a gradual transition from a purely metallic substrate (stainless steel) to the functional amorphous carbon layer. Many experiments were made with several combinations and the best procedure turned out to be the following structure: thin Cr layer / thin W layer / thick W+a-C:H layer / thick a-C:H layer. These interlayers were deposited using a chromium or tungsten target. All the transitions in this stack are between two similar structures. A

scheme of this stack is shown in Fig. 2(a) while the corresponding Auger electron depth profile in Fig. 2(b).

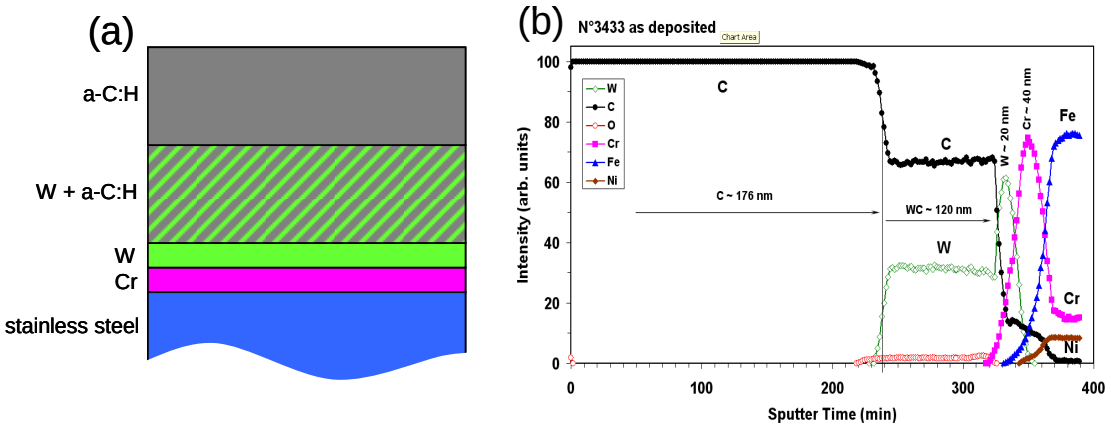

Figure 2: The a-C:H deposit with the most appropriate interlayer combination for enhanced adhesion: (a) scheme, (b) AES depth profile

It has to be pointed out that purely from the fusion point of view (etching of deposits) the only relevant layer is the topmost a-C:H. However, to enable sample stability, the interlayers are of utmost importance.

The result of the above described procedure were samples, which were afterwards etched by the other project group in different plasma environments. The sputtering coeficients were measured for different deposit types: a-C, a-C:H and W+a-C:H, with several combinations and variations. For different functional layers, different interlayers were applied. The results were published in [1–4].

A limited number of depositions were perfomed using magnesium targets. The Mg+a-C:H deposits thus played a role of a reasonable non-toxic substitute for beryllium deposits.

2.2. Deposition of amorphous carbon by a target-less ion source

Triode sputtering is not the only method to deposit amorphous carbon coatings. Within the well-established collaboration between Joanneum Research, Laser Center Leoben (Leoben, Austria) and Jožef Stefan Institute we performed an extensive analysis of the a-C:H coatings, deposited by a target-less ion source called the "anode layer source" (Fig. 3). The apparatus consists of two cathodes and one anode, and is able to hold a plasma (2000 V / 0.1 A) in a cavity. By feeding the apparatus with a working gas, the gas is ionized and the ions accelerated towards the substrates. An a-C:H coating can thus be deposited by using only C_2H_2 gas, without any solid targets. By adding another gas, say N_2, a different coating can be deposited (in this case the a-C:N).

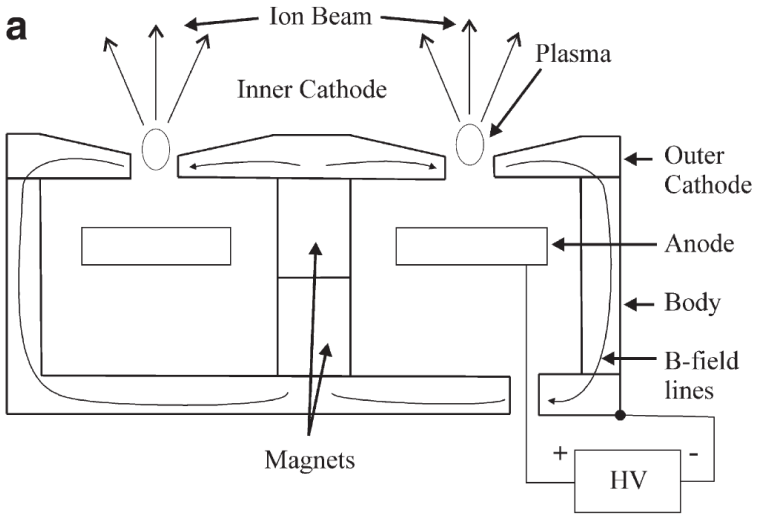

Figure 3: Cross-section of the target-less anode layer source

The amorphous carbon films deposited by the anode layer source (or any other technique, eventually) suffer from the above mentioned problem of poor adhesion. The anode layer source is a relatively new technique with very few publications on carbon deposition (it is primarily used for ion cleaning of surfaces). For this lack of reference data we performed a thorough analysis, how do individual deposition parameters influence the film properties. We were primarily investigating the discharge voltage, C_2H_2 and N_2 flow, and interlayer tape. The properties investigated included the Raman spectra (to determine the sp^2:sp^3 ratio), microhardness, adhesion, and chemical composition (C:N ratio). We found out that a trade-off is necessary between high hardness on one hand and good adhesion on the other – there is no overall best coating. A thick metallic chromium interlayer worked well to ballance the high internal stress and thus further improve the adhesion. An SEM micrograph of a cross-section through the optimized coating is shown on Fig. 4(a). We published several papers on individual aspects of amorphous carbon coatings deposited by the anode layer source [5–8].

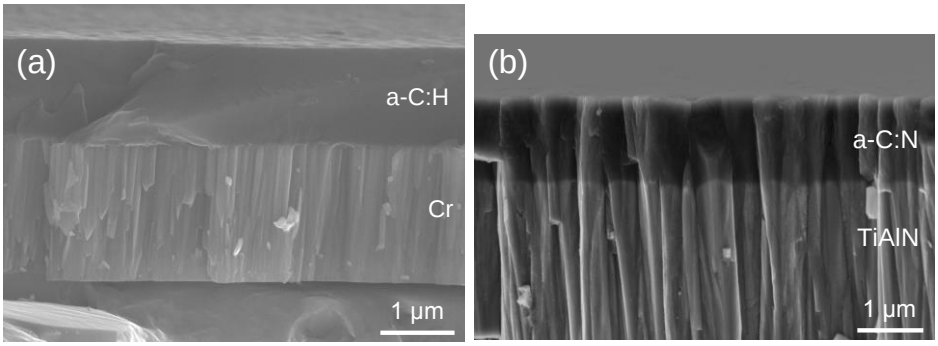

Figure 4: SEM micrograph of the cross-section of amorphous carbon structures, deposited by: (a) anode layer source, (b) magnetron sputtering

2.3. Deposition of amorphous carbon by magnetron sputtering

Yet another technique for deposition of amorphous carbon is the well-established magnetron sputtering. For the sake of improving the adhesion, additional steps were necessary in this case as well. This included lowering the internal stress through incorporation of nitrogen, and using an extended interlayer of TiAlN. This work was based on depositions carried out in an industrial apparatus CemeCon CC800/9, with an extended application of using these coatings in machining.

These coatings were extensively investigated too, and a lot of comparison has been done between the ones deposited by the anode layer source and the magnetron-sputtered ones. The former are distinguished by an extremely smooth morphology (owing to the absence of a solid target), and the latter by high deposition rate, a prerequisite for industrial application. A paper was published specifically on this comparative issue [9]. Part of the work has been done in the scope of a PhD thesis completed in our group [10]. Though it was not directly a fusion-oriented thesis, it contributed a lot to the knowledge of fusion-relevant materials such as amorphous carbon deposits.

3 CONCLUSIONS AND OUTLOOK FOR FURTHER WORK

The outcome of this project is an extended knowledge of amorphous carbon in various forms: elementary (a-C), hydrogenated (a-C:H) and metal-doped (e.g. W+a-C:H). They were succesfully deposited by three diverse deposition techniques: lab-scale triode sputtering, lab-scale anode layer source, and industrial-scale magnetron sputtering. In all these three techniques we encountered the problem of poor adhesion (connected primarily to large internal stress) which was succesfully overcome by introducing interlayers or manipulating the structure/composition through various deposition parameters.

The amorphous carbon samples produced in our group served as substitutes for carbon deposits encountered in tokamak walls, with the primary advantage of being available in large quantities at a low price. The sister group of this project used these samples to study the plasma cleaning phenomena and was able to perform enough experiments to quantify them.

In addition to narrow fusion-related goals this work contributed in expanding the knowledge of amorphous carbon, both in the basic scientific aspect as well as in the applied one. Our group was able to adapt the magnetron-deposited amorphous carbon coating in industrial production, and there is an ongoing research of tribological phenomena in amorphous-carbon-based coatings.

4 REFERENCES

1 DRENIK, Aleksander, VESEL, Alenka, MOZETIČ, Miran, PANJAN, Peter. Recombination of atomic oxygen and hydrogen on amorphous carbon, Journal of nuclear materials, ISSN 0022-3115, vol. 442, no, 1/3, suppl. 2013, p. 751-754

2 ZALAR, Anton, KOVAČ, Janez, PRAČEK, Borut, PANJAN, Peter, ČEH, Miran. Ion sputtering rates of W-, Ti- and Cr-carbides at different Ar[sup]+ ion incidence angles. Appl. surf. sci., 2008, vol. 254, no. 20, str. 6611-6618.

3 VESEL, Alenka, MOZETIČ, Miran, PANJAN, Peter, HAUPTMAN, Nina, KLANJŠEK GUNDE, Marta, BALAT-PICHELIN, Marianne, Etching of carbon-tungsten composite with oxygen plasma, Sur. Coat. Technol. 204 (2010) 1503-1508
4 VESEL, Alenka, MOZETIČ, Miran, PANJAN, Peter, HAUPTMAN, Nina, KLANJŠEK GUNDE, Marta, BALAT-PICHELIN, Marianne. Interaction of hydrogen plasma with carbon-tungsten composite layer. Nucl. Eng. Des., 2011, vol. 241, no. 4, str. 1255-1260. M. Kalin, S. Novak, J. Vižintin, Surface charge as a new concept for boundary lubrication of ceramics with water, J. phys., D, Appl. Phys., 39 (2006), 3138-3149.
5 KAHN, Markhus, ČEKADA, Miha, BERGHAUSER, R., WALDHAUSER, Wolfgang, BAUER, C., MITTERER, Christian, BRANDSTÄTTER, E. Accurate Raman spectroscopy of diamond-like carbon films deposited by an anode layer source. Diamond and related materials, 2008, vol. 17, no. 7/10, str. 1647-1651.
6 KAHN, Markhus, ČEKADA, Miha, SCHÖBERL, Thomas, BERGHAUSER, Roswitha, MITTERER, Christian, BAUER, Christian, WALDHAUSER, Wolfgang, BRANDSTÄTTER, Elmar, Structural and mechanical properties of diamond-like carbon films deposited by an anode layer source, Thin Solid Films, 517, 24 (2009) 6502-6507
7 KAHN, Markus, PASKVALE, Srečko, ČEKADA, Miha, SCHÖBERL, Thomas, WALDHAUSER, Wolfgang E., MITTERER, Christian, PELICON, Primož, BRANDSTÄTTER, Elmar. The relationship between structure and mechanical properties of hydrogenated amorphous carbon films. Diamond and related materials, 2010, vol. 19, no. 10, str. 1245-1248
8 ČEKADA, Miha, KAHN, Markus, PELICON, Primož, SIKETIĆ, Zdravko, BOGDANOVIĆ-RADOVIĆ, Iva, WALDHAUSER, Wolfgang E., PASKVALE, Srečko. Analysis of nitrogen-doped ion-beam-deposited hydrogenated diamond-like carbon films using ERDA/RBS, TOF-ERDA and Raman spectroscopy. Surf. coat. technol., 2012, vol. 211, str. 72-75
9 PASKVALE, Srečko, KAHN, M., ČEKADA, Miha, PANJAN, Peter, WALDHAUSER, Wolfgang E., PODGORNIK, Bojan. Tribological properties of diamond-like carbon coatings prepared by anode layer source and magnetron sputtering. Surf. coat. technol., 2011, vol. 205, suppl. 2, str. S99-S102,
10 PASKVALE, Srečko, Carbon based protective coatings prepared by physical vapour deposition technique, PhD thesis, Ljubljana, 2012

ADVANCED VISUALIZATION TOOLS FOR EFDA INTEGRATED TOKAMAK MODELLING FRAMEWORK

Leon Kos
Association EURATOM-MESCS, University of Ljubljana, Faculty of Mechanical Engineering, LECAD Laboratory
leon.kos@lecad.fs.uni-lj.si

1 INTRODUCTION

The European Integrated Tokamak Modelling (ITM) project aims to provide to the European fusion community a suite of validated codes for the interpretation of present experiments and predictive modelling of future reactors. Verification and validation of predictive and interpretative simulation runs require that modelling platform allows combining experimental and simulation-data at various stages throughout scientific workflow development. Traceability (provenance) in Kepler workflow engine used within the EU ITM framework should provide easy verification and validation at the modelling level. Sharing workflows between scientists is "easy part" of the workflow-based provenance and must be accompanied with often big data that orchestrated codes needs to trace. Data model seems to be one of the challenges that cannot be universally addressed for all domains. Fusion-oriented framework DataSpaces separates data model into server–client model with distributed hash tables with the goal of providing transparent memory-to-memory transfer (staging) to applications. For "expensive to get" data, lookup and meta-data is provided in the DataSpaces three-layered architecture. The EU ITM data model currently relies on a single-layered Universal Access Layer (UAL) that concentrated on accessing a tailored (tokamak) datastructure description. Data gathered within CPOs (Consistent Physical Objects) is used for "partitioned" interchange between codes in "strongly" coupled workflows. Similarly to CPOs, ADIOS system provides groups that describe collections of data written at once. ADIOS as a HPC library for input/output (IO) provides simplified and configurable write strategy to parallel codes. The EU ITM approach uses UAL library routines in upgraded fusion codes for data exchange through a structured CPOs database. Staging and write strategy is a part of the UAL configuration and can range from direct file access, memory-cached or parallel access. The UAL back-end responsible for storage uses MDSplus and HDF5 database formats. Both formats are commonly used in scientific and experimental (fusion) environments. As mentioned before, single-layered UAL is providing simple IO with minimal number of functions to codes for fetching and storing CPOs. UAL adaptation to hashed client–server model as in DataSpaces, DART asynchronous data communication layer or using ADIOS should not change the UAL front-end routines used in codes. Code specific data transport configuration and provenance can be governed by the workflow engine (e.g. as XML

file used in ADIOS). For distributed workflows where database access is not easy to arrange on must rely on serialization of CPOs for exchange between compute sites. One such approach in fusion modelling is MAPPER project that can couple codes with enveloping them into communication kernels and configure into workflow.

The EU ITM effort turned its focus into creation of workflows for specific physics applications that can easily include similar physics codes for verification and comparison in integrated modelling. Key principle for these workflows is not UAL but rather datastructure description (ontology) consisting of CPOs. Consistency enforced by CPO data model requires that existing codes need to be "adapted" to be able to retrieve/store results in database. This task requires developer's knowledge of the code and CPOs description that needs to be mapped to each other in enforced units (MKSA and eV). After (necessary) adaptation, code can be executed as a black-box within scientific workflows that couples different codes in a compatible way and sequence. Similarly to CPOs, ITER Integrated Modelling & Analysis Suite (IMAS) foresees the development of a datastructure composed of Interface Data Structures (IDSs) as standardized entities for use between physics components. The collection of CPO descriptions form together a complete data model for diverse simulations that can also contain imported experimental data. This approach enables a direct comparison of results with the experiment and/or use experimental data as an input. The implementation phases and continuous development of the EU ITM framework are simplified by the fact that the CPO data structures are described by an XML schema definition (XSD), which can be easily modified. This semi human-readable description allows rigorous validation, creation of data bindings and translations for different purposes. The XSD data-structure description is mainly used to generate CPO definitions in an XML format obtained by applying the XSL translation (XSLT) language. Consistency of CPO definitions is assured by the XSD description, so that the derived CPO definitions in XML are consistent too.

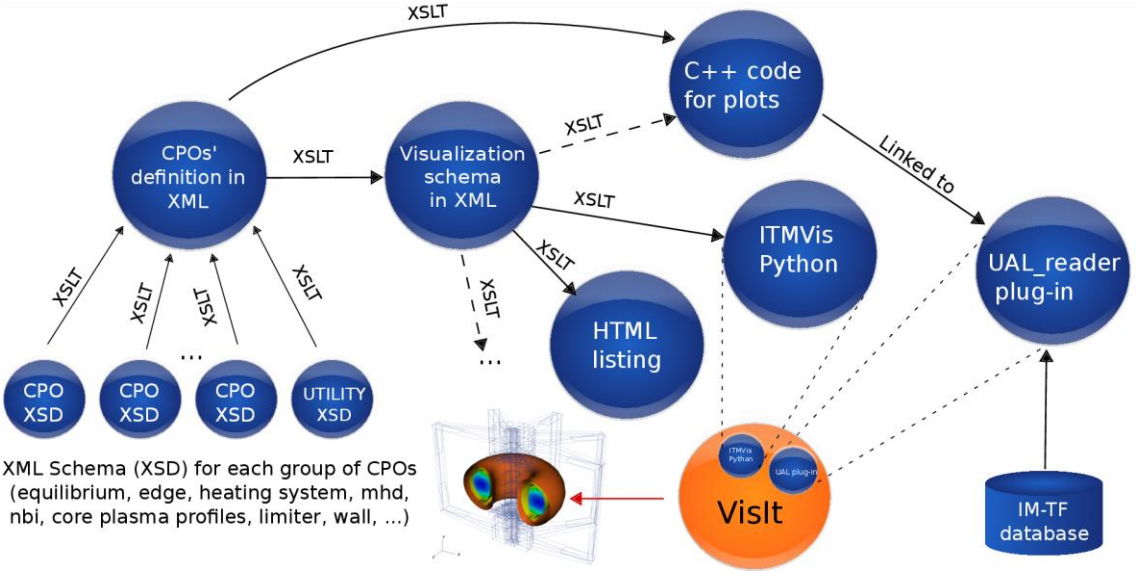

Figure 1. XSLT flowchart for standard representation transformations used for visualization.

From the CPOs schema one can automate (through XSLT processing) generation of "include" definitions and UAL linking for all supported languages. From

each CPO defined with XSD we then translate into single CPODef.xml file that includes complex and common structure types defined in utility.xsd. Figure 1 on the left shows this initial transformation from many CPO definitions into single CPOs' definition in XML. The fundamental purpose of CPODef.xml is a description of the EU ITM persistent storage database. As most of the CPOs are time dependent, the EU ITM database stores slices of each CPO during simulation iterations or experiment sampling. Slicing occurs at different time scales for each CPO depending on the physics involved .

Described data model and its access is a basis for visualization tools that are aimed to support users in all stages of modelling framework usage. To support the diagnostic of the time-dependent data in CPOs, several visualization tools are used depending on the scales and representation of the data that is regularly used in simulations. For many simulations, custom visualization are created using general-purpose graphics libraries. To avoid such custom approaches and to provide standardized sets of visualizations EU ITM aims to provide tools that can be used for visualizations without the need for scientists to manually program each plot and allow creation of reusable custom visualizations.

2 WORK PERFORMED IN 2010 - 2013

The work performed in the »ITM Advanced visualisation tools« was carried under priority support within the following tasks: WP10-ITM-ISIP-ACT13-T1, WP11-ITM-ISIP-ACT2-T11, WP12-ITM-ISIP-ACT2-T11, WP13-ITM-ISIP-ACT2. It should be noted that the priority support was continuation of our work within the EUFORIA (EU Fusion for Iter Applications) project where we collaborated with University of Strassbourg on JRA4 that provided some visualisation support prototypes for ITM described in continuation.

EU project EUFORIA was not part of MHEST/SFA programme and was carried separately by University of Ljubljana, Mech. Eng., LECAD laboratory in the years 2007-2010. The EUFORIA and ITM projects were closely related. EUFORIA aimed to provide HPC and GRID computing support to ITM framework together with acompanying visualisation tools [1]. In 2010 porting and support for these visualization tools was included within ISIP (Infrastructure and Software Integration Project), which is in charge of developing and maintaining the Integrated Tokamak Modeling Task Force (ITM-TF) simulation infrastructure where we mostly collaborated with IPP Garching, CEA and CIEMAT.

2.1. Visualization support in the EU ITM framework

Graphical inspection of data in variety of ways becomes more difficult with increasing data complexity. As time is a key physical quantity of tokamak modeling, this quantity is included in nearly every CPO and can be assumed as an additional dimension when time-varying properties are inspected. Usually, time-dependent visualization is done by specifying a time point or selecting a cycle (frame or time-slice) from the UAL database. From that point data can be retrieved and visualized with different tools in a variety of ways. Visualization tools capable of accessing UAL data directly (without exporting or converting) were developed to provide required visualizations.

Table 1. The EU ITM visualization tools capable of UAL direct access

EU ITM Tool	Graphical plot config (user level)	Non-interactive processing	Input data pre-processing	Publication ready figures
ITMVis	no (basic)	yes	yes	yes - matplotlib
VisIt	yes (basic)	yes	limited	yes - raster gr.
Matlab	yes (expert)	yes	yes	yes - builtin
ISE	yes (basic)	no	no	no

Three approaches are used by the EU ITM for producing visualization: (i) programming languages, (ii) general tools, and (iii) specialized tools with capabilities as shown in Table 1. Scripting languages like Python and Matlab are suited for all kinds of data processing. However, their use requires development effort. Non-scripting languages (C++, Java, Fortran) for producing visualizations are even less attractive. They are used for application programming and within visualization tools. In fact, there are no general purpose tools available that can cover all aspects of usage. The Integrated Simulation Editor (ISE) was designed with Kepler workflow control in mind in a "study"-like manner and currently only provides simple 2D signal editing and visualization.

2.2. ITMVis

One goal of the EU ITM effort is to consolidate and extend the visualization capabilities of the platform[3,4], providing developers with tools for (automated) creation of specialized plots that can be easily distributed to end users and tools for creating plots for code/workflow development and debugging. Eventually, users will benefit from easy-to use, interactive tools for data exploration, easily available custom visualizations for specific physics problems/workflows and tools that are capable of producing publication-ready plots. Towards this goal the EU ITM developed a structured 2D Python visualization library — ITMVis which unifies the existing approaches, provides extensibility and enables reuse of custom visualizations for various target visualization tools (back-ends). The ITMVis library encompasses the following:

- A standard front-end consisting of command line Python scripts for accessing UAL database by prescribing run, shot, time, user, tokamak and CPOs needed for visualization.
- A structured repository of code fragments for computing data required for plot, possibly combining data from various CPOs. For each plot metadata and plotdata function is provided.
- A collection of "standard" processing functions which can then be shared among multiple visualization scripts.
- Collects and makes code owned/developed by specific projects available to everybody in a central place and provides a plot sharing mechanism for users to reference exported visualization scripts.

Developers/users need to concentrate only in data processing and plot description by providing metadata and plotdata functions. Metadata describes the plot

and verifies data availability so the user is informed whether a specialized plot can be produced or not. Only if a database contains the required data, the plot data function can be executed. To detect modules containing metadata and plot data functions in the Python search path, some function naming conventions are prescribed. Backends implemented as outputs are text, VisIt and matplotlib library with several graphical formats. ITMVis implemented a Python library can be included in all Python scripts that can regularly include matplotlib along with UAL wrapper library that requires NumPy/SciPy stack.

2.3. VisIt

For complex 3D visualizations the EU ITM effort adopted VisIt visualization software (open-source, maintained by LLNL) upgraded with custom UAL_reader plugin developed under EUFORIA/JRA4 project[1]. VisIt is popular and extensible visualization software that provides various representation modes and data post-processing in interactive and non-interactive (batch or scripting) mode. With custom plugin is able to read CPOs from the the EU ITM database directly. VisIt as a general visualization tool is capable of complex visualizations that are primarily 3D. Experimental data that is imported into UAL by the EU ITM tool exp2itm mostly comes in 1D time-dependent[2] (TD) form and can be inspected by surplus of graphing tools. VisIt role in workflows is primarily dedicated to inspection of 3D or even 4D data resulting from "integrated modeling". Normally, insight into 3D data is extracted by variety of operators at selected cycle (moment in time). Animation and time-slider can be useful TD tools for general overview of inspected phenomena. VisIt uses FlipBook animation for showing time-varying databases. Controls for moving though cycles/time are similar to many software players (or VCR). UAL plug-in for VisIt (UAL_reader) enables VisIt fusion data reads through the UAL in order to build the resulting visualization. In order to connect VisIt with UAL two components of the plugin was developed as shown in Fig. 2. Standard visualizations are fetched directly from the database. For custom plots ITMVis library is included through plugin-embedded Python interpreter and accesses database by Python UAL interface.

VisIt is built on top of Analysis and Visualization Toolkit (AVT) that has strong correlation to VTK Toolkit made by Kitware. Data structures from UAL needs to be represented in AVT compatible way. When CPO is read into memory all data is available and information on how this data can be "naturally" represented in coordinate system is being amended by physicists. "Natural" representation of data of interest is related to conventions and physicist's way of thinking. For example, one needs to decide which field represent x and y-axis for 1D Curve. A representation is, in fact, a description of the visualization. There can be multiple representations of the same data.

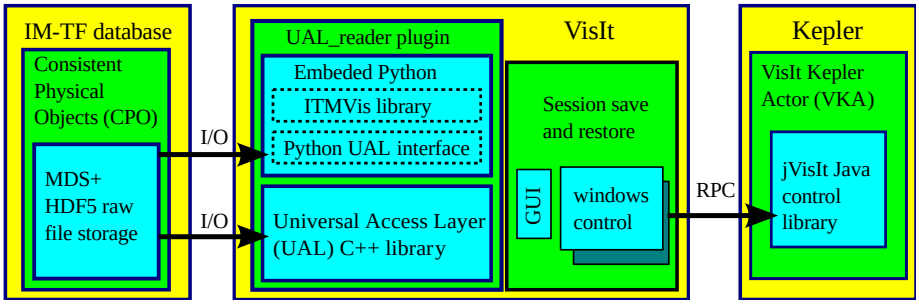

Figure 2. Schematics and communication of basic components for visualization with VisIt under Kepler workflows.

The UAL_reader plugin for VisIt (see Fig. 1) utilizes representation tags that are included in the XSD files describing the CPOs. This means that datastructure "knows" how it can be visualized. This is similar to the concept of views in SQL, which are stored in a database directly (except that these would be stored directly in the database). Representation tags are just a description that does not enlarge storage but facilitates views on data. Each representation consists of name, mesh type, links for the axes, and data attributes. The representation name is arbitrary and is shown as the last name in the VisIt path when adding plots. The data attribute can be either a scalar or a vector and describes the kind of data mapped on the mesh represented by one or more links. Meshtype describes the type of variable mapping in space. Several meshtypes exist: i) curve as a polylines plot, ii) axis1D0 X axis given as a link1 vs. a bunch of curves from a matrix; iii) mesh1D0 Contours (closed curves) as a (2D) surface mesh, iv) rectlinear0 or curvilinear0 meshes in 2D and 3D. Each meshtype can have a variable number of links (link1, link2 and/or link3) and thus different kind of visualizations that are constructed as VTK objects in VisIt. Links provide axis mapping to corresponding vectors or matrices that constitute a mesh. The topology name at the end of the meshtype means (0D - points, 1D - lines, 2D - surface, 3D - volume). The number at the end distinguishes variations of the same meshtype (0, 1, ...). If no topology is given, a general description is assumed (2D and 3D). UAL_reader plugin is a basis for all kinds of visualizations with VisIt.

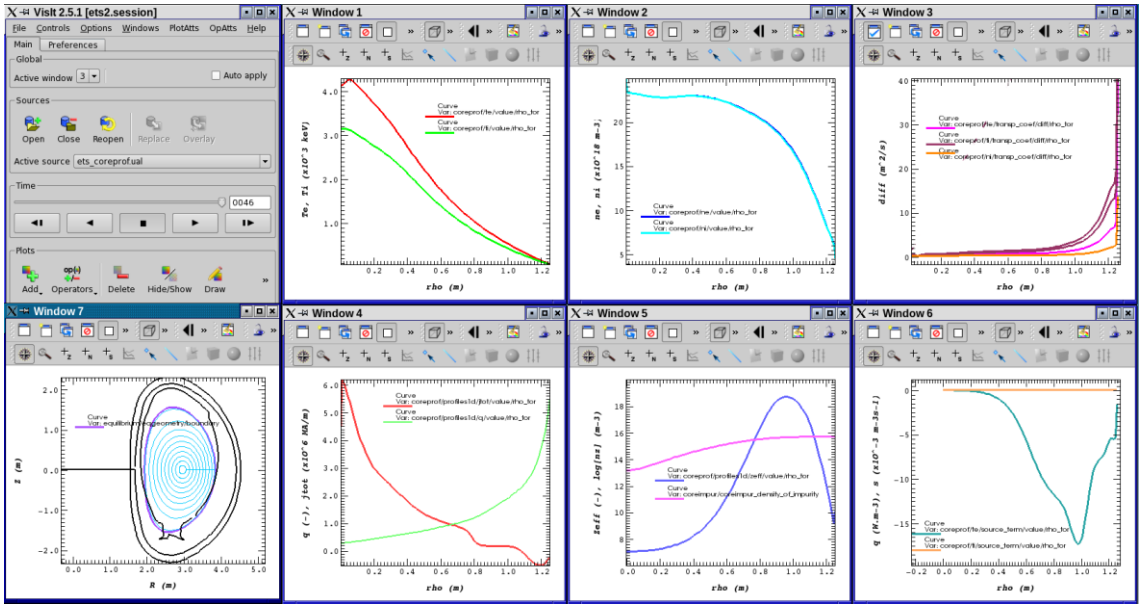

Figure 3. European Transport Solver (ETS) convergence monitoring with VisIt.

As shown in Fig. 2 customized plots can be accessed through ITMVis library and standard plots by direct translation from datastructure. Both parts of the plugin are complementary and can be used together in a dashboard-style setup for European Transport Solver shown in Fig. 3 where some difficult to combine data were rather prepared by custom plots.

2.4. Visit Kepler Actor

The EU ITM selected the Kepler scientific workflow engine which enables graphical programming of workflows. Data flow between processes (called actors) is modelled by wires. Through wires only small amount of data (signals) are passed, usually just single numbers, strings and structures with CPO names, which identify database entries. The Actual data exchange between ITM actors encapsulating fusion codes is then implemented by direct access to the "real" data through the UAL library. For inclusion of VisIt in the Kepler workflows the VisIt Kepler Actor (VKA) was developed. The VKA in Fig. 2 can restore session created previously within VisIt but with new source database. Session saved within VisIt graphical user interface (GUI) consists of all windows, applied plots, operators and attributes. This means that user can configure session under VisIt GUI inside or outside Kepler. Then user builds a particular visualization for the quantities of interest. Finally, user stores a VisIt session file which contains all the information needed to restore the state of VisIt when the session file is generated. In the second stage, the user launches Kepler, inserts the VKA to his workflow and add as parameter of the VKA the session file generated at stage 1. When the workflow is executed, once the VKA is activated by the workflow, one or several visualization windows will pop up with the data contained in the incoming database. The resulting visualization is rendered with the parameters contained in the session file. This means that session files are special tailored descriptions of visualizations with expected inputs. Normally most scripting languages (IDL, Matlab, gnuplot, ROOT, ...) that require visualization also generate scripts for visualization by

coding. VisItUAL is a similar approach but without coding as user can with GUI save XML session file. Such session can then be shared and collected for visualizations of interest and used as standalone or within Kepler workflow. Such approach is useful for fusion codes and experiments that output complete results in UAL database but researchers are interested in specific phenomena and selected variables and ranges that needs to be monitored within larger scientific workflow supported by Kepler.

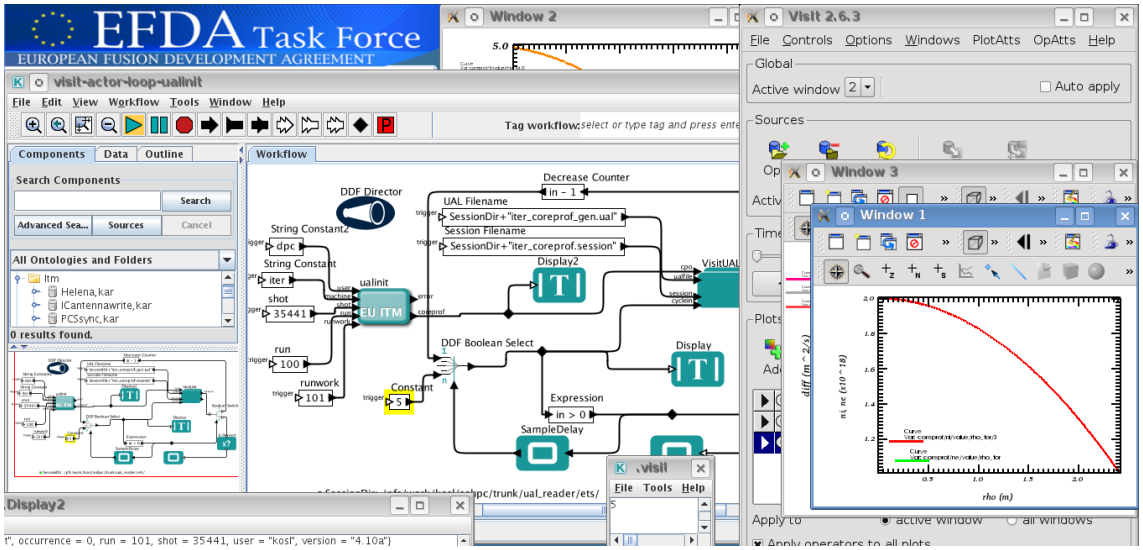

Figure 4. The VisIt Kepler Actor – VisItUAL in a workflow within a loop reading data through the Universal Access Layer. Multiple VisIt windows configured with session save/restore mechanism are shown and updated during iterations.

For UAL database and CPO support composite actor Coupling VisIt to UAL is supported by UAL_reader database plugin. Fig. 4 shows such a workflow with user supplied visualization settings. Location of the ualfile is given for automatic creation at the specified location. This location can be the same as previously manually generated session file. VKA allows visualizations of multiple CPOs and includes its own GUI written in Java for controlling interactive work under Kepler and restoring VisIt GUI. It can also be used in a synchronized loop as in Fig. 4 that cycles through prescribed time steps found in CPOs.

3 CONCLUSIONS AND OUTLOOK FOR FURTHER WORK

Visualization in a mission to assist researchers in achieving their research goals needs to provide proper analytics with tools that tackle specific domain. Our introduction of the *visualization schema* into the *datastructure* unifies and reduces efforts required to develop different visualization tools. A set of *standard* visualizations provided by the visualization schema enables users to browse through CPOs available. In cases of custom requirements, scripting for plots can be used by *ITMVis* library that was embedded in VisIt UAL database reader. How to provide more sophisticated (algorithmic) mappings in the schema is ongoing question. The present state and requirements for visualization tools may be considered as a general view for integrated modelling problematics and a starting point for a future work. Additionally, initiative

for collaboration from CCFE on Kitware tools (VTK, ParaView) will start in 2014 under EUROfusion consortium.

4 REFERENCES

1 Haefele, Matthieu, Kos, Leon, Navaro, Pierre, Sonnendrücker, Eric. *EUFORIA Integrated Visualization*. 18th Euromicro International Conference on Parallel, Distributed and Network-Based Processing, 17-19 Feb. 2010, Pisa, Italy. Los Alamitos: IEEE Computer Society, 2010, pp. 498-502 doi: 10.1109/PDP.2010.76, http://www.ieeexplore.ieee.org/xpls/abs_all.jsp?arnumber=5452425&tag=1,

2 L. Kos, O. Hoenen, S. Kulovec, P. Huynh, J. Duhovnik, F. Imbeaux. *Towards 3D time dependent visualization within ITM-TF infrastructure*. 20th International Conference Nuclear Energy for New Europe 2011, September 12-15, 2011, Bovec, Slovenia. *Proceedings*. Ljubljana: Nuclear Society of Slovenia, 2011, PP. 1008.1-1008.

3 L. Kos, H.-J. Klingshirn, P. L. García Müller, F. Imbeaux, *Extension of the visualization capabilities within the European Integrated Tokamak Modelling platform*", 21st International Conference Nuclear Energy for New Europe, Ljubljana, Slovenia, September 5-7, 2012, pp. 1117.1-1117.8

4 L.Kos, H.-J. Klingshirn, P.L,Garcia Muller, F. Imbeaux and EFDA ITM-TF contributors, *Unified Approach to Visualizations within the European Integrated Tokamak Modelling Framework*, 22nd Int. Conf. Nuclear Energy for New Europe, Bled, Slovenia, 9–12 Sept. 2013, pp.1402.1–1402.8

INTEGRATED TOKAMAK MODELLING WITH EXTERNALLY COUPLED CORE AND EDGE TRANSPORT CODES

Leon Kos, Mladen Stanojević, Janez Krek, Nikola Jelić, Jožef Duhovnik
Association EURATOM-MESCS, University of Ljubljana, Faculty of Mechanical Engineering, LECAD Laboratory
leon.kos@lecad.fs.uni-lj.si

1 INTRODUCTION

The P1 project started in October 2006. It is closely related to the EFDA's Integrated Tokamak Modelling Task Force (ITM-TF) Integrated Modelling Project 3 (IMP3): Transport Code and Discharge Evolution, in particular to its topic 3E: Interfaces to boundaries. The P1 project is focused on the core-edge coupling and includes the following activities:

1. review of the "state-of-the-art" in the integrated tokamak modeling with the existing fluid transport codes (in 2006 - 2007);
2. analysis of the physical models used in the existing core and SOL transport codes, which are main candidates for the coupling, with the objective to identify and formulate possible necessary changes and improvements to be implemented in these codes in order to achieve more efficient coupling (in 2006 - 2007);
3. analysis of the software architecture and numerical methods used in the codes mentioned above with the objective to identify and formulate possible necessary changes or improvements to be implemented in these codes in order to achieve more efficient coupling (in 2007);
4. implementation and testing of the changes or improvements identified and formulated in the activities 2. and 3. (in 2007);
5. specification and prototyping of the interfaces for the core-edge coupling (in 2007 - 2008);
6. development of either the interface module for at least one example of the core-edge coupling with the existing codes or the standardized interface module for all core and edge transport codes considered in the project according to the recommendations of the ITM-TF (in 2008);
7. testing, verification and validation of the modules produced (in 2008 - 2009); Documenting the work and results in the activities 1. - 7. (in 2006 - 2009).
8. Collaboration after P1 continued in EUFORIA (EU Fusion for Iter Applications) project (2008-2010) and then in Integrated Tokamak Modelling (ITM) (2010-2013).

2 WORK PERFORMED IN 2007 - 2013

The following activities were performed:

1. review of the "*state-off-the-art*" in the integrated tokamak modelling with the existing fluid transport codes, including the analyses of the physical models and numerical methods used in these codes with the objective to identify and formulate possible necessary changes or improvements to be implemented in these codes in order to achieve more efficient coupling, and implementation of the necessary changes or improvements of the codes identified and formulated in the review mentioned above.
2. The review and analysis of the COCONUT code package [1, 2] gave a valuable information for developing new and more advanced core-SOL coupling schemes and interfaces. However, due to limited portability and accessibility of the COCONUT code package, which is located at JET computer system, we decided to continue our work on this project with the core transport code ASTRA [3] and SOL transport code SOLPS-B2.5 [4].
3. The latest standard or master version of the latter code was installed at LECAD Laboratory computer system and supplemented with the boundary conditions (or boundary source terms) developed in our previous research project on the boundary conditions for fusion plasmas (Cost-Sharing Action: Contract No. FU06-CT-2003-00321, see Project Related Publication 1).

Regarding the coupling of the core and SOL codes at a specific location, which is usually the separatrix, we identified the following physical and computational problems to be investigated and solved in the continuation of the project:

- since the exact location of the separatrix may be unknown or may change during the tokamak operation, coupling core and SOL transport codes at a prescribed location of the separatrix may give unrealistic results for the plasma parameters and related fluxes near the separatrix;
- it is well-known from the experiments and theory that the plasma transport in the core edge or pedestal region has a crucial role in tokamak plasma confinement (especially in the H-mode), so that the coupling at the separatrix or at a location within the core, which includes poloidal averaging of the plasma parameters and related fluxes or simplification of the transport models in that region, may give very unrealistic results;
- although the computational mesh of the SOL transport codes can be extended deeply into the core, they do not include appropriate transport coefficients and various source terms (e.g., due to plasma heating) appropriate for the core region, therefore modifications and improvements of the SOL codes in that sense will be necessary in order to obtain more realistic results of the coupled core and SOL plasma simulations, even if only few layers of the SOL code computational cells within the core are used in the simulation.

In ASTRA there are numerous theory-based and empirical models of the radial transport in the core, which can optionally be employed in the simulations. The ASTRA

library includes about one hundred different neoclassical and anomalous transport coefficients which can be expressed as formulas.

Recently, more complicated routines for evaluation of the transport coefficients were developed and some of them can be included in ASTRA as separate modules. Therefore we decided not to add any additional transport models or modify the latest version of ASTRA for the purpose of our project. On the other hand, the number of various radial transport models in SOLPS-B2.5 is rather small and different transport models for the core and SOL plasma cannot be used.

The anomalous transport coefficients can be prescribed by the user as constant parameters or calculated with simple semi-empirical formulas using free input parameters or their radial profiles can be prescribed with the input file 'b2.transport.inputfile'. The latter option was used by Bürbaumer et al. in their one-directional coupling of ASTRA and SOLPS-B2.5 [5]. Since the original technical documentation and coupling code were lost, we developed a new coupling code - ASTRA2SOLPS, in order to reproduce their results and possibly use their approach in our project (see Project Related Publication 2.1).

In their coupling scheme, presented in Figure 1, ASTRA is run in the interpretative mode and its output data are processed by ASTRA2SOLPS, which produces 'b2.transport.inputfile' and 'b2.sources.profiles' files. These two files are input files for SOLPS-B2.5 and include the radial profiles of the transport coefficients and particle, momentum and heat sources due to plasma heating and fueling in the core region, respectively.

Thus the transport coefficients and source terms in SOLPS-B2.5, which are calculated with inappropriate expressions for the core region, are replaced with the values of these parameters calculated with ASTRA. Detailed testing of this coupling scheme is pending.

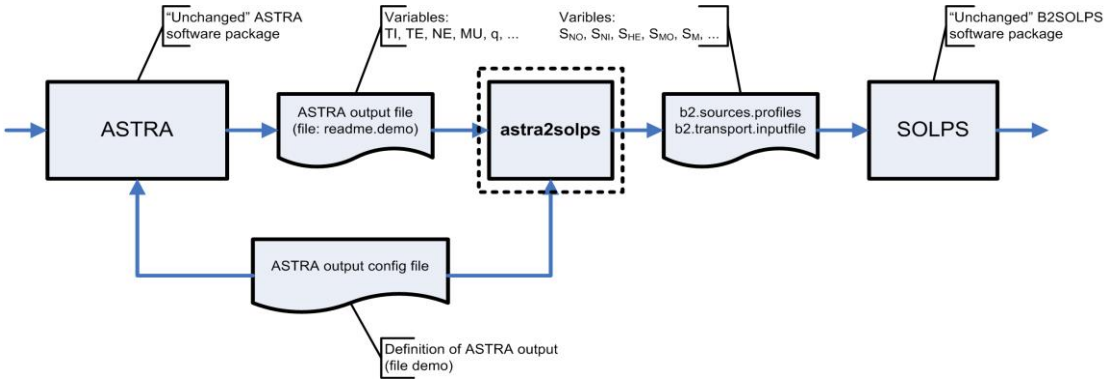

Figure 1. One-directional coupling of ASTRA and SOLPS-B2.5.

Nevertheless, in order to improve SOLPS-B2.5 by adding new theory-based anomalous transport models applicable either in the SOL or in the core region, we investigated the existing theoretical models of tokamak core and SOL plasma transport.
Considering their applicability for interpreting experimental data, we identified limited number of anomalous transport mechanisms or models to be implemented in the modified SOLPS-B2.5 as follows.

- In the core plasma (i.e., in the SOLPS-B2.5 computational cells within the core region), the anomalous transport coefficients (i.e., density and pressure driven particle diffusion coefficients, radial pinch velocity, viscosity, ion and electron thermal diffusivities, electrical conductivity and thermo-electric coefficient) should be prescribed or calculated by using one of or sum of several of the following constituents [6-13]:
  - constant value,
  - Bohm transport,
  - gyro-Bohm transport,
  - critical gradient transport model (or "stiff" transport model, which is basically modified
- gyro-Bohm transport model [12, 13]), and
  - neoclassical transport.
- In the SOL plasma (i.e., in the SOLPS-B2.5 computational cells within the SOL region), the following possible transport mechanisms or constituents should be taken into account [14-18]:
  - constant value,
  - endplate MHD interchange instability depending on the pressure gradient,
  - endplate MHD interchange instability depending on the density gradient,
  - drift instability with collisionless skin depth,
  - drift instability with collisionless skin depth taking into account different density and
- temperature gradients,
  - Bohm transport,
  - collisionless MHD interchange instability near ,
  - collisionless skin depth,
  - charge-exchange collisions, and
  - classical and neoclassical conduction.
- In the semi-analytical expressions for the transport coefficients, the relative contributions of these transport mechanisms can be prescribed with free input parameters.

2.1. References of *Theoretical support in P1* to Fusion

1 M. Stanojević: **Review of the boundary conditions in the SOLPS-B2.5 code**, Research Work Report (2007), LECAD Laboratory, Faculty of Mechanical Engineering, University of Ljubljana, 2007.

2 J. Krek, N. Jelić, J. Duhovnik, M. Stanojević: **Coupling of ASTRA and B2-SOLPS**, Research Work Report (2007), LECAD Laboratory, Faculty of Mechanical Engineering, University of Ljubljana, 2007.

3 S. Kuhn, N. Jelic, D.D. Tskhakaya (sr.), and L Kos, **Theoretical and Numerical Modelling of the Plasma Sheath for ITER,** Invited lecture presented on 14th October 2011 by Siegbert Kuhn at the Joint ITER-IAEA-ICTP Advanced Workshop on Fusion and Plasma Physics, Trieste, Italy, 3-14 October 2011

4 N Jelic **Cutoff effects of electron velocity distribution to the properties of plasma parameters near the plasma-sheath boundary,** *Phys Plasmas 1*8, (2011)

5 N Jelic **Fluid plasma parameters near electrodes biased close to plasma potential ,** *Phys. Plasmas* Nov 2011

6 KOS, Leon, TSKHAKAYA, D., JELIĆ, Nikola. **Potential profile near singularity point in kinetic Tonks-Langmuir discharges as a function of the ion sources temperature**. *Phys. plasmas*, 2011, vol. 18, iss. 5, p. 053507-1-053507-11.

7 N JELIC, L Kos **Particle in cell simulations on the effects of electrically biased grid to the plasma parameters.** V: ZAJC, Baldomir (ur.), TROST, Andrej (ur.). *Proceedings of 20th ERK 2011, 19. - 21. september 2011, Portorož, Slovenija*, Ljubljana: IEEE Region 8, 2011, p. 291-295.

8 J Krek, N Jelić, J Duhovnik **Grid-Free Treecode Method in Particle-In-Cell (PIC) Simulations**, 20th International Conference: Nuclear Energy for New Europe 2011, p 311.1 2011

9 JELIĆ, Nikola, KOS, Leon, DUHOVNIK, Jože. **Thermodynamic plasma properties near the sheath edge in kinetic Tonks-Langmuir model with finite ion source temperatures**. *Scientific publications of the State University of Novi Pazar. Series A, Applied mathematics, informatics and mechanics*, 2011, vol. 3, no. 2, p. 71-83.

10 J. Krek, N Jelić, J Duhovnik, **Particle-in-cell (PIC) simulations on plasma-sheath boundary in collision-free plasmas with warm-ion sources.** *Nucl. Eng. Des.*., 2011, vol. 241, issue 4, p. 1261-1266, doi: 10.1016/j.nucengdes.2010.04.005.

11 KOS, L., TSKHAKAYA, D.D., DUHOVNIK, J., JELIĆ, N.. **Analytic solution to the Bissell-Johnson model.** 30th International Conference on Phenomena in Ionized Gases (ICPIG), Belfast, Northern Ireland, August 28th - September 2nd 2011. *ICPIG 2011 Conference*. Belfast: Queen's University, cop. 2011, p. [B5136-1-B5136-4],.

12 N. Jelic and L. Kos. **Particle in cell simulations on the effects of electrically biased grid to the plasma parameters.** In 20th International Electrotechnical and Computer Science Conference ERK, volume A, pages 291–295, Portoroz, Slovenia, 2011. IEEE Slovenia.

13 N. Jelic, L. Kos, J. Duhovnik. **Thermodynamic plasma properties near the sheath edge in kinetic Tonks-Langmuir model with finite ion source temperatures.** Scientific publications of the State University of Novi Pazar. Series A, Applied mathematics, informatics and mechanics, 3(2):71–83, 2011.

14 L. Kos, D. D. Tskhakaya, N. Jelić, J. Duhovnik, **Analytic properties of the sheath solution with warm ions**, 39th EPS Conference on Plasma Physics [and 16th International Congress on Plasma Physics : 2-6 July 2012, Stockholm, *Sweden*, [Mulhouse], European Physical Society EPS, 2012, PD6.006, http://ocs.ciemat.es/epsicpp2012pap/pdf/PD4.006.pdf.

15 N. Jelić, L. Kos, D. D. Tskhakaya, S. Kuhn, **Analytic solution to the plasma equation with warm ions**, : 39th EPS Conference on Plasma Physics and 16th International Congress on Plasma Physics : 2-6 July 2012, Stockholm, Sweden, [Mulhouse], European Physical Society, EPS, 2012, PD4.007, http://ocs.ciemat.es/epsicpp2012pap/pdf/PD4.007.pdf.

16 N. Jelić, L. Kos, J. Krek, **Warm plasma-boundary properties**, 21st International Conference Nuclear Energy for New Europe, Ljubljana, Slovenia, September 5-7, 2012, pp. 1118.1-1118.9

17 S. Kuhn, D. D. Tskhakaya, N. Jelić, L. Kos, J. Duhovnik, **Polytropic-Coefficient Function (PCF) vs. polytropic-exponent function (PEF)**, 39th IEEE International Congress on Plasma Science, ICOPS 2012 : 8-12 July 2012, Edinburgh, Scotland, Edinburgh, IEEE Nuclear and Plasma Science Society, 2012.

18 N. Jelić, L. Kos**, Ion-sound Velocity at the Plasma Edge in Fusion-Relevant Plasmas**, Nuclear Engineering and Design (2013), doi:10.1016/j.nucengdes.2012.12.004. **261** (2013) 269–274.

19 L. Kos, D.D. Tskhakaya, Sr., S. Kuhn, N. Jelić, **Debye-sheath properties in the Tonks–Langmuir discharge with warm neutrals**, Journal of Plasma Physics (2013), doi: 10.1017/S0022377813000949. **79** (2014),
20 N. Jelić, L. Kos, **Towards Possible Control of Plasma Outflow in Fusion-Relevant Devices via Employing Virtual Terminating Surfaces**, 22nd Int. Conf. Nuclear Energy for New Europe, Bled, Slovenia, 9–12 Sept 2013, 1403.1–1403.8
21 S. Kuhn, D. D. Tskhakaya, L. Kos, **The non-marginal Bohm condition in the collisionless plasma diode**. 40th European Physical Society Conference on Plasma Physics, Espoo, Finland, 1 – 5 July 2013, P1.410[1– 4] http://ocs.ciemat.es/EPS2013PAP/pdf/P1.410.pdf
22 N. Jelić, L. Kos, J. Krek, J. Kovačič, T. Gyergyek, A. J. Christlieb, J. P. Verboncoeur, **Ionization front in a gas-filled diode during electrical breakdown**. 49th International Conference on Microelectronics, Devices and Materials & the Workshop on Digital Electronic Systems, Sept. 25 - 27, 2013, Kranjska Gora, Slovenia, 109–114.
23 T. Gyergyek, J. Kovačič, N. Jelić, L. Kos. **Sheath formation in front of a negative electrode close to plasma potential studied by PIC simulations**. 49th International Conference on Microelectronics, Devices and Materials & theWorkshop on Digital Electronic Systems, Sept. 25 - September 27, 2013, Kranjska Gora, Slovenia. 115–120.
24 N. Jelić, L. Kos, J. Krek, J. Duhovnik, **Kinetic theory and simulations of moderately strong stationary double layers with warm ions**. IEEE International Conference on Plasma Science (ICOPS, 16-21 June 2013, San Francisco, California, USA, doi: 10.1109/PLASMA.2013.6633373

3 CONCLUSIONS AND OUTLOOK FOR FURTHER WORK

Integrated tokamak modelling with externally coupled core and edge transport codes enabled our participation in EUFORIA and ITM-TF projects. Possible future activities on this subject should include coding of these new transport models in SOLPS-B2.5 and testing of these transport models by means of simulations of experiments in various tokamaks. Further theoretical model development (plasma wall transition under complex conditions, localized electrostatic structures in plasmas i.e., sheaths and double layers paralllel and normal to magnetic field lines), probe theory. Future developments of computational methods and applications i.e., upgrading of existing kinetic PIC and hybrid codes and development and applications of new codes e.g., 3D treecode package - from scratch, for applications for simulating plasma wall transition phenomena and diagnostic probes. Further theoretical work in numerical method development for solving demanding sets of integro-differential equations for solving plasma sheath transition problems under complex conditions.

4 REFERENCES

1 Fichtmüller M. et al 1999 J. Nucl. Mater. 266-269 330
2 Lönnroth J.-S. et al 2003 Plasma Phys. Control. Fusion 45 1689
3 Pereverzev G. V. and Yushmanov P. N. 2002 ASTRA – Automated System for Transport Analysis, IPP 5/98
4 Schneider R. et al 2006 Contrib. Plasma Phys. 46 3
5 Bürbaumer H. et al 2001 J. Nucl. Mater. 290-293 571
6 Erba M. et al 1997 Plasma Phys. Control. Fusion 39 261
7 Bateman G. et al 1998 Phys. Plasmas 5 1793
8 Tardini G. et al 2002 Nucl. Fusion 42 258
9 Tala T. J. J. et al 2002 Plasma Phys. Control. Fusion 44 A495
10 Garzotti L. et al 2003 Nucl. Fusion 43 1829
11 Becker G. 2004 Nucl. Fusion 44 933
12 Garbet X. et al 2004 Plasma Phys. Control. Fusion 46 1351

13 Garbet X. et al 2005 Plasma Phys. Control. Fusion 47 957
14 Counsell G. F. et al 1999 J. Nucl. Mater. 266-269 91
15 Connor J. W. et al 1999 Nucl. Fusion 39 169
16 Fundamenski W., Sipilä S. and JET-EFDA Contributors 2004 Nucl. Fusion 44 20
17 Kirnev G., Fundamenski W. and Corrigan G. 2007 Plasma Phys. Control. Fusion 49 689
18 Fundamenski W. et al 2007 Nucl. Fusion 47 417

MCNP TRANSPORT CALCULATIONS FOR THE JET TORUS – UPGRADE OF THE JET MCNP MODEL – CALCULATIONS FOR THE GAMMA RAY CAMERA

Igor Lengar, Luka Snoj

Jožef Stefan Institute
igor.lengar@ijs.si

1 INTRODUCTION

Calculations of neutron/gamma fields are an essential part to be performed in parallel to the experiments, connected to diagnostics in fusion devices. Transport calculations, mainly with the widely used code MCNP, have been performed at JET for a long time. One issue is, however, that MCNP models had become outdated, since the recent changes in the torus were not introduced into them.

The aim of the project was the upgrade of the MCNP models of the JET torus, which have originally mimic the situation as of the year 1998, when they were prepared. The emphasis was on the MCNP model of octant 3 and it has been updated to the last C-wall state and to the state after the Be-wall introduction.

A verified MCNP model is necessary for quality results. The new updated MCNP model has thus been tested, uncertainty analyses was performed and the model used in order to check for hidden errors and additionally modified for specific purposes. The upgrade of the MCNP model was done mainly on the basis of the available CATIA files. The verified model then enabled the determination of the neutron field inside the torus and at specified location outside of the torus.

A lot of calculations have been performed with the new model, most of them as a support for neutron diagnostics systems and activation of some of the torus components following neutron irradiation. A large set of calculations were performed as a support for Gamma-Ray Camera (the KN3) upgrade – in the frame of the Neutron Attenuators Project. The final calculations were made as a support for the neutron calibration, which was performed in April 2013.

The most important calculations performed are described in the continuation.

2 WORK PERFORMED IN 2007 – 2013

The upgrade of the MCNP model is a continuous task, the major results, obtained are briefly presented in the continuation.

2.1. Upgrade of the JET MCNP Model of Octant 3

A general feature of all MCNP models for the JET torus is that their underlying geometry is much simpler as in case of the real engineering model. A few of the upgrades to the model, as used for the calculations, are described below.

Intermediate vacuum port

The irradiation end KN2-3U is one of the major diagnostics for neutrons. The vacuum port closest to this irradiation end (IE) has been changed to represent the true double walled, rounded structure. The IE has been reduced in size, since it was found, that the previous model, based on an available engineering drawing, does not correspond to the recently obtained pictures of the IE and was even too large to fit into the port. The structures around the IE within the double wall vessel structure have also been modelled.

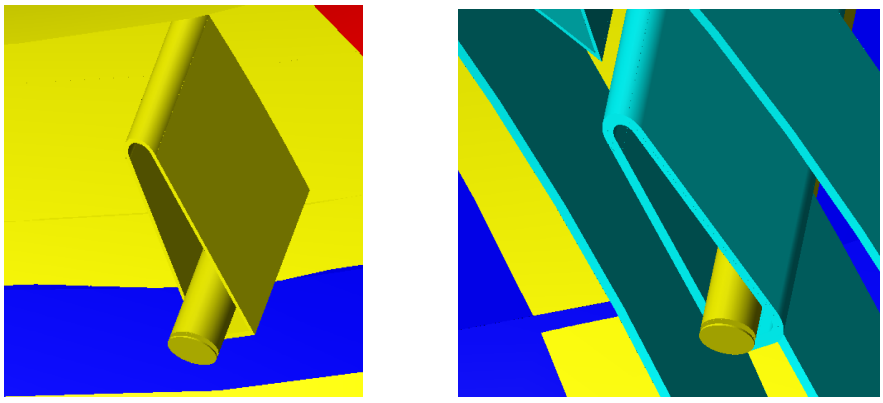

Figure 1: Comparison of the details of the Intermediate Vacuum Port between the last two MCNP models (pictures produced with MCAM).

Double vessel wall

The vessel wall was homogenised in the original model. In reality the wall is composed of two layers with a hollow space in-between, which is adequately modelled.

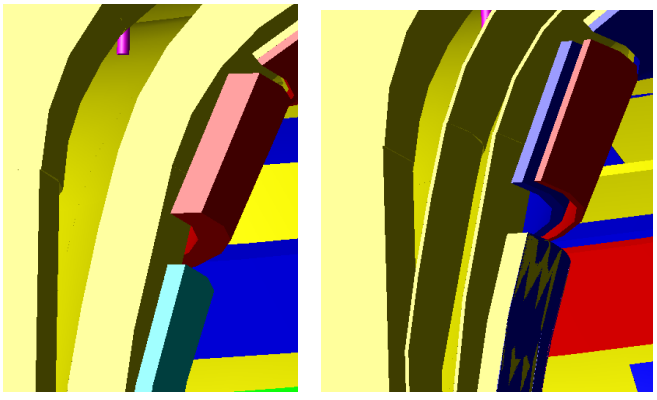

Figure 2: Change of the homogenised vessel to the real double wall structure.

Adjustment of the vacuum-vessel shape

It was found that the vessel in the previous MCNP models is of a slightly different shape and size than presented in the engineering models. The difference in the position of particular vessel points ranged from 1 to 5 cm between both models. The MCNP model was modified in order to correspond to the engineering model.

2.2. Analyses of the Change in Neutron Field Between the C-Wall and Be-Wall Models

Difference in flux distribution

One of the aims was the estimation of the changes in the flux distribution due to the change from C-wall to Be-wall torus. The emphasis was given on the calculation of detector response of the KN2-3U Irradiation end. An analysis of the differences in neutron fields, calculated with both models, was performed.

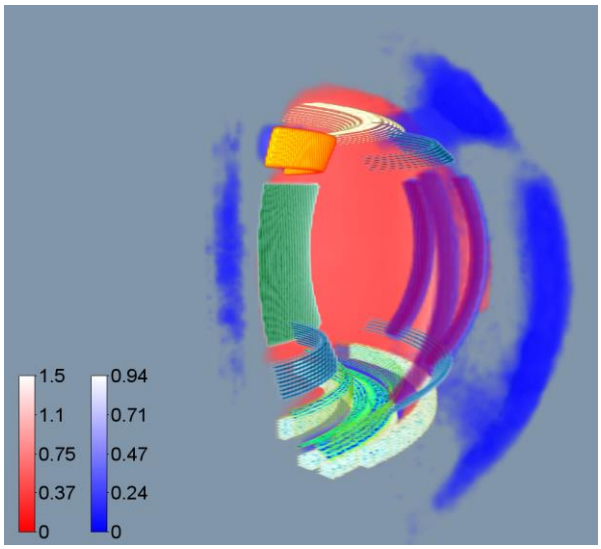

Figure 3: Graphical distribution of the difference in the thermal (En < 0.625 eV) neutron flux: red shaded – higher flux in Be-wall model; blue shaded - higher flux in C-wall model.

The calculations were performed by using the MCNP5 1.40 code with a set of FENDL 2.1 cross-section data libraries; for the nuclides, for which the FENDL data is not available the ENDF 7.0 cross-sections were used. In order to get insight of the influence of the wall change on the neutron flux distribution, the difference in the neutron flux between both models was calculated. These calculations have been performed for three energy groups: thermal (below 0.625 eV), epithermal (0.625 eV – 100 keV) and fast (above 100 keV). The change in the neutron flux distribution between the C-wall and Be-wall models was examined. Long runs have been performed with both models and the neutron flux was tabulated. The difference between both flux distributions has been examined. Examples of the changes between the neutron fluxes are presented in Figures 3 to 5 for the three energy bins, in which the regions with the higher neutron flux in the Be-wall model are red or orange shaded and the regions with the higher flux in the C-wall model are blue or purple shaded. The graphics results are presented in the form of the relative difference: 0 on the color scale means equal flux, 1 means 100% difference.

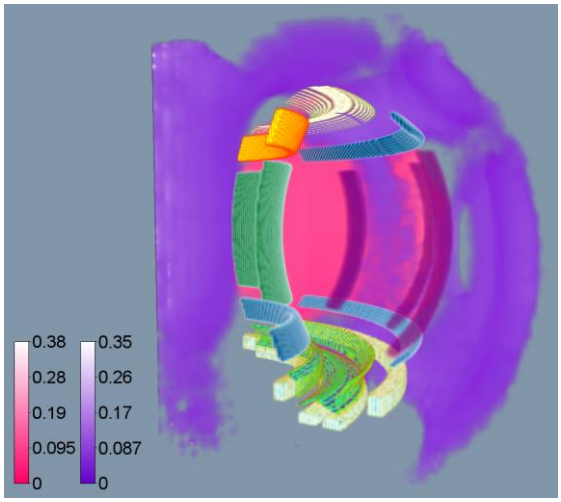

Figure 4: Graphical distribution of the difference in the epithermal (0.625 eV < En < 100keV) neutron flux: cyan shaded – higher flux in Be-wall model; purple shaded - higher flux in C-wall model.

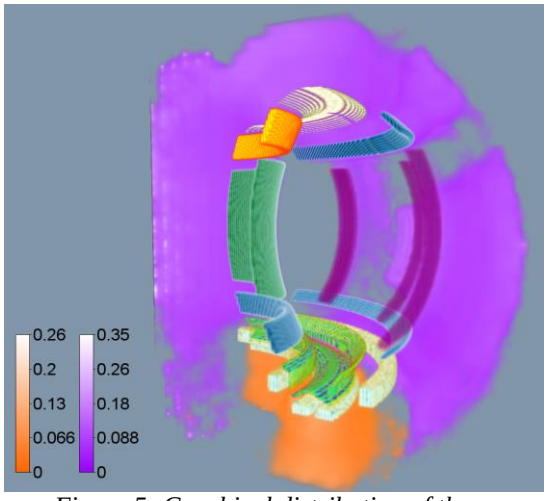

Figure 5: Graphical distribution of the difference in the fast (En >100keV) neutron flux: orange shaded – higher flux in Be-wall model; purple shaded - higher flux in C-wall model..

The shape of the in-vessel structures can be easily deduced from the figures and it can be seen that in general the flux inside the vacuum vessel is higher in the Be-wall model and lower outside. In case of the fast flux a change below the divertor is visible, implying that the fast flux below the new tungsten divertor is somewhat higher than in the case of the previous carbon divertor. This could be attribu table to the smaller moderation of neutrons down to epithermal energies in the case of tungsten with regards to carbon. Tungsten also has a lower number density as carbon but a higher total neutron cross-section.

Difference in the neutron flux

The neutron flux was monitored at several positions. The changes in the values of the neutron flux in three energy groups, corresponding to different components, which were exchanged in the C-wall to obtain the Be-wall model, are presented in Table 1. The flux was monitored on larger areas at the specified positions of the torus: inside the horizontal vacuum port, below the divertor and above the saddle tile. These three positions are presented in Table 1, divided into three energy groups.

energy range	**< 0.625 eV**			**0.625 eV – 100 keV**			**> 100 keV**		
introduced change	inside horiz. port	below divertor	above saddle tile	inside horiz. port	below divertor	above saddle tile	inside horiz. port	below divertor	above saddle tile
	Contribution / difference in % *								
inner limiters, wall	-2.4	-7.4	-3.6	-0.2	0.7	0.3	0.4	1.4	1.7
divertor	-1.3	-13.0	-4.9	-0.8	2.8	-0.4	0.2	13.5	0.2
coil protection	-1.0	-1.4	-0.6	-0.2	-0.3	0.2	0.0	0.5	0.9
poloidal limiters	1.4	-2.2	-1.6	0.7	0.2	-0.2	0.7	0.6	0.4
mushroom limiters	-0.1	-0.2	-0.2	0.0	0.0	0.0	0.0	0.0	0.0
Be saddle tiles	0.7	3.3	1.8	0.2	0.4	0.5	-0.1	-0.1	-5.8
LHCD	-1.8	-0.6	-0.4	0.0	-0.1	-0.2	1.9	0.2	0.1
RF antenna	-0.7	-2.2	-1.0	0.0	-0.1	-0.3	0.2	0.2	0.1
C-wall to Be-wall model	**-5.2**	**-23.8**	**-10.4**	**-0.3**	**3.7**	**-0.1**	**3.5**	**16.4**	**-2.3**

Table 1: Contribution of the change of individual components to the neutron flux, divided into the thermal, epithermal and fast component, at three positions in the torus. Positive values represent flux higher in the Be-wall model.

2.3. Support of neutron yield calibration

Calculations with the model were performed in parallel with calculations, carried out by Luka Snoj with a simpler but quick-running model of the JET tokamak in order to support the neutron yield calibration, which was carried out in April 2013. The quick-running 360° model of the JET torus and its torus hall has a rectangular cross-section. The model, developed in the frame of this project is of larger detail and helped in studying effects of the simplification of the calculations with the former model.

A strong Cf-source was deployed in the torus and the detector responses and correction factors for individual detector positions for many effects, e.g. corrections which originate from the undesired shielding of the source by the mascot robot arm holding the source, were calculated. During the source calibration all together more than 200 calibration points were measured. All correction factors were calculated also with the detailed 360° model for comparison with results obtained from other models.

Upgrade of the 360° model – inserting unsymmetrical components

The mascot robot boom, holding the ^{252}Cf source during the calibration, was modeled in the frame of the task for calculation of correction factors with the simplified model. A visual presentation of the MCNP model of the boom is pictured in Figure 6.

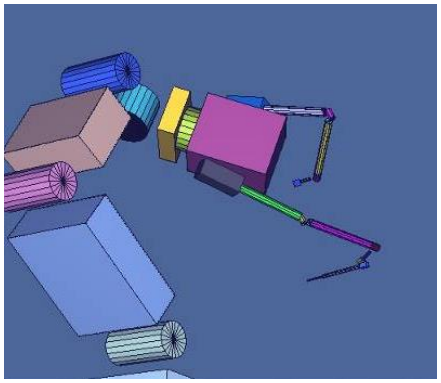

Figure 6. Visual presentation of the mascot robot boom.

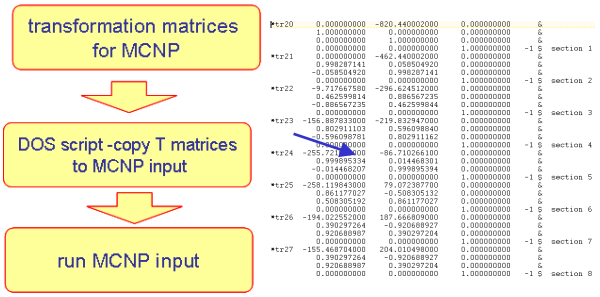

Figure 7: schematic presentation of the script for automatic insertion of the boom into the 200 MCNP models.

For each of the calibration points the boom has a different shape and consequently the MCNP models differ from each other. The number of calibration points is large, over 200, which makes an automatic conversion of the remote handling boom teach files into the boom MCNP models necessary. The second step, which has been done in parallel in the frame of the task of calculation the correction factors with the simplified model, is the insertion of the appropriate boom into the MCNP model of the torus, which jointly present the model for correction factor calculations. For this reason the present model was accordingly adjusted for automatic insertion of the more than 200 boom configurations. Three steps automatic procedure of insertion of the transformation matrices into the MCNP input file and its usage are presented in Figure 7. The visualisation of the boom inside the torus is presented in Figure 9, using the visualisation module of the automatic conversion tool MCAM.

The original model comprised only a 90° sector of the torus. A 45° sector of this model was then used in order to fill the whole torus. The previous step was a model of the torus, filled with eight identical sectors, i.e. eight equal octants (Figure 8 (a)).
The individual sectors were filled with according components. For this reason the structure of the whole torus was broken down into the vacuum vessel, which is duplicated 8 times, and into the components inside the vacuum vessel, which are individually modeled, i.e. the ILW antenna, lower hybrid, wide poloidal limiters, narrow poloidal limiters or different sets of inner limiters.

Each of these components was modeled in its own universe and positioned into the right place, possibly several times replicated as in the case of poloidal limiters. The obtained model is pictured in Figure 8 (b)).
Additionally some ex-vessel structures as the transformer limbs and torus hall were inserted. A visualization of the last model including the boom inside the torus is presented in Figure 9. The vessel is removed from the picture for the in-vessel structures to be visible.

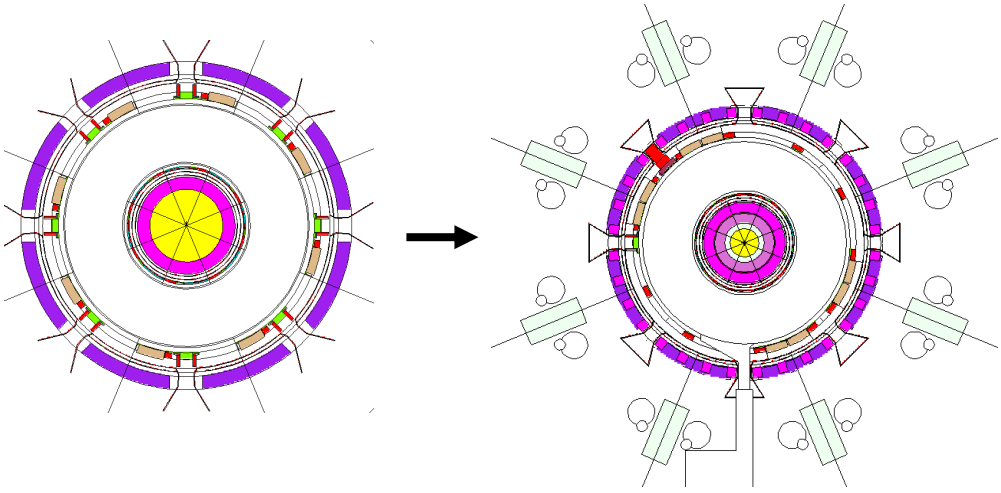

Figure 8: Graphical presentation of the change from the torus model composed of 8 identical sector models to the model, in which in-vessel components are modeled individually. The later model is also adapted to insertion of the boom (from below) and includes some ex-vessel structures.

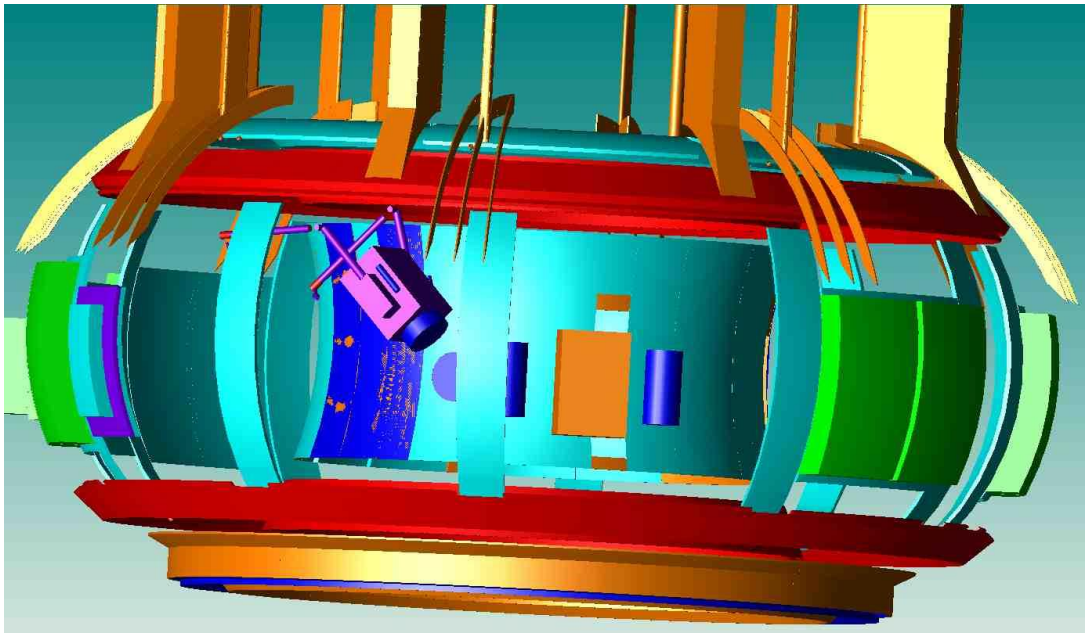

Figure 9: Presentation of the major in-vessel structures and the boom, inserted into the model. Graphics by MCAM.

2.4. Calculation of correction factors for KN2-3U and KN1

The calculation of correction factors using the MCNP Monte Carlo program is computationally a demanding task. For each configuration two runs with the ^{252}Cf source have to be performed; one with the remote handling boom in the model and one without the boom. The results are then compared in order to estimate the correction due

to the boom. Each single run takes from one week to over a month to run on a single processor. Usage of larger computer clusters is thus necessary in order to perform the calculations in a reasonable time.

During the neutron source calibration, two neutron detector systems are measured – the KN2-3U in-vessel activation system and the KN1 ex-vessel fission cell system. During the actual calibration of detector systems with the Cf source the large majority of calibration points, more than 200, was chosen to calibrate the KN1 system, only three locations were chosen for dedicated calibration of the KN2-3U system.

KN2-3U calculations

The calculated response including the calibration factors for three dedicated points, are presented in Table 1. Each calibration factor is presented in the form of the ratio of the corresponding response (activations of Indium atoms for the KN2-3U system and counts of the fission counter for the KN2 system per 10^9 source neutrons) for two cases: response (boom present)/ response (boom absent), i.e. the introduced perturbation due to the boom.

location	absoutle source position			response (no. of activated atoms, boom absent)	correction factor
	x	y	z		
midplane	-288.5	-58.3	30.2	35.1	1.02
middle position	-290.9	-59.1	104.7	97.7	1.00
upper position	-315.6	-63.6	159.6	744.8	0.99

Table 1: Calculated KN2-3U response (boom absent) and corresponding correction factors for three source points (presented in absolute numbers relative to the torus coordinate system).

It can be observed from the table that the remote handling system for the three configurations does not present a significant influence on the calibration. The absolute values for the response have been confirmed by calculations with a MCNP model for JET by Sean Conroy. The model is suitable for KN2-3U response and calibration factors calculations.

KN1 calculations

The number of calculations performed for the KN1 correction factors was larger than for the KN2. The results were compared to calculations with a MCNP model from Sean Conroy (CCFE, UU), also calculating KN1 correction factors. That model was to a fair amount adjusted in order to fit the measured data. In addition Sean Conroy uses a low density Inconel ring on the outer side of the torus structure in order to mimic the many components, found around the torus, which cannot be modeled explicitly for MCNP calculations.

The comparison shows, that lacking these ring of low density Inconel around the torus increases the value of the response of fission chambers by a factor of a few. The conclusion was that the model was not suitable in the present form for quantitative calculations of the detector response, it can however be used for qualitative estimation of the response and for calculation of correction factors for the KN1.

2.5. Gamma-Ray Cameras - Neutron Attenuators Project

A coherent set of upgrades of the gamma-ray spectrometry systems were performed at JET in for the better support the experimental program. In particular, by using adequately chosen neutron-attenuating materials to reduce both the neutron background, and the neutron-induced gamma-ray background, the measurements of the fast ions could be performed in every JET discharges. With the previous diagnostics capabilities the gamma-ray signal was completely wiped out by the neutrons even in JET discharges using a few MW's of neutral beams.

The aim of the larger project GCR was the installation of attenuators for neutrons, which should shield the KN3 camera (neutron-gamma vertical camera at JET). The attenuator material is water. The task for the particular project was to estimate the influence of the proposed KN3 neutron attenuators on the neutron field. The calculations were performed on the basis of Monte Carlo method using the MCNP code. The three major problems addressed were:

- attenuation factors for neutrons and gammas in the neutron attenuator
- neutron induced gammas in the neutron attenuator
- possible inscattering of neutrons into the detector region from the attenuator in the parking position.
- neutron cross-talk between cannels

The transmission factors for neutrons have been found to amount to roughly 0.01 for DD neutrons and 0.001 for DT neutron, depending also on the camera cannel. In addition to the transited neutrons, some an equal or larger neutron flux was found to scatter into the detectors from the neutron attenuator, the energies of these neutrons being however thermal and thus separable form the original neutrons.

The attenuators are meant to attenuate neutrons but not disturb the gamma flux. It is thus also important, that there is not too many induced γ radiation from the attenuators, which could disturb the signal. The number of the induced γ rays hitting the detector per original neutron, which would reach the detector is 1% is or less. The main γ line in the spectrum of the induced gammas is the line due to thermal neutron capture on hydrogen with an energy of 2.22 MeV; more than half of all induced γ rays in the attenuator are concentrated in this line and there are virtually no γ rays with higher energies.

Another problem studied was the value of the neutron cross-talk between channels, i.e. the ratio of neutrons, reaching a particular detector, traveling at some point through another channel's flight tube, to the total flux in the detector; a schematic presentation and three examples of calculated neutron paths, contributing to the cross-talk, are graphically presented in Figures 10 and 11.

It is found, that the cross-talk is virtually zero for neutrons of energies above 2 MeV, i.e. energies with significant neutron fluxes. At lower energies, at which the fluxes are however significantly smaller, the cross-talk is considerable. This cross-talk should not present a significant problem, since the absolute value of the flux is small

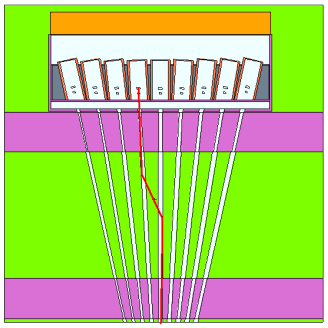

Figure 10: Neutron cross-talk

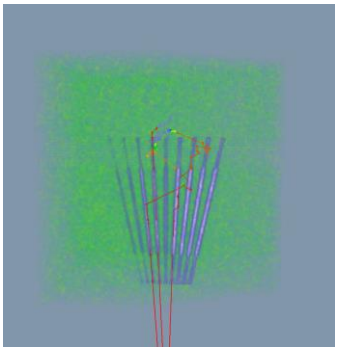

Figure 11: Graphical presentation of three typical neutron tracks, contributing to the cross-talk of the central channel.

with respect to the peak of direct neutrons. Furthermore, the neutron detectors discriminate between the low and high energy neutrons.

3 CONCLUSIONS AND OUTLOOK FOR 2014

The 3D MCNP model of JET was upgraded in order to be optimized for calculation of diagnostics response and of the correction factors, needed for the neutron source calibration. The boom was inserted into the upgraded 360° MCNP model, the correctness of the insertion was examined. The model is optimized for the automatic insertion of the boom to the necessary more than 200 positions (automatic insertion of transformation cards).

The correction factors in the frame of the calibration of JET neutron detector systems with a Cf source were performed with the final model. The calculations for the calibration points for the KN2-3U were found to be adequate and that the detector response and calibration factors can be used.

A large effort in computer time was invested for the calculation of the correction factors for the 200 calibration points of the KN1 system. Analyses shows that due to the lack of a low density Inconel ring in the surrounding of the torus, which approximates the many ex-vessel components, a too high detector response is obtained.

In the frame of the present task, the MCNP model was further upgraded. It will be used in the future for calculations of the detector responses, in particular of the KN2-3U, needed as support for experimental work. In the year 2017-2018 a DT campaign is planned at JET, what will be preceded by a DT calibration. The model is planned to be used for calculation of correction factors in support of this calibration and for the subsequent DT plasma measurements.

The work on addressing the neutron flux in narrow flight channels will be continued by the study of the KX1 beam line in the frame of the Gamma Ray Spectrometer Upgrade Project.

CALCULATIONS TO SUPPORT JET NEUTRON YIELD CALIBRATION

Luka Snoj, Igor Lengar, Aljaž Čufar, Andrej Trkov

Jožef Stefan Institute
luka.snoj@ijs.si

1 INTRODUCTION

Neutron yield measurements are the basis for the determination of the absolute fusion reaction rate and the operational monitoring with respect to the neutron budget during any campaign for the Joint European Torus (JET).

After the Carbon wall to ITER-Like Wall (Beryllium/Tungsten/Carbon) transition in 2010-11, confirmation of the neutron yield calibration will be ensured by direct measurements using a calibrated ^{252}Cf neutron source (NS) deployed by the in-vessel remote handling (RH) boom and mascot manipulator inside the JET vacuum vessel [1]. This calibration will allow direct confirmation of the external fission chambers (FC) calibration which was the original JET standard [2] and provide the first direct calibration of the JET activation system inside the torus.

In total more than 200 locations of the NS inside the tokamak will be used for neutron monitor calibrations. The locations of all NS calibration points inside the torus are schematically presented in Figure 1. There are 40 locations in the toroidal direction round the torus, each location having 5 positions: one is centrally located (C) in the plasma centre 30 cm above the tokamak midplane and 4 positions are offset from this central one by 0.5 m in the, upper (U), lower (L), inner (I) and outer (O) directions. These point source measurements simulate 5 rings round the torus, a central ring, plus up, down, in and out.

These desired locations and the preferred source-baton orientations for physics needs were given to RH group who produced the required virtual reality (VR) files of the RH dispositions of the mascot and the boom.. These files contain the orientation information for all joints in the boom/mascot and enable the movements between successive locations.

Preparation of all RH movement files and simulating all RH movements in advance is needed in order to ensure that the boom + mascot move within strictly approved safety limits, e.g. away from the vessel edge.

In order to safely handle the neutron source, it will be placed inside and at one end of a specially designed tube (the ‘source baton’) which is small enough to be carried within a shielded transport flask. At JET, the neutron source will be deployed into the JET vessel via the octant 5 ‘mascot’ manipulator. The source baton can be picked up by and locked on to a specific RH tool called the ‘mascot baton’ which is borne by the

mascot. The 2-baton combination provides remote source handling, while ensuring adequate separation of the neutron source from the mascot body. That separation is required in order to reduce neutron scattering from the mascot manipulator, to reduce activation of the manipulator and to limit the dose on the manipulator cameras [4].

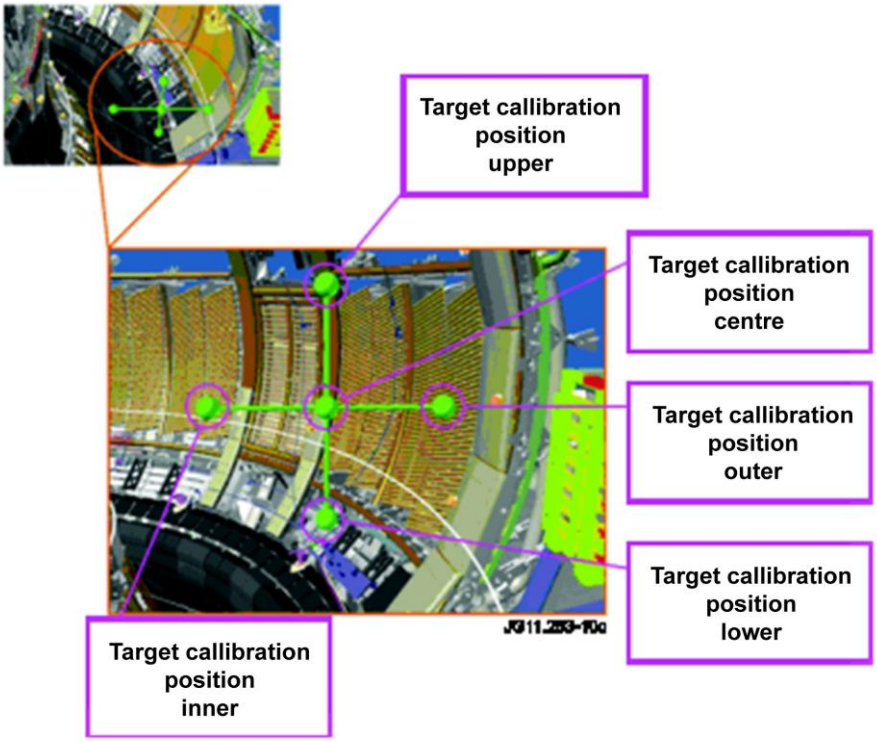

Figure 1: Draft of in-vessel scan pattern. There are 5 points at each toroidal location round the vessel, i.e. 5 rings of points, plus some subsidiary points at other particular locations. Only part of the JET structure is shown. KN1 denotes external neutron monitors and KN2 denotes the JET activation neutron monitoring system.

As in all such calibrations, neutronic calculations are required to support the physics, safety and engineering efforts. Many are based on Monte Carlo modelling using the advanced Monte Carlo transport codes, such as MCNP [5].

2 WORK PERFORMED IN 2007 - 2013

Results or our work performed in the period 2007-2013 are described in the sections below. It is important to note that the majority of result were directly applicable in the experimental neutron yield calibration. Practically all milestones and deliverables were achieved with some exceptions, which occurred due to rescheduled experimental campaign, which was not under our control. During this period we attended several mobility missions in order to improve the efficiency of our collaboration with the JET operator. Here we could expose two long missions, one 6 – month mission in 2010 and on two month mission in 2013. The results of our work were published on several conferences and in SCI journals. More publications will follow in the coming months.

2.1. Contributions to the external neutron monitor responses

Firstly we perform a set of calculations using a simplified model of the JET tokamak to understand and estimate the various effects on the JET FC systems, such as: neutron source position, neutron source spectrum, importance of the ports, presence of large structures outside the tokamak (e.g. plasma diagnostics, plasma heating systems, iso-containers, etc.) and scattering back from the torus hall wall (room return effect).

The results of the calculations will serve as a guide to features which are important in the calibration. In addition the results will provide guidelines in optimizing the neutron source positions for detector calibrations. A thorough analysis of the external neutron monitor response is presented in the paper [3]

The structures (e.g. vacuum vessel, coils, mechanical structure, etc.) of the simplified JET model are modelled as homogeneous layers. The cross section of the model in the poloidal plane is rectangular in shape as in the model of Laundy and Jarvis, 1993 [2]. However we conserved as much as possible the most important neutron transport parameters, consistent with the information available at the time, i.e. component mass, material composition, major dimensions and vacuum vessel surface to volume ratio. The geometrical MCNP model of the JET tokamak is depicted in Figure 2.

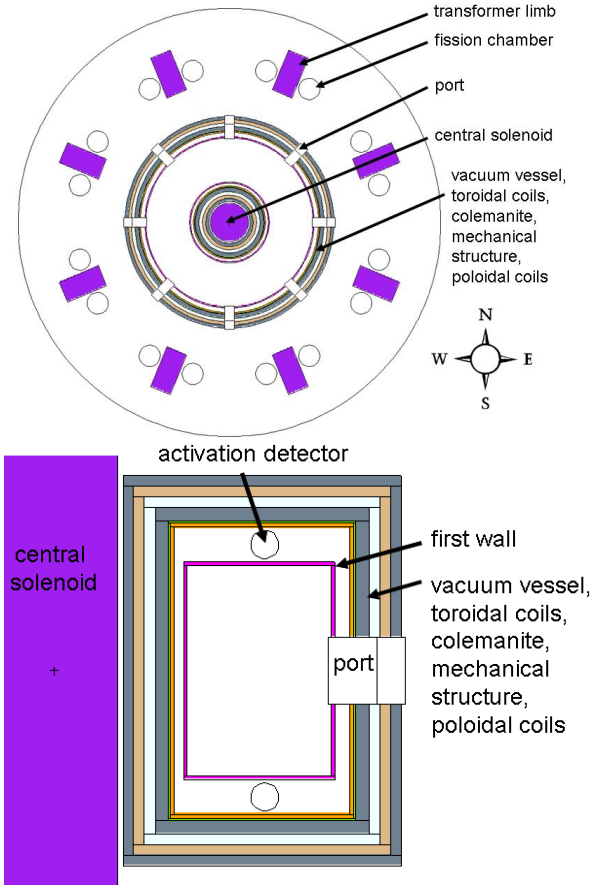

Figure 2: Cross sectional view of the MCNP JET geometrical model. Horizontal section of the JET tokamak (top) and half of the vertical section of the tokamak (bottom).

The FC response was calculated in the FC detectors located on the transformer limbs. It is important to note that most of the results are presented as detector response versus detector position rather than detector response versus point neutron source position. If we wanted to calculate certain detector response versus source position, we had to run as many calculations as many source positions we would want to examine. As it takes approximately one day to run single calculation, such approach would be very time-consuming and inconvenient. Hence the approach of tallying several detectors at different positions in a single run is much more time-effective. Especially as the simplified JET tokamak model used in our calculations is rotationally symmetric around the vertical axis.

The first measurement in the neutron detector calibration campaign will be measurement of the FC response versus source position in the torus. As discussed above we actually calculated the FC response versus FC position. The calculations were performed for two limiting source positions, one in front of the E port (0 °) and one exactly between the E and NE ports (22.5 °). By performing additional runs with source at 5 °, 10 °, 15 °, 20 °, and 25° and considering the symmetry relations in the computational model of the tokamak we were able to reconstruct the FC response versus source position for the simple model without any perturbations (Figure 3). The FC response versus detector position is symmetric as the detectors are arranged symmetrically in the computational model.

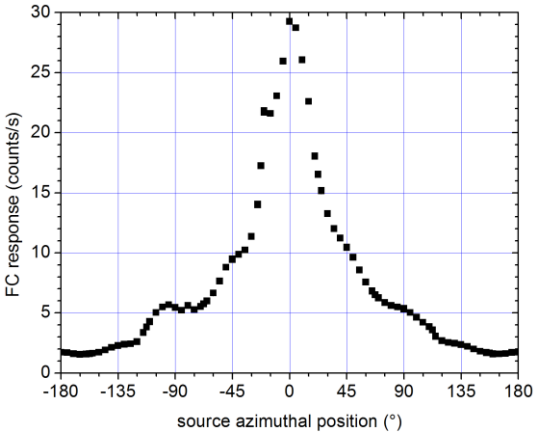

Figure 3: FC response versus source position

The FC response versus source position is strongly asymmetric due to the position of the detector on one side of the transformer limb, which shields the detector from neutrons from ports behind that limb (Figure 3). A step like function of FC response versus position with steps around the ports suggests that the neutron source position relative to the ports is extremely important for external neutron detectors indicating that the majority of neutrons reach the detector via ports.

2.2. Effect of the JET remote handling system

The JET RH system contains some substantial objects, which will be inside the vacuum vessel during the calibration, hence it is expected that these objects will significantly affect the neutron transport from the NS to the neutron monitors. The purpose of this paper is to begin the study of the effects of major components of the JET RH system on neutron monitor response.

Firstly we developed a simplified geometrical computational model of the JET RH system in MCNP based on the engineering drawings. In parallel we developed a script that translates the RH movement data to transformations of individual geometrical parts of the RH model (boom + mascot) in MCNP. Secondly we performed a benchmarking of the model to confirm accordance of the target source and RH system positions from our model with the originals. In the last phase we placed the RH system model in the simplified MCNP model of the JET tokamak [12] and studied its effect on neutron monitor response for some characteristic deployment configurations. As mentioned earlier the purpose of our work is to be able to calculate the neutron monitor response correction factors for every calibration point, i.e. for every JET RH system configuration. Hence we have to prepare MCNP input for every source point, each featuring a different arrangement of the JET RH system components. In order to do this we wrote a script named RH2MCNP (in Fortran 77) that reads the JET RH coordinates

and calculates the transformations of each RH system component in the MCNP model and computes the location of the neutron source.

Additional scripts and batch procedures in DOS are then used to couple the RH teach files containing all RH coordinates with the RH2MCNP script and then take the script output (translations, rotation matrices, NS positions) to prepare the MCNP input files run them and extract the necessary data (various neutron monitor responses) from the MCNP output. For easier understanding a simple flowchart of the process is presented in Figure 4.

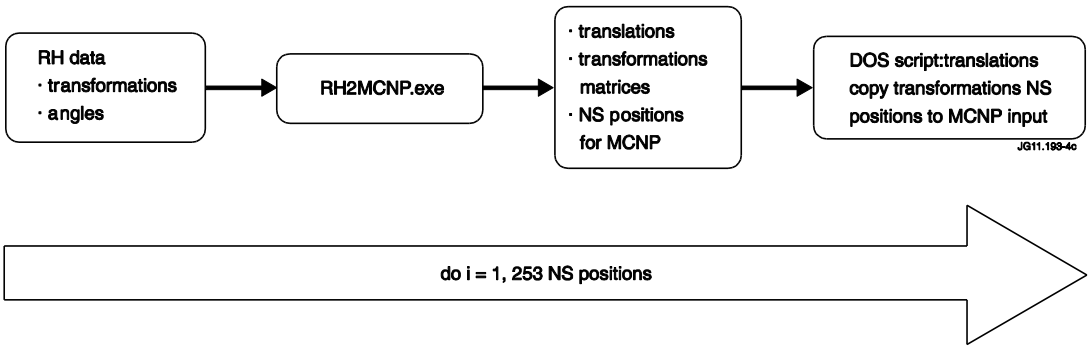

Figure 4: Flowchart of the procedures to model the JET RH system in MCNP.

Estimation of the effect of the major components of the JET RH system (the mascot manipulator and the boom) on the JET neutron monitor response, from the external fission chambers on the transformer limbs inside the vacuum vessel was performed in the following way. Firstly we calculated the undistorted neutron monitor response versus NS position for every calibration point, i.e. a response without the JET RH system in the vessel. Secondly we did the same calculation with the exception that the JET RH system consisting of the boom and the mascot manipulator holding the NS holder was modelled inside the tokamak in a particular configuration. Then we calculated the RH calibration factor for the i-th NS position, $C_{RH,i}$, as the ratio between the distorted neutron monitor response, $\Phi_{RH,I}$ and the undistorted response, $\Phi_{0,i}$:

$$C_{RH,i} = \frac{\Phi_{RH,i}}{\Phi_{0,i}} \qquad (1)$$

The computational model of the JET tokamak featuring the JET RH system is depicted in Figure 7. In order to understand the effects of the JET RH system on the external neutron monitor response, the calculations of the correction factors were performed for all the 16 notional fission chambers in the model. However special attention was paid to the three fission chambers, denoted by D1, D2 and D3 in Figure 7, which are located at the positions of the real fission chambers at JET tokamak. Presenting final RH correction factors for all calibration points is out of scope of this paper. Hence the RH correction factors are presented only for D1, D2 and D3 and for some representative NS positions.

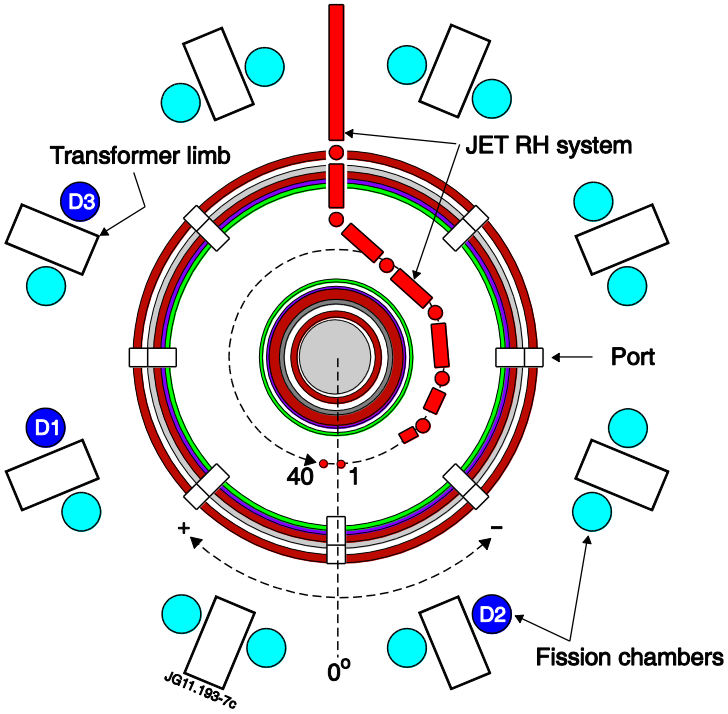

Figure 5: Top view of the MCNP JET geometrical model with the JET RH system deploying the source at location 1 C. The section is made at the tokamak midplane (z=0). As the mascot manipulator is tilted relative to the XY plane only the boom is visible. The positions of the JET external neutron monitors are denoted by D1, D2 and D3.

Our previous studies showed that the highest contribution to a certain FC is via the closest port and the second highest contribution is via the port closest to the neutron source. There is an additional effect due to the massive boom blocking neutron exit from the Octant 5 port. The effects of the JET RH system depend on the RH configuration and on the neutron monitor location. The response can be decreased by the boom blocking a port or increased by favourable scattering.

Calculation of final RH correction factors for all calibration points is out of scope of this paper. Hence the RH correction factors are presented only for some particular cases and for the central NS positions, which are the most representative as they correspond to the plasma centre. Special attention was paid to the three fission chambers, denoted by D1, D2 and D3 in Figure 5, which are located at the positions of the real fission chambers at the JET tokamak.

First we calculated the undistorted detector response for the central NS position (Figure 6 above). The FC response curve versus NS position represents the contribution to individual detector response from a certain NS position. It is found that the results are in agreement with [3], i.e. the neutron monitor response is the highest when the NS is closest to the detector, except for the position, which is approx. 30° from the detector. The peak at the latter position is due to a direct line of sight effect through the port, exaggerated because the size of the notional detectors is larger than their real size. Hence the location, shape and height of the peak strongly depend on the shape of the port and of the neutron detector in the computational model.

Secondly we calculated the RH correction factor (as defined in Equation 1) for the NS at the central position and for the FCs at D1, D2 and D3 positions (Figure 6 below). It can be observed that FC response at location D3 is the most affected by the RHS as it is closest to the RH entrance port in Octant 5, which is blocked by the boom. Moreover the FC response for D1 and D2 positions is the most affected by the RHS when the NS is located in Octant 5. It is interesting to note that when the NS is located in the octant close to the FC position, the FC response is only slightly affected by the RHS, i.e. the RH correction factor is slightly larger than unity, mainly due to increased back-scattering from the mascot robot body. All these findings are in agreement with our previous studies showing that the highest contribution to a certain FC is via the closest port and the second highest contribution is via the port closest to the neutron source [3]. The effects of the RHS depend on the RH configuration and on the neutron monitor location. The response can be decreased by the boom blocking a port or increased by favourable scattering.

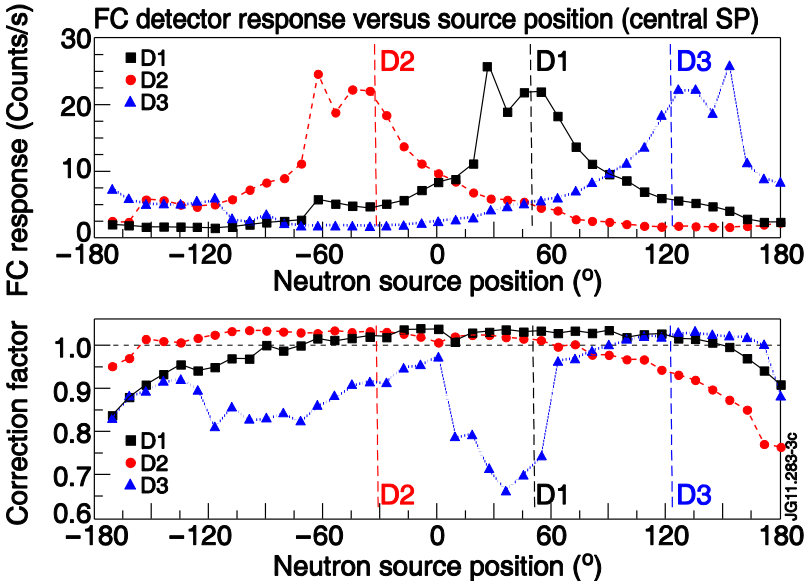

Figure 6: External FC response versus NS position for D1, D2 and D3 FCs (above). Remote handling correction factor versus NS position for D1, D2 and D3 FCs (below). NS is located on the central ring.

The RH correction factors are required for each of the 200 measurement positions. In order to obtain the plasma (volumetric neutron source) relevant response these should then be convoluted with the fission chambers position-dependent response (e.g. Figure above) to generate the integrated ring responses for each detector. First we calculated the ring correction factors for each of 5 poloidal NS positions:

$$C_{RH-IW}^{i,k} = \frac{\sum_{j=1}^{40} \Phi_{RH}^{i,j,k}}{\sum_{j=1}^{40} \Phi_{0}^{i,j,k}} \qquad (1)$$

Secondly we calculated the total correction factor:

$$C^{\,i}_{RH-IW,tot} = \frac{\sum_{k=1}^{5}\left(w_k \cdot \sum_{j=1}^{40} \Phi^{i,j,k}_{RH}\right)}{\sum_{k=1}^{5}\left(w_k \cdot \sum_{j=1}^{40} \Phi^{i,j,k}_{0}\right)}, \qquad (2)$$

where w_k denotes the ring importance factor, which is proportional to the neutron emission from that part of the plasma and strongly depends on the poloidal plasma profile.

In calculations presented in Table, we assumed a flat plasma profile, meaning that all rings contribute equally to the detector response. This is not necessary true for all plasma shapes, especially the common ones which have highly peaked poloidal profiles. For such peaked plasma emission profiles, the data will be biased towards the central ring values.

All final importance-weighted correction factor results for D1, D2, and D3 detectors are presented in Table. For D3 detector the CF is by far the largest for the upper NS position, as its distance from the tokamak midplane is the largest (80 cm).

During the investigation of the effect of the JET RHS on the neutron monitor response, we closely interacted with the remote handling team trying to find the optimal configuration, i.e. the one with the smallest correction factor. For example we changed the RHS deployment geometry for some of the most affected NS points in Octant 5. One such example is presented in Table 1, showing the total correction factors for two RH configurations.

The differences are relatively small meaning that already initial configurations were well optimised. However it can be seen that a reduction in the correction by~ 0.8 % was achieved for the most affected detector D3.

Table 1: Importance weighted RH correction factors for all NS position for two RHs configurations, basic (old) and improved (new).

detector →	old Oct 5 positions			new Oct5 positions			new/old-1 [%]		
NS position ↓	D1	D2	D3	D1	D2	D3	D1	D2	D3
C	1.018	1.013	0.954	1.019	1.016	0.964	0.13 %	0.26 %	1.04 %
L	1.017	1.015	0.965	1.018	1.018	0.974	0.13 %	0.22 %	0.87 %
O	1.013	1.009	0.949	1.016	1.013	0.964	0.27 %	0.37 %	1.58 %
I	1.018	1.014	0.949	1.019	1.016	0.948	0.03 %	0.12 %	-0.09 %
U	1.014	1.009	0.918	1.015	1.011	0.923	0.09 %	0.18 %	0.49 %
total	1.016	1.012	0.948	1.017	1.015	0.956	**0.13 %**	**0.23 %**	**0.81 %**

C-centre, L-lower, O-outer, I-inner, U-upper

For D1 and D2 positions the integral correction factor is ~1.015, which is mainly due to neutrons back-scattered from the mascot body. In D3 position however the integral correction factor is approx. 0.95, mainly due to the boom blocking the port in Octant 5, which is relatively close to the D3 position in Octant 6.

3 CONCLUSIONS AND OUTLOOK FOR FURTHER WORK

Activities such as experimental neutron yield calibrations should always be supported by calculations, in order to guide the planning process and in order to evaluate experimental uncertainties and biases. The work performed in 2009 – 2013 greatly assisted in performing the experimental JET neutron yield calibration as well as to understanding of results. In 2014 we will work on gathering all results and writing papers to be submitted to SCI journals. In addition in 2014 we will start working on calculations to support JET DT calibration, where knowledge and experience gained in the past projects will be very valuable. It should be noted that this whole process of understanding & improving the knowledge of the neutron yield calibration for JET is of great interest for ITER, where the methods and procedures for calibrating the neutron yield monitors have yet to be finally defined.

4 REFERENCES

1 Syme D.B. et al., Fusion Yield Measurements on JET and their Calibration, Nuc. Eng. Des., article in press,
2 Laundy B.J., Jarvis O. N., Numerical study of the calibration factors for the neutron counters in use at the Joint European Torus, , Fusion technology, vol.24, pages 150-160, September 1993.
3 Snoj L. et al., Calculations to support JET neutron yield calibration: contributions to the external neutron monitor responses, Nuc. Eng. Des., vol. 246, p. 191-197, 2011, doi:10.1016/j.nucengdes.2011.07.011
4 Snoj L. et al., Calculations to support JET neutron yield calibration: neutron scattering in source holder, Fus. Eng. and Des., Vol. 87, Issue 11, November 2012, Pages 1846–1852.
5 X-5 Monte Carlo Team, MCNP - A general Monte Carlo N-particle Transport code, Version 5, LA-UR-03-1987, April 24, 2003 (revised June 30 2004).
6 Mindham, T.J., et al., Developments in remote metrology at JET. Fusion Engineering and Design. In Press, Corrected Proof.
7 Haist, B., S. Mills, and A. Loving, Remote handling preparations for JET EP2 shutdown. Fusion Engineering and Design, 2009. 84(2-6): p. 875-879.
8 http://www.jet.efda.org/remote-handling/how/ (August, 2011)
9 Murcutt P. et al.,High level integration of remote handling control systems at JET, Fusion Engineering and Design, In press, doi:10.1016/j.fusengdes.2011.03.072
10 J. P. Both, A. Mazzolo, O. Petit, Y. Peneliau, B. Roesslinger: User Manual for version 4.3 of the TRIPOLI-4 Monte Carlo method particle transport computer code, CEA-Report : CEA-R-6044, DTI, CEA/Saclay, France, 2003
11 TRIPOLI code available from OECD-NEA Databank, http://www.oecd-nea.org/tools/abstract/detail/nea-1716
12 Snoj L. et al., Calculations to support JET neutron yield calibration: modelling of the JET remote handling system, Nuc. Eng. and Des., Vol. 261; str. 244-250, 2013

DEVELOPMENT OF SiC-BASED COMPOSITE MATERIAL FOR FUSION APPLICATION

Saša Novak[1], Goran Dražić[1], Aljaž Iveković[1], Tea Toplišek[1], Katja (Mejak) Köenig[1], Jaro Bele[1], Zoran Samardžija[1], Miran Čeh[1], Kristina Žagar[1], Medeja Gec[1], Aleksander Ford[2], Stephen Skyle-Henney[3]

[1] Department for nanostructured materials, Jožef Stefan Institute, Jamova cesta 39, Ljubljana

[2] Imperial College London, Prince Consort Road, London SW7 2BP, UK

[3] TISICS, 22 Invincible Road, Farnborough, Hampshire, UK
sasa.novak@ijs.si

1 INTRODUCTION

Nuclear fusion offers a prospect of a safe, economical and environmentally friendly source of energy. For the advanced concepts of nuclear fusion, SiC-based fibre reinforced composites were proposed as a structural material for the first wall of the reactor vessel, enabling higher operating temperatures and efficiencies. Already developed techniques for fabrication of SiC_f/SiC composites are currently unable to achieve all of the design assumed values for these materials, therefore further development is needed. The main drawback in fabrication of SiC_f/SiC composites is densification of SiC matrix in 3D woven fabric preform using low activation elements and at temperatures at which the properties of the fibre reinforcement are preserved.

2 WORK PERFORMED IN 2007 - 2013

The work conducted within the fusion programme was focused on the development of low-activation SiC_f/SiC composite material suitable for application in advanced fusion concepts. Projects consisted of development of a new fabrication technique, coupled with in depth examination of individual composite constituents, e.g. matrix, fibre, interface.

2.1. Interphase and Fibre characterisation

Fibers in ceramic composites determine the final properties, and thus knowledge of the microstructure and mechanical properties of an individual fibre is very important. In depth analysis of Nicalon, Hi-Nicalon S (Nippon Carbon Ltd.) and Tyranno SA

Grade 3 (UBE Industries Ltd.) SiC fibres, was performed in order to determine the composition, stability and the mechanical performance of each "fusion" grade fibre.

Nicalon and Hi-Nicalon-S

Nicalon fibres were characterised by an amorphous matrix with limited amount of very small nanocrystals of β-SiC, with size between 1 and 3 nm. The diameter of fibres were around 14 μm, the surface was smooth, without visible defects. The average roughness, determined using Atomic-force microscopy (AFM) was around 2 nm. First-generation fibres, synthesised from organo-metal polymer precursors contain high amount of oxygen (12 wt.%) which limit the high-temperature use of the fibres (above 1100 °C). As a result of microstructural analysis we have summarised that the low conductivity of Nicalon SiC fibres (3 - 8 W/mK) is a consequence of their amorphous structure and are not suitable for high-temperature application also due to high oxygen content and tendency to recrystallize and consequently deteriorate mechanical properties.

Hi-Nicalon-S fibres, on the other hand, were found already well-crystallised at room temperature with the grain size of 5 to 20 nm. Crystals were mostly in cubic (β) form. Between the grains amorphous pyrolitic carbon was found. Surface of Hi-Nicalon-S fibres is smooth, without visible defects. Fibre diameter is around 12 μm. EDXS-analysis showed just traces of oxygen (estimated concentration below 1 wt.%). Hi-Nicalon-S fibres are already crystalline, so no additional recrystallization is expected during thermal treatment. The thermal conductivity is 18 W/mK. The high content of (pyrolitic) carbon may have some negative effect when used in fusion reactor (like tritium retention). Also the presence of high amount of hexagonal (α) SiC phase is not welcome for fusion application (due to higher amount of irradiation defects as compared to cubic (β) phase).

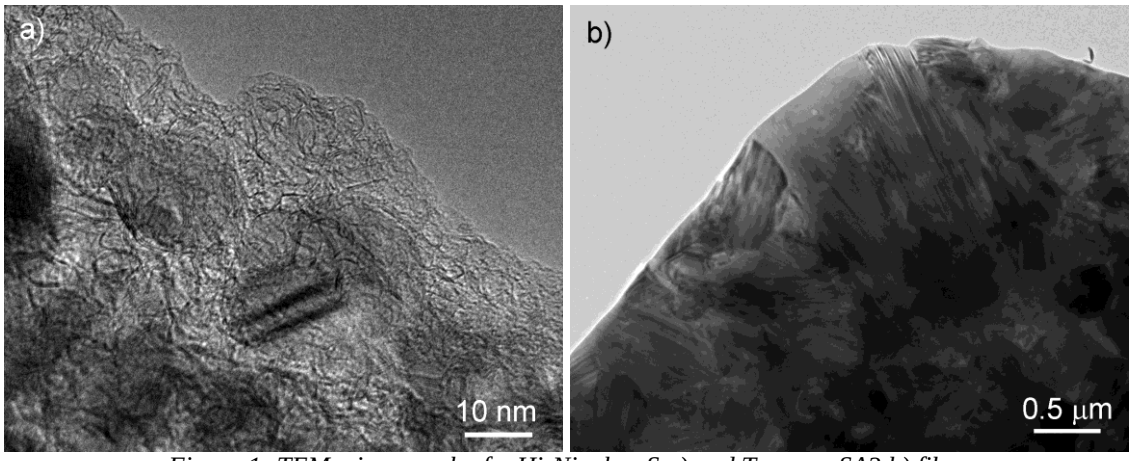

Figure 1: TEM micrograph of a Hi-Nicalon-S a) and Tyranno SA3 b) fibre.

Tyranno SA Grade 3

The newest SiC fibres, Tyranno SA3, have diameter of 7.5 μm. The surface is relatively rough without visible defects. Using AFM we measured that the average roughness was around 9 nm. Also Tyranno SA3 SiC-fibres were found to be crystalline already at room temperature. The size of the grains was around 50 nm. Fibres are composed of both SiC phases, cubic and hexagonal. Planar defects inside the grains are

characteristic for polytype structures (simultaneous presence of both phases inside one grain). Grains are crystallographically randomly oriented. Tyranno SA3 SiC-fibres have also relatively high amount of α-SiC phase and coarse grains that limits mechanical properties (toughness). The thermal conductivity of these fibres is 65 W/mK. Comparing the results of microstructural analysis and thermal conductivity we have concluded that the high degree of crystallinity (volume fraction of crystalline vs amourphous phaseses) and larger grain size increase the thermal conductivity of SiC fibres.

TISICS

Since low availability of SiC fibres represents a major issue in the production of SiC-fibre reinforced composites in Europe, an attractive option appeared to involve the UK producer of W-core SiC fibres (TISICS Ltd, UK) and to adapt the state-of-the-art fibres to the needs of the target composite. Incorporation of additional phases with high thermal conductivity, such as tungsten (which is so and so expected to be used in fusion reactors) would be also beneficial for the increase of through-thickness thermal conductivity, one of the restricting properties of SiC-based composites.

The analyses of a range of the TISICS products in revealed that some adaptations would be needed. The currently rather thick fibers (90 - 140 μm) contain tungsten core with diameter of 15 - 20 μm and a thick SiC rim. As such, due to their high rigidity the fibres seem to be very difficult, if not impossible, to weave. In the best case they can be placed in-plane that, however, cannot substantially contribute to the through-the- thickness thermal conductivity. These thick fibres could be possibly incorporated into the SiC- based material, if a special architecture is developed to assure appropriate mechanical and thermal properties. The adapted architecture should follow the goal to achieve the required high mechanical strength and reliability and high thermal conductivity. Another way is to produce much thinner fibres.

The main problem of the TISICS fibres is the extensive reaction between W and SiC already at 1000 °C. Careful selection of thin interphase which would inhibit the interdiffusion of W and Si (and thus inhibit the chemical reaction) is a possible solution of this serious problem. Incompatibility of W and SiC, found in this work, could be a serious draw-back for application of SiC based materials in future fusion reactor. We expect that certain buffer layer with stable and relatively rigid structure would inhibit interdiffusion of W and Si atoms. Our first choice was TiC, and samples of W-core SiC fibres with thin interlayer of TiC were recently produced in company TISICS.

2.2. SITE process

The novel process “SITE” is a **pressure-less moderate-temperature process**, in which the key step is **electrophoretic infiltration** of **3-D** fibre preform with powder prior further densification. It has been developed in order to adapt the composite matrix composition to better fit the expected neutron activation and might hence serve as a promising gateway to a suitable fusion-relevant material. In its original form the densification was first achieved by aid of transient eutectoid (the origin of the name SITE -“Slip Infiltration and Transient Eutectoid”), similar as in the NITE process, but

was later substituted by PIP in order to avoid oxides and to fulfil the target of low-activation.

The process is composed of a two-stage infiltration followed by a moderate temperature densification. The matrix material is introduced into the 3D woven SiC-fibre performs with electrophoretic deposition, an electric-field-assisted colloidal process, where the charged particles in the aqueous suspension are forced to move toward the oppositely charged electrode through the SiC-fibre fabric preform. A volume of work was dedicated to the study of electrokinetic properties of submicron and nanosized SiC powders optimal for the formation of high-density deposits from aqueous suspensions [1]. The process of electrophoretic deposition was also investigated as a possible pathway to produce a thin fibre interface coating in order to replace current time-consuming and expensive processes for application of interphase coating. Feasibility of such process was shown by application of a thin, carbon nanotube (CNT) interphase coating on SiC fibres [2].

By separation of fibres from the deposition electrode, electric field penetration through the thickness of the preform was ensured in order to provide a driving force for migrating particles. Due to the same polarity of zeta potential of migrating SiC particles (> 60 mV, pH10) as for the fibres (>50 mV, pH10), the particles were able to penetrate throughout the 5.4 thick fabric preform and thus filled the voids within it. Best results were obtained from suspension with 50 wt. % of solids loading at current density of 2.5 $mAcm^{-2}$.

In the original, so called SITE-A version, densification of the SiC matrix within SiC fabric was achieved by the use of magnesia, yttria or alumina as sintering additives for the low-temperature sintering of a SiC-matrix material. A small amount of P_2O_5 was employed as a transient additive that lowers the viscosity of the secondary phase during the particles' rearrangement process, while silica, found in a thin layer on the particles' surfaces, acts as the third component for the secondary phase in the system $MeO–SiO_2–P_2O_5$ (Me stands for Y, Mg or Al). Various procedures were used for the preparation of the matrix ceramics. Sintering additives were added to the SiC powder, simply by mixing or by forming a coating of sintering additives on SiC powders. As expected, the samples prepared from the coated powders were more homogeneous and exhibited a lower porosity than those prepared by mixing the powders. The amount of the secondary phase did, however, increase slightly.

The microstructural observations of the matrix-material samples sintered using different additives confirmed that the P_2O_5 significantly decreases the densification temperature and, after playing its role in viscous-flow sintering, it evaporates. The samples with the MgO addition sintered in an argon atmosphere were highly porous due to the reaction of the MgO with SiC forming gaseous products, while sintering in the open air resulted in dense ceramics with a large amount of silica-rich amorphous secondary phase. The system $Y_2O_3–P_2O_5–SiO_2$ did not result in dense ceramics; it is, however, supposed that hot pressing might result in sufficient densification. The lowest porosity for the matrix material was obtained with a secondary phase of $Al_2O_3–P_2O_5–SiO_2$, which was therefore used in the fabrication of the fibre-reinforced composite. The SiC-fibre preform was first infiltrated with a silicon carbide powder suspension employing the electrophoretic deposition technique that was followed by the vacuum infiltration of an aqueous solution of Al-phosphate and sintering at 1300–1400 °C. The

results suggested that the presented technique offers a promising way for producing SiC-fibre-reinforced SiC ceramics in a moderate temperature regime. The drawback of the process, however, was the presence of secondary oxide phases which limit materials thermal conductivity and due to its composition their applicability in fusion environments is questionable. Consequently, efforts have been done to avoid the oxide-based secondary phase by substituting the densification step.

2.3. SITE-P

In contrast to the initial SITE process, SITE-P process was developed in order to form a matrix composed of only low-activation elements [3]. The development of "fusion-grade" SiC fibres and their increased temperature stability (up to 1800 °C) enabled the use of higher processing temperatures in order to obtain the desired material.

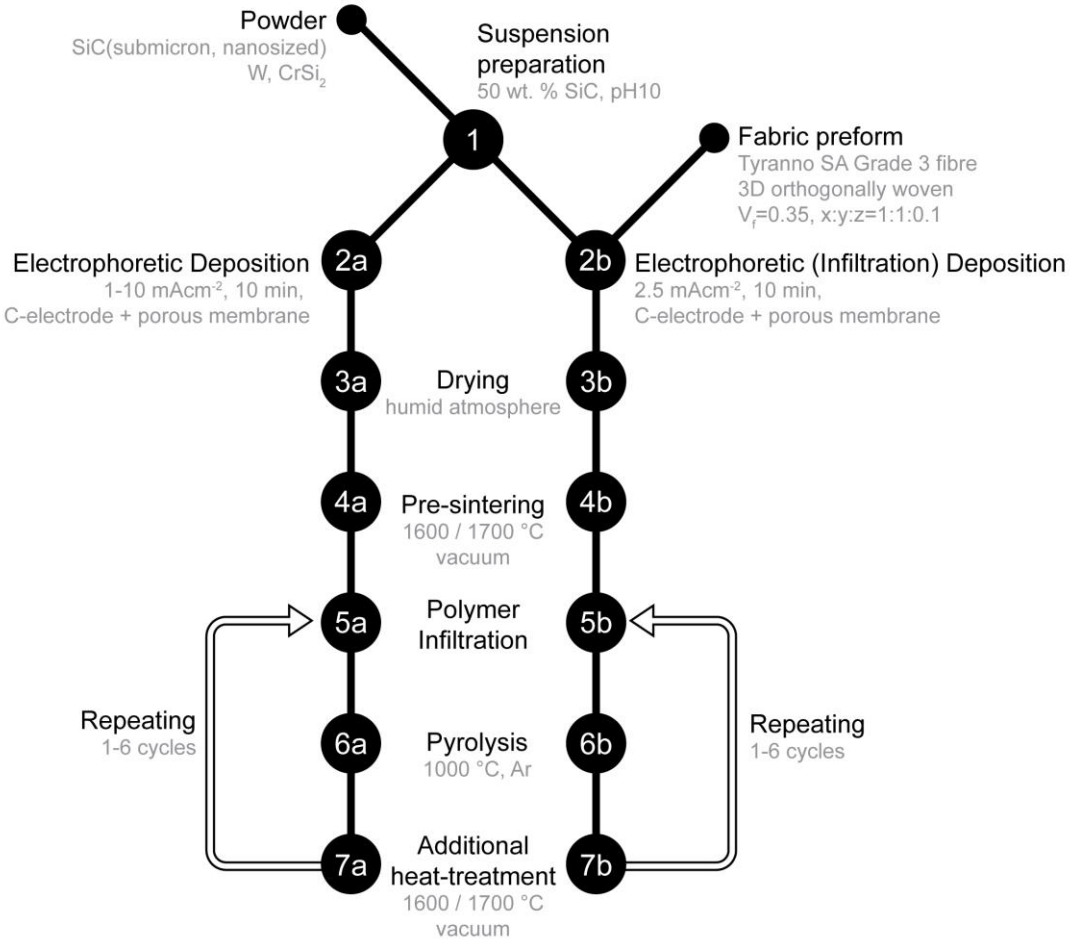

Figure 2:Shematic representation of SITE process. (druga slika SITE-A + SITE-P)

In the SITE-P process, SiC powder was introduced into 3D fabric preform in the same way as in the original SITE-A process, by using electrophoretic deposition. Low pressure, moderate temperature densification was achieved by using polymer infiltration and pyrolysis (PIP) process. By six cycles of polymer infiltration and pyrolysis process followed by additional heat treatment at 1600 °C or 1700 °C (EP6) resulted in pure, crystalline SiC matrix material with ~87 % TD. Six PIP cycles were selected for densification, since further cycles did not increase the density of the material, most likely due to inability to further infiltrate the material with pre-ceramic polymer. Further densification might be achieved by application of pressure in the next polymer infiltration steps

After densification of the material by six polymer infiltration and pyrolysis cycles, a SiC_f/SiC composite was formed, composed of pure, crystalline SiC with a more favourable microstructure in terms of pore size and porosity distribution in comparison to other fusion-grade composites prepared by state-of-art techniques (CVI, PIP).

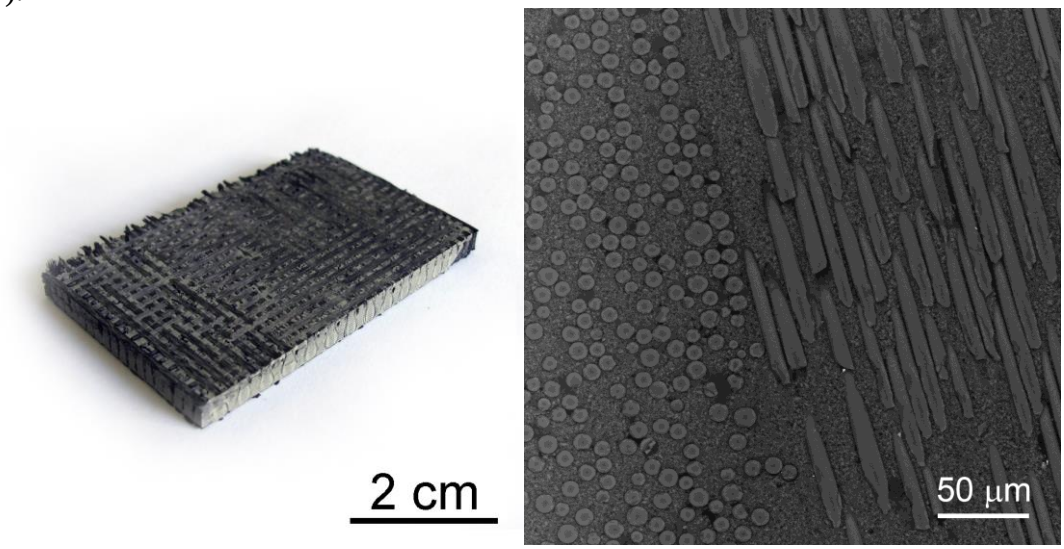

Figure 3: Macroscopic image and polished cross-section of SITE-P SiC_f/SiC composite

The resulting SiC_f/SiC composite was characterised by high thermal conductivity in achieving 60 $Wm^{-1}K^{-1}$ at room temperature and 30 $Wm^{-1}K^{-1}$ at 1000 °C, which is one of the highest thermal conductivities reported for such material [4]. Initial mechanical properties characterisation of the composite material revealed a need for a more stable interphase layer between the matrix and the fibres.

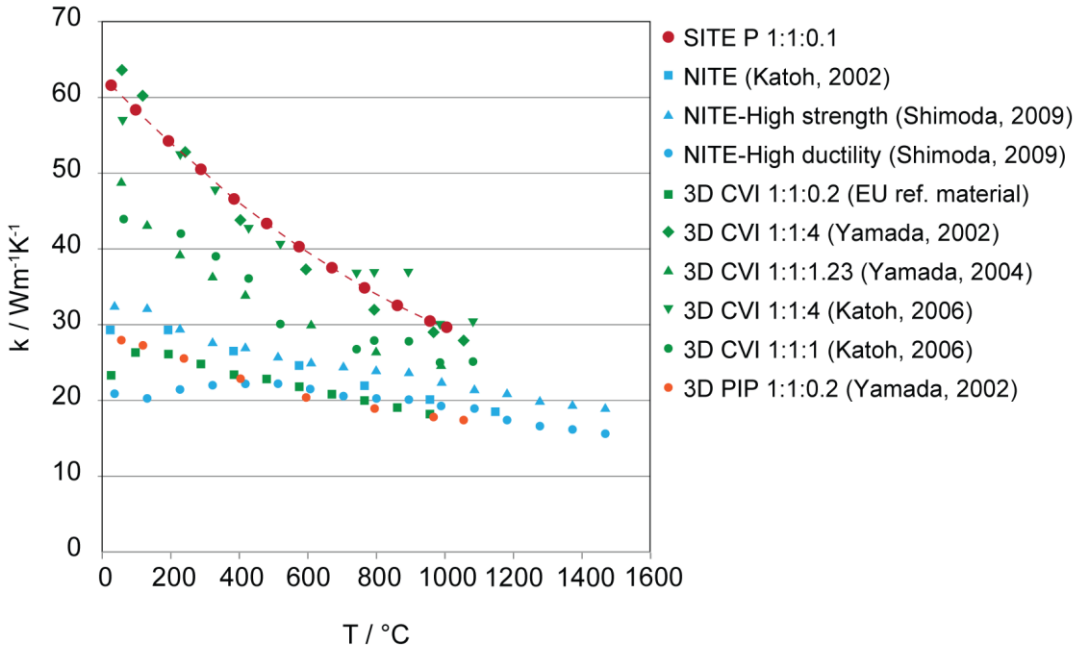

Figure 4: Thermal conductivities as a function of temperature for various grades of SiC_f/SiC composites.

In order to further increase the matrix density, a possibility to use tungsten as active filler during polymer infiltration and pyrolysis was investigated. The role of W is twofold; first, it would contribute to faster densification due to the reaction with polymer decomposition by-products and second, it would further enhance the materials through thickness thermal conductivity.

3 CONCLUSIONS AND OUTLOOK FOR FURTHER WORK

The combined process of electrophoretic (infiltration) deposition and polymer infiltration and pyrolysis was confirmed as a good route for densification of 3D SiC-fibre reinforced SiC at moderate temperatures (<1800 °C) and pressures.

Electrophoretic deposition has proven to be an effective way of infiltration of thick conductive substrates such as 3D woven fibre preforms as well as a possible technique to form an interface layer between fibres and the matrix. Several important finding were identified in order to successfully infiltrate thick conductive preforms by EP(I)D. It is essential that the fibres are separated from the electrode to prevent electric field shielding and deposition only on the proximal side of the preform. By separating the fibres from the electrode, the particles stream through the thickness of the preform due to the potential gradient between the electrodes. To prevent particle deposition on the fibres and to achieve full penetration of powder through the preform an electrostatic repulsion force must exist between the particles and the fibres. Both constituents (particles, fibres) had a similar electrokinetic behaviour in aqueous suspensions and depositions were performed at pH10 where both possessed a high (negative) zeta potential. To promote infiltration wetting of the fibres with aqueous suspension was enhanced by treating the surface of fibres with anionic surfactant. To prevent any air entrapment within the preform, fabric was also evacuated and gradually filled with the

suspension prior to electrophoretic (infiltration) deposition. The process resulted in a preform infiltrated through the entire thickness (5.4 mm) with excellent infiltration in the interbundle areas and partial infiltration of intrabundle areas. Further improvement of infiltration might be achieved by infiltration by nanosized particles. As-deposited composites were carefully dried to mitigate the formation of drying cracks.

Prior to polymer infiltration and pyrolysis, dried EP(I)D compacts were strengthened to prevent cracking associated with dimensional changes of polymer precursor during polymer-to-ceramic conversion. Strengthening without shrinkage was accomplished by pre-sintering the deposits at temperatures < 1700 °C, which resulted in neck formation and facetation of particles and increase in pore size, beneficial for further infiltration with polymer precursor. For a successful infiltration, polymer precursor was heated up to 100 °C to reduce its viscosity. Densification by polymer infiltration and pyrolysis resulted in a gradual filling of the voids within the infiltrated material. After six PIP cycles the composite SiCf/SiC material density was 2.8 gcm^{-3} (87 %TD). Full densification was not achieved, however, a more homogeneous microstructure with majority of pores < 1μm without the presence of large voids in interbundle areas, typical for standard PIP (and CVI) processing shows a significant improvement in comparison to these processes. The resulting composite material was composed of β-SiC with minor amounts of α-SiC, which was attributed to the α-SiC present in the starting materials (powder, fibres).

SITE-SiCf/SiC samples exhibited brittle fracture behaviour and low mechanical strength, much lower than that for the SiC matrix alone. Such result is the consequence of the unfavourable microstructure in which the fibre-matrix interphase layer, essential for pseudoplastic behaviour in ceramic matrix composites, was not present after final processing. Obviously, during heat treatment above 1600 °C the PyC fibre-matrix interphase layer reacted with the polymer derived SiC. In order to ensure non-brittle behaviour of the material and to justify the role of fibres within the material, PyC interphase should be replaced by a more stable interphase such as (PyC-SiC)n multilayer.

Through thickness thermal conductivity of SITE SiCf/SiC is among the highest measured values in comparison to other state-of-art materials. Comparable values were obtained by CVI-SiCf/SiC, however only in the case where the amount of fibres oriented in the z-direction was much higher; therefore we can conclude that the contribution of matrix phase in case of SITE samples was much higher than in the case of CVI. A more uniform matrix with larger grain size and the absence of large interbundle voids, play a crucial role in high thermal conductivity of the material.

The SITE, a novel process combining EP(I)D and PIP was presented as a promising technique for fabrication of SiC-based ceramic matrix composites. For full implementation of such material optimisation of the interphase layer would be needed.

4 REFERENCES

1 König K, Novak S, Iveković A, Rade K, Meng D, Boccaccini AR, Kobe S (2010) Fabrication of CNT-SiC/SiC composites by electrophoretic deposition. Journal of the European Ceramic Society 30 (5):1131-1137

2 Iveković A, Dražić G, Novak S (2011) Densification of a SiC-matrix by electrophoretic deposition and polymer infiltration and pyrolysis process. Journal of the European Ceramic Society 31 (5):833-840

3 Iveković A, Novak S, Dražić G, Blagoeva D, de Vicente SG (2013) Current status and prospects of SiCf/SiC for fusion structural applications. Journal of the European Ceramic Society 33 (10):1577-1589

4 König K. The production of advanced ceramic materials by electrophoretic deposition: PhD thesis, University of Ljubljana, 2011

5 Bele J. Priprava keramične matrice na osnovi SiC z uporabo infiltracije in pirolize polimera: BSc thesis. University of Ljubljana, 2011. XIV, 73

6 Iveković A. Development of SiC-based composite material for fusion application: doctoral dissertation, Jožef Stefan International Postgraduate School, Ljubljana, 2013.

7 Toplišek Tea, Dražić G, Bukovšek V, Novak S, Kobe S. Electron microscopy and microanalysis of the fiber, matrix and fiber/matrix interface in SiC based ceramic composite material for use in a fusion reactor application. V: WUNDERLICH, Wilfried (ur.). Ceramic materials. Rijeka: Sciyo, 2010, str. 99-114

DIVERTOR HIGH HEAT FLUX HELIUM COOLING

Boštjan Končar, Martin Draksler, Samo Košmrlj, Igor Simonovski

Jožef Stefan Institute, Jamova cesta 39, 1000 Ljubljana, Slovenia
bostjan.koncar@ijs.si

1 INTRODUCTION

A successful design of the helium-cooled divertor should be able to remove very high heat fluxes of at least 10 MW/m^2. Preliminary divertor design was developed at Karlsruhe Institute of Technology (KIT) [1] and is based on modular design consisting of small cooling fingers, each cooled by 25 high pressure helium jets. The main heat transfer and flow characteristics to meet the design requirements are to increase the heat removal capability of the divertor and at the same time minimize the pumping power for the coolant flow. A comprehensive analysis of main operation parameters as well as design variants was performed. Detailed numerical predictions of heat and thermal stress loads in the divertor structures and pressure drop in the helium flow were carried out to ensure that the design constraints and material limits are not exceeded.

2 WORK PERFORMED IN 2007 - 2013

The work on the project Divertor high heat flux cooling started in 2008. The common goal of all performed activities was to develop a reliable computational model and use it for development and optimisation of the divertor design. The activities were related to thermal-hydraulic and thermal stress analyses of the reference hexagonal design, evaluation and improvement of modelling accuracy, investigation of alternative cooling finger concepts considering different material as well as geometry options and last but not least a detailed investigation of flow and heat transfer phenomena at multiple jet impingement. The results of performed tasks are summarized hereinafter, while more details can be found in annual reports of Slovenian Fusion Association (SFA).

2.1. Thermo-hydraulic and thermal stress analyses of the reference hexagonal finger design

The finite-element structural methods in combination with the computational fluid dynamics (CFD) analysis can be successfully used to analyze the cooling efficiency and thermal stresses of different finger designs. Furthermore it was demonstrated that such approach can be used to predict the finger structure response subjected to periodic heat flux loading.

Effect of cartridge nozzle sizes on the heat transfer and thermal stresses in the hexagonal finger

The size and arrangement of the jets in the cooling finger affects the heat transfer, pressure drop characteristics and thermal stresses in divertor plasma facing structures. Five different jet arrays with varied hole sizes were analyzed numerically using a combined CFD and structural finite element model. The most critical parameters, such as structure temperature, heat removal ability, pressure drop, cooling efficiency and thermal stress loadings in the cooling finger were investigated.

The results have shown that different jet arrangements have a relatively small effect on the peak values of thermal stress (up to 10%). For all analyzed cases, the maximum stresses appear on the thimble's inner surface and exceeded 515 MPa. The lowest thermal stress peak is predicted for the finger design with no jets in the last row (19 jets) and equal jets cross-section as the reference design (25 jets). The work is reported in detail in SFA annual reports 2009 and 2010.

Thermo-mechanical simulation of the cooling finger at cyclic heat flux loading

Divertor should withstand high flux loads for a number of load cycles since initially the DEMO reactor is expected to operate in a pulse mode. To simulate the structure response under the cyclic heat flux loading, a combined CFD and structural model was developed. The selected Efremov experimental test case with cyclic heat flux boundary conditions was simulated. During the experiment the upper tile surface was subjected to the variable surface heat flux up to 14 MW/m^2. Up to 10 cycles with a cycle period of about 60 seconds were applied for each heat flux level.

The simulated thermal stresses show that there are three potential areas where the cracks in the structure could occur (Figure 1): the thimble inner surface in the regions with high thermal gradients, the tile's outer left and right edges where high equivalent stresses are observed and the brazing layer in the tile-thimble joint where the temperature may exceed the melting temperature of the filler material.

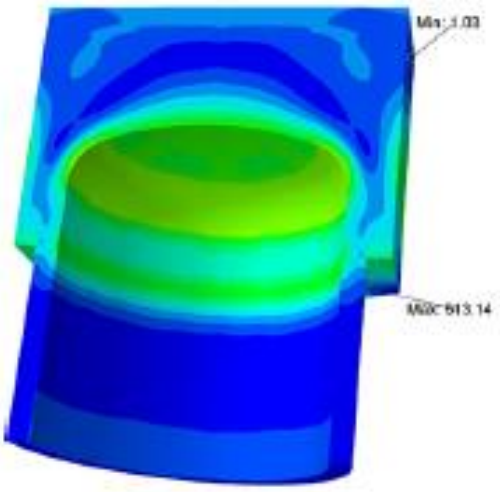

Figure 1: Mises stress distribution at the heat flux 11.63 MW/m^2

The numerical predictions of stresses qualitatively agree with the experimental observations [2]. Post-examination of irradiated mock-ups also revealed the separation of the tile-thimble joint, which indicates that the melting temperature of the tile-thimble brazing material was exceeded. Details are provide in SFA annual reports 2008 and 2009.

2.2. Evaluation of modelling accuracy of cooling finger experiments subjected to cyclic heat loads

Although the cooling performance of the divertor finger has been successfully high-heat-flux tested under real DEMO conditions in a combined helium loop and electron beam facility at the Efremov Institute, Russia [2], an accompanying numerical simulation of the experiments is of great importance leading to better understanding of complex thermo-hydraulic conditions with the aim to accurately predict different load cases. In 2011 and 2012, the numerical analyses of the third series of High-Heat Flux (HHF) experiments performed at Efremov Institute were carried out. The finger tile shapes (developed at KIT) with rounded lower edge were used in these tests. The main focus of our studies was accurate representation of experimental boundary conditions and estimation of uncertainties due to modelling assumptions. Transient calculations of the heat transfer in the solid structure were validated against the cyclic heat flux experiments.

Modelling uncertainties

The ANSYS-CFX code was used for simulations of HHF experiment. In thermal-hydraulic analyses of cooling finger, several modelling assumptions can be used that do not always correctly reflect the experimental conditions or material properties. The most common assumptions are the following: constant heat flux profile on the top of the tile, adiabatic boundary conditions on the side of the finger, neglecting the heat losses or inaccurate modelling of solid properties. Modelling uncertainties associated with these assumptions were evaluated and are briefly described in this section. Details are given in SFA annual report 2011.

To accurately reproduce the experimental heat flux distribution on the tile's top surface exposed to the electron beam, the Gaussian-like shape of the absorbed heat flux density was modelled, which depends on the beam power density and its raster pattern.

The tile surfaces can be heated up to 2000 K, therefore some of the input energy may be lost due to the radiation. About 3% of the absorbed heating power can be submitted through the radiation losses as compared to the adiabatic model. Modelling of radiation losses may reduce the temperatures inside the finger structure by up to 30 K.

The effect of thermal conductivity modelling on the simulation results was found to be essential. The simulated temperatures may vary by almost 100 K at top of the tile, and over 30 K at the tile-thimble interface. The available material data from the ITER handbook [3] should be used very carefully. More recent data on tungsten and tungsten alloys [4] provide significantly different thermal conductivity values moreover they are highly dependent on the way how the mock-up is manufactured.

Transient simulations

Transient simulations of the cyclic heat flux experiments were performed using the heat transfer coefficient (HTC) distribution obtained from the steady-state analyses. It was found that the HTC value mainly depends on the mass flow rate and inlet temperature. The mass flow rate throughout the considered experiment was relatively constant, but the inlet temperature varied for about 40 K. The estimated maximum error associated with inlet temperature variation and with constant HTC approximation was about 5 K at the helium-thimble interface and about 1 K on the top surface of the tile. A good agreement between the experimental and simulated tile surface temperatures was obtained.

2.3. Thermal-hydraulic analyses of alternative cooling fingers

These analyses were focused on investigation of alternative He-cooled divertor target concepts for updated design requirements in an early DEMO. The research activities were carried out mainly in 2012 and 2013 within the framework of the PPP&T programme, workpackage Design Assessment Studies (DAS). The main objective of the task was to perform thermal-hydraulic analyses of alternative cooling finger designs in terms of material choice and geometry of the tile. Two possible incident heat flux conditions were studied, 10 MW/m^2 and 8.7 MW/m^2, where the lower heat flux value is based on the relaxed parameters of the "early-DEMO" design. The scoping analyses were carried out in two directions. In the first case the alternative material, Ta-alloy (T-111) for the thimble with a much lower Ductile to Brittle Transition Temperature (DBTT) was investigated that allow a reduction of the coolant temperature and a better operational temperature window of the materials (e.g. steel). Thermal loading of the finger structures and pressure drop in the cooling channel are compared with the reference design at high helium temperature. In the second case, the alternative finger geometries (the hexagonal finger being the reference) at high helium outlet temperature were investigated. These analyses were performed as a cross-border activity with WP12-DAS-02-T05 from the perspective of shadowing of the target plate edges against damage caused by the incident particles. The work was carried out in close cooperation with the Karlsruhe Institute of Technology (KIT) - Institute for Applied Materials-Materials Processing Technology. Based on thermal-hydraulic analyses of different cooling finger concepts, a new finger design with the square shape of the tile was constructed and fabricated at KIT. The new design had the same upper surface of the tile as the reference hexagonal-shaped finger. The CAD model of the fabricated square finger was used to construct a detailed CFD model in order to evaluate its thermal-hydraulic performance and heat loading on the finger structures.

Low temperature Helium cooling using T-111 as a thimble material

Ta-based alloy (T-111) for the thimble was analysed at lower helium temperatures ranging from 400 to 500 ^{o}C. The alloy T-111 has a lower DBTT value (rough estimation ~ 400 ^{o}C) at irradiation conditions than the reference thimble material WL10 (600 ^{o}C). Thermal loading of the finger structures and pressure drop in the cooling channel are compared with the reference design at high helium temperature. At

400 ºC of the helium inlet temperature, the maximum thimble temperature for T-111 is about 100 ºC lower and does not exceed 1100 ºC. The pressure drop in the cooling channel is also reduced by more than 25% compared to the reference case. It is shown that the maximum thermal loading increases linearly with the increased helium inlet temperature. To reflect the recent data for the early DEMO design (the so-called DEMO1), additional sensitivity cases were calculated with the lower peak heat flux 8.7 MW/m^2. The inlet helium temperature was varied between 450 ºC and 650 ºC to cover the estimated uncertainty range of irradiated DBTT of T-111.

Alternative finger designs for the toroidal edge of the target plate

Alternative finger geometries were investigated from the perspective of shadowing of the target plate edges against damage caused by the incident particles. In order to form a flat toroidal edge of the target plate, alternative tile geometries (non-symmetric pentagon, square) were analysed with respect to the reference hexagonal design. CFD analyses were performed from the point of view of maximum allowable thimble temperature and minimum required helium flow through the finger module. The results have shown, that apart from the reference hexagonal finger, the square-shaped finger with a 16.5 mm edge shows the best performance (6.8 g/s at 124 kPa pressure loss). This indicates that a helium cooled divertor could be composed entirely of the square-edged fingers, which would simplify the manufacturing process and assembling of the target plate. Thermo-hydraulic analyses show that square fingers need to be slightly smaller (only 1%) than hexagonal fingers to reach equivalent performance. Detailed results can be found in SFA annual report 2012.

Analyses of fabricated square-shaped cooling finger

Prerequisites for the new finger design were the square shape of the tile (with the same plasma facing area as in the case of hexagonal tile) and the use of Ta-alloy for the thimble material. A square tile with 17.1 mm of edge width was designed and fabricated at KIT. For fabrication purposes, the commercially available Ta-alloy T-222 was used for thimble structure in order to enable low temperature cooling below 450 ºC. The cartridge design was slightly changed; the upper, wider part of the cartridge was shorter than for the reference hexagonal finger. Its thermal-hydraulic performance and temperature loading on the structure materials was evaluated using the CFD code ANSYS-CFX (Figure 2). The sensitivity analyses were performed for two different surface heat fluxes (10 MW/m^2 and 8.7 MW/m^2), two mass flow rates (6.8 nad 9 g/s) and two helium inlet temperatures (350 and 450 ºC). The results were compared with previous simulations of 16.5 mm square finger (task WP12-DAS-02-T06). The tile temperature was higher for the new finger as a consequence of larger tile edge (17.1 mm). On the contrary, the maximum thimble temperature was slightly lower for the new finger design, originating from different shape of the cartridge upper part. Details are provided in the SFA report 2013.

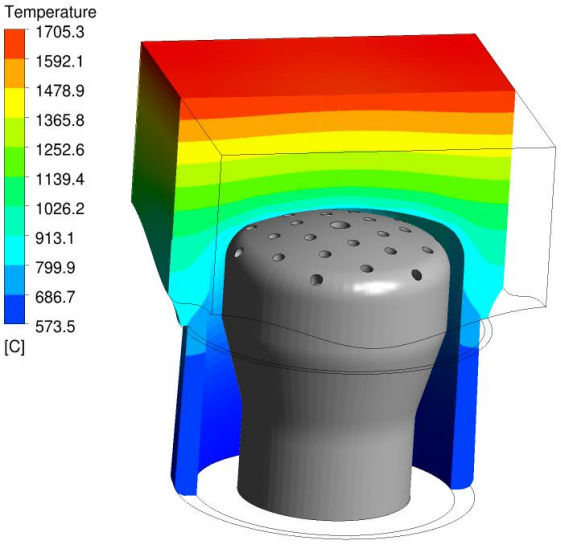

Figure 2: Temperature distribution across the finger structures for the case qw= 210 MW/m^2, mfr= 6.8 g/s, T_{He},inlet=450 ^{o}C

2.4. In-depth study of multiple impinging jets (RANS and LES simulations)

The heat transfer characteristics for two different multiple jet configurations have been validated on the simple experimental case by the means of Reynolds Averaged Navier-Stokes (RANS) approach. This approach can provide main local flow characteristics of jet impingement with an acceptable accuracy and reasonable computational times. The main goal of this study was to evaluate the effect of jets arrangement on the heat transfer enhancement. In particular, the connection between jet flow structures and heat transfer coefficient distribution was sought. For the purpose of such analysis an experimental case [5] was selected, where the air from an open-circuit wind tunnel is blown through a flat nozzle plate. The flow impinges a flat horizontal glass plate after issuing the nozzles. Two different arrangements of the nozzles were tested, the in-line configuration with 9 nozzles and the hexagonal one with 13 nozzles). For all tested cases the nozzle diameter was 13 mm. Reynolds numbers were comparable to those in the cooling finger of helium-cooled divertor. The comparison of results at different jet configurations clearly show better heat transfer characteristics at the hexagonal jet arrangement, which is also adopted in the case of divertor cooling finger. To estimate the accuracy of RANS simulations and to carry out in-depth study of the flow characteristics and heat transfer at hexagonal jet configuration, the same experiment was simulated using the Large Eddy Simulation (LES) approach. LES modelling and simulation work started in 2012 with simulations of the instantaneous flow fields and setting up the necessary statistical methods for analysis of transient results. In 2013 the LES simulations were continued with the focus on validation against experimental data, interpretation of results and carrying out the LES simulations of the heat transfer. LES simulations of the flow field and secondary turbulent stresses show very good agreement with experimental data.

RANS simulation of two multiple-jet configurations

Steady-state RANS simulation together with the two equation turbulence model is a preferable choice for optimization studies of multiple jet configurations, which require fast and efficient analyzing technique. Two different jet configurations (hexagonal and in-line) were simulated showing similar patterns of the local heat transfer, which is enhanced in the vicinity of flow structures. The results show that the local heat transfer maximum is shifted away from the stagnation point, which can be connected to a small vortex ring formation around the stagnation point. The comparison of the flow structures sizes between both jet arrangements shows that the jets interactions are more pronounced in the hexagonal case, resulting in higher local values of the turbulence kinetic energy and consequently higher heat transfer. Due to the geometry nature, the effect of the cross flow is less pronounced for the hexagonal configuration. In general, the sizes of flow structures are smaller for the in-line configuration, which is manifested also as a smaller local Nusselt number. More details on RANS simulations can be found in SFA annual reports 2009 and 2010.

LES simulation of multiple-jet experimental case

The vast majority of physical phenomena and mechanisms of turbulent impinging jets can be sufficiently captured by Large Eddy Simulation (LES), where all larger spatial scales can be solved directly without any additional modelling. Additional models are required only on smaller, subgrid scales to capture the simpler, isotropic turbulence. LES simulations were carried out in order to study the flow characteristics and heat transfer of multiple circular impinging jets at configurations and Reynolds numbers comparable to those in divertor cooling finger. The mean flow field is obtained by time-averaging of transient results. A validation study on experiment with hexagonal configurations of jets was performed. The results show that the LES simulation accurately predicts the key flow phenomena of multiple highly turbulent impinging jets. Flow field and secondary turbulent stresses show very good agreement with experimental data (Figure 3). Minor discrepancies between experiment and simulation were still observed that may originate from inaccurate modelling of experimental inlet boundary conditions. Therefore three different flow profiles at the exit of the nozzles were tested; uniform velocity profile, the profile obtained from precursor RANS simulation and uniform profile with additional pseudo-random fluctuations. Results show that additionally imposed turbulence is rapidly dissipated from the flow, and that the levels of the stresses downstream the nozzles do not exceed the values that occur anyway (with the flat profile without additional fluctuations). Accurate LES results could serve either as a benchmark case for validation of RANS turbulence models or could contribute to in depth interpretation of the local flow and heat transfer phenomena in multiple impinging jets. Ultimately, these results can serve as a validation benchmark for CFD models used in pre-conceptual and optimisation studies of divertor cooling finger. The work was performed in cooperation with the Paul Sherrer Institute (PSI), Laboratory for Thermal-Hydraulics, Switzerland.

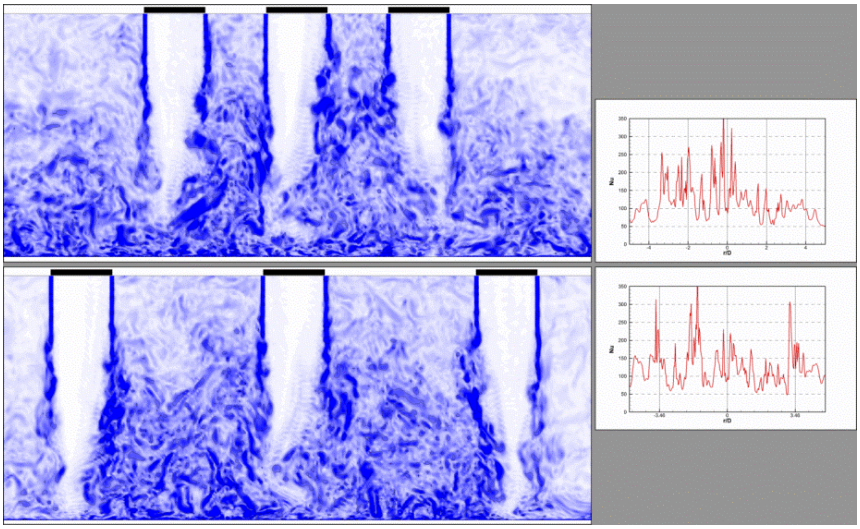

Figure 3: Flow of multiple impinging jets, shown in two characteristic planes. Vortical structures (colored by vorticity magnitude) and the profiles of the local heat transfer coefficient

3 CONCLUSIONS AND OUTLOOK FOR FURTHER WORK

Thermal-hyudraulic and stress analyses of divertor cooling finger proved to be an essential tool for pre-conceptual design and optimisation studies of helium-cooled divertor. The presented results together with the experimental work performed at KIT contributed to an improved design of the DEMO divertor. Besides, part of the project activities also resulted in a PhD work. The SFA research group will continue with numerical analyses related to DEMO reactor also in the frame of Eurofusion program.

4 REFERENCES

1 P. Norajitra P., Conceptual design of a He-cooled divertor with integrated flow and heat transfer promoters (PPCS subtask TW3-TRP-001-D2), Part II: Detailed Version. Forschungszentrum Karlsruhe, Scientific Report, FZKA 6975, April 2004.
2 A. Gervash, R. Giniyatulin, A. Kokoulin, A. Komarov, V. Kuznetsov, A. Makhankov, et al.,, 2006. Manufacturing and testing the He-cooled target module mock-ups for DEMO fusion reactor divertor, Status report, EFREMOV Institute STC Sintez St. Peterburg, 2006.
3 ITER Material Properties Handbook, 2001.
4 M. Rieth, et al, Tungsten as a Structural Divertor Material, Adv. Sci. Tech., 73, (2010), 11-21.
5 L. F. G. Geers, K. Hanjalić, and M. J. Tummers. Wall imprint of turbulent structures and heat transfer in multiple impinging jet arrays. J. Fluid Mech., 546:255, 2006.
6 The Annual Report 2008 of the Slovenian Fusion Association EURATOM-MESCS, 2008.
7 The Annual Report 2009 of the Slovenian Fusion Association EURATOM-MESCS, 2009.
8 The Annual Report 2010 of the Slovenian Fusion Association EURATOM-MESCS, 2010.
9 The Annual Report 2011 of the Slovenian Fusion Association EURATOM-MESCS, 2011.
10 The Annual Report 2012 of the Slovenian Fusion Association EURATOM-MESCS, 2012.
11 The Annual Report 2013 of the Slovenian Fusion Association EURATOM-MESCS, 2013.

ASSESMENT OF INTERFACE BETWEEN MCNP AND ANSYS CFX FOR THE BLANKET TEST CASE

Matjaž Leskovar, Boštjan Končar, Igor Lengar, Samo Košmrlj

Jožef Stefan Institute, Jamova cesta 39, 1000 Ljubljana, Slovenia
matjaz.leskovar@ijs.si

1 INTRODUCTION

The development of the DEMO fusion power plant blanket is a complex task, because it is necessary to take into account several branches of physics, including fluid dynamics, volumetric heat generation due to neutrons, heat transfer etc. Therefore, in order to support the development of the DEMO breeding blanket it is important to develop a computational model, which will take into account all the relevant data and physical processes. The volumetric heat generation in a Helium Cooled Pebble Bed Test Blanket Module due to neutrons, together with the surface heating from the plasma and the removal of heat by the helium coolant was investigated.

The breeding blanket in a fusion reactor has the function of removing the heat, generated by fusion reactions in the plasma. Additionally, it produces tritium, required for fusion reactions, from Lithium Orthosilicate (OSI). The surface heat load from plasma heating amounts up to 500 kW/m2 and the volumetric heat generation from neutrons ranges up to 8 MW/m3 in the region of OSI, closest to the first wall. The absorbed heat is removed by a helium coolant loop.

2 WORK PERFORMED IN 2007 - 2013

The research activities were carried out in the year 2012 in the framework of the PPP&T programme, workpackage Design Tools and Methodologies (DTM), Task DTM01-T03 Assessment of ANSYS Workbench hybrid platform. They were partly carried out in the frame of EFDA Priority Support. The main objective of the task was to test the possibilities for data transfer from the MCNP neutronic analysis to the ANSYS CFX thermo-hydraulic analysis. The assessment of the data transfer was performed for the Blanket Test Case [1], defined by the Karlsruhe Institute of Technology, which provided also the nuclear heating data [2], calculated with MCNP. For testing purposes a simplified blanket model was used, where only a slice of the actual blanket unit was simulated. Furthermore, the helium region of the manifold was neglected, since it was estimated, that the manifold itself does not play a significant role in the heat balance of the blanket unit.

2.1. ANSYS CFX Modelling and Simulation Results

Geometry of simulated region

A blanket module consists of six breeder units. The constituent materials absorb a lot of energy from the neutrons produced in the fusion reactions and have to be cooled effectively to prevent damage. Additionally, OSI has a relatively low thermal conductivity, which requires it to be cooled by an additional coolant loop running around it. The layout of the breeder units, consisting of beryllium, Eurofer, helium and OSI domains, is shown in Figure 1 (note: breeder units are held in place by an Eurofer structure, which also contains vertical and horizontal helium loops, but these are not shown).

Only part of the actual blanket module was simulated, as proposed in the Blanket Test Case Definition by Karlsruhe Institute of Technology [1] that should serve as a benchmark case for data transfer between CFD and neutronic codes on the two tested platforms (ANSYS CFX and Salome). The so called "slice" model takes into account a vertical slice of the blanket module.

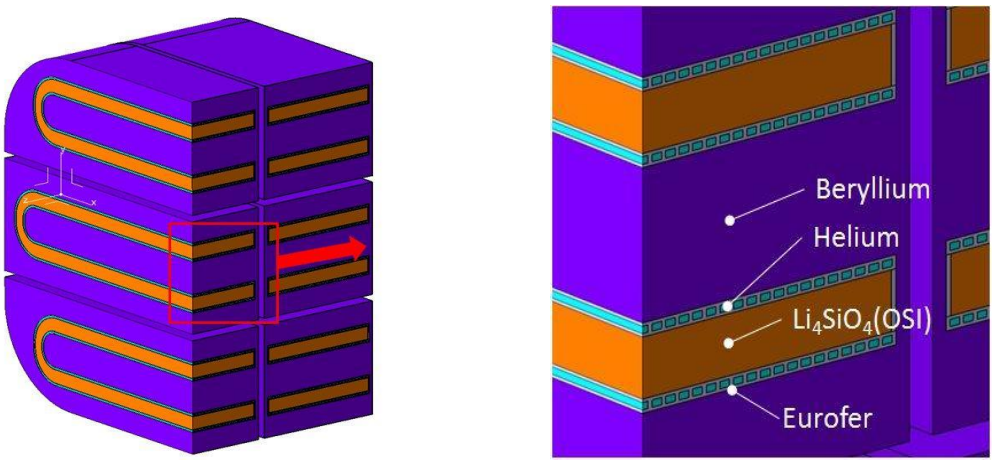

Breeder units in a single module Detailed view

Figure 1: Breeder unit layout.

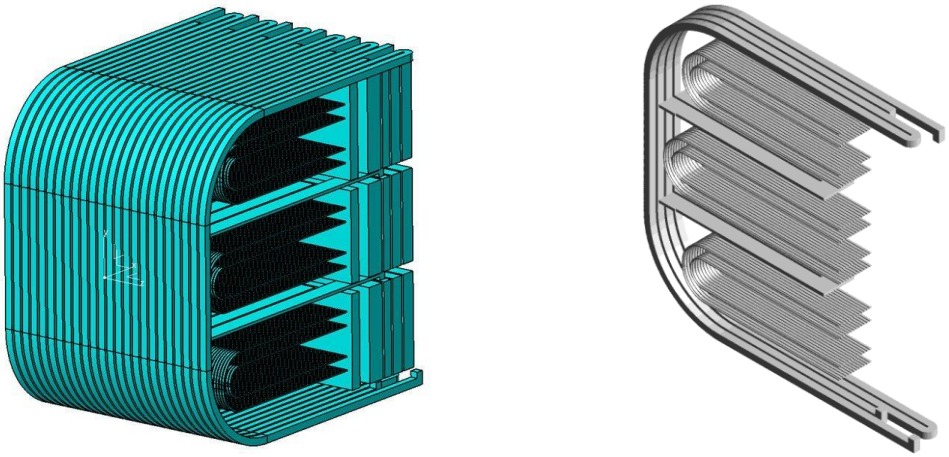

Entire helium domain Simplified helium domain in slice

Figure 2: Helium loops.

For simplicity, the helium domain in the manifold was ignored. Even though this would mean a violation of physics in reality, the simulation has no problems with that, as we can define inlets and outlets anywhere in the domain without needing to actually connect it with the helium source. Figure 2 shows the complete helium domain in a blanket module and the simplified helium domain in the slice. To overcome the absence of heat removal, the neutron heat generation was set to zero in the manifold region.

Numerical mesh

The blanket module was meshed using a fully hexahedral mesh. The mesh consists of 1.49 million elements. The standard mesh quality criteria were taken into consideration when constructing the mesh. The minimum mesh angle was mostly kept above the safe angle 20 degrees, 250 elements were between the (still acceptable) angle of 10 degrees and 20 degrees. The 2x2x2 determinant of all elements was above 0.1, which is considered to be the limit for fast convergence. The close-up of the mesh of the breeder unit closest to the first wall is shown in Figure 3.

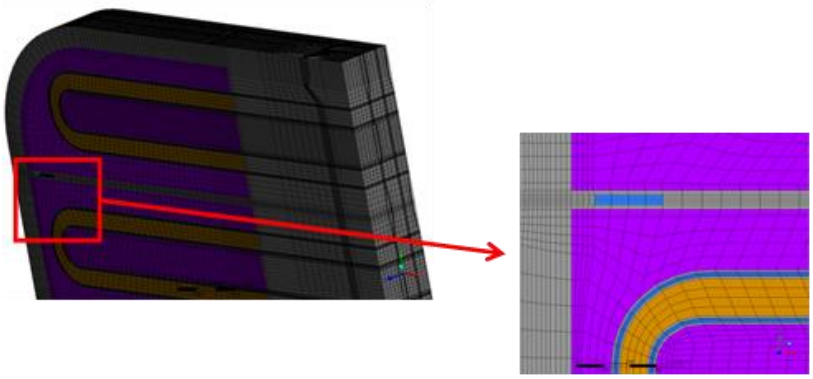

Figure 3: Detail of the mesh near the first wall.

Model setup and boundary conditions

The simulations were performed with the ANSYS CFX 13.0 code. Three solid domains (Beryllium, OSI and Eurofer) and one fluid domain (helium) were modelled. The heat transfer was solved simultaneously in the solid and fluid domains using the conjugate heat transfer approach. In the fluid domain the momentum and thermal energy equations were solved. Due to the low velocities (well below the sound of speed) the helium was treated as incompressible. The fluid turbulence was solved using the two-equation Shear-Stress-Turbulence model (SST). The boundary conditions for the simulated case are listed in Table 1.

Parameter	*Value*
He inlet mass flow rate	as defined in [1]
He inlet temperature	300 °C
H inlet pressure	8 MPa
FW surface heat flux (front)	500 kW/m^2
FW surface heat flux (bending)	0 to 500 kW/m^2

Table 1: Boundary conditions for the slice blanket module model

Setting up the volumetric heating in CFX-PRE

The data for the volumetric absorbed power density was obtained from neutronic calculations using the Monte Carlo Neutron Program (MCNP) [2]. The 3D volumetric absorbed power density was provided in the form of txt files, where the coordinates and heating power density columns were separated by a comma - the so-called comma separated values format (csv), which is the default format for CFX, i.e. import and export of numeric values is primarily done in csv format.

To add volumetric heating to a CFX model, it is required to define an additional subdomain inside a domain (in Beryllium, Eurofer and OSI), which serves as a heat source. The source can be defined by a constant value, equation or by a user function, which is in our case represented by a 3D table of values. The table of values is imported into CFX-PRE via a user function. The user function requires the users to define the argument units, which are measurement units in the first column (in case of 1D data) or in the first three columns (in case of 3D data), and result units, which are measurement units in the last column. The data can be imported from the file by right clicking into the coordinate/value field. When importing the data, it is not possible to import several files, because every import overwrites the previous one. This is overcome simply by merging input files (by copy+paste). When the user function is defined, it can be applied (after specifying which quantities should be used for the arguments, usually the x, y and z coordinates) into the source subdomain.

The volumetric heating data was provided in several separate files, where files for the beryllium and lithium orthosilicate regions were some 100 KB in size, but files for the steel support structure were about 6 MB in size. Considering the fact, that the steel structure is about the same volume as beryllium, this means that the data points are much more close together, which is probably the main reason why the loading time in both the CFX-PRE and the CFX-Solver was unreasonably increased (from 3-4 minutes to several hours). The significant increase of the volumetric heating data processing time was not a consequence of insufficient RAM, which would result in the much slower data operation on the disk. The data processing time can also not be speed up by parallel computing, as parallelized data processing is not available in CFX-PRE and CFX-Solver. This shows that special care should be taken in the nuclear heating data preparation to not impose unnecessary computational demands.

It seems that it is currently impossible to import external data to CFX directly through the ANSYS Workbench, i.e. to import the data through the module called “External Data”, as the “External Data” module does not support transferring data to CFX. Also if it would be possible to import the data through the “External Data” module, this would not simplify the setup of the simulation, because similar steps would be required as when importing data with the user function.

Simulation results

The simulation converges to the final stable state in less than 500 steps. The temperature distribution in the middle of the slice model is shown in Figure 4. The highest temperatures occur in the OSI region due to its high volumetric heating and the low thermal conductivity. The maximum temperatures in the slice in various material regions are the following – OSI: 996 K, Eurofer: 751 K and Beryllium: 679 K. The temperature in the lower parts of the breeder units is a bit higher than in the upper parts,

because the helium coolant, which comes from the inlet and passes through the upper parts of the tubes has a lower temperature than in the lower parts, where it has already taken the heat from the upper parts. The manifold region receives some heat flux due to conduction through the solid, but that region is far away from the regions of interest and the temperature gradients are low. Therefore it is expected, that replacing the helium region of the manifold with Eurofer should not significantly affect the area of interest near the first wall.

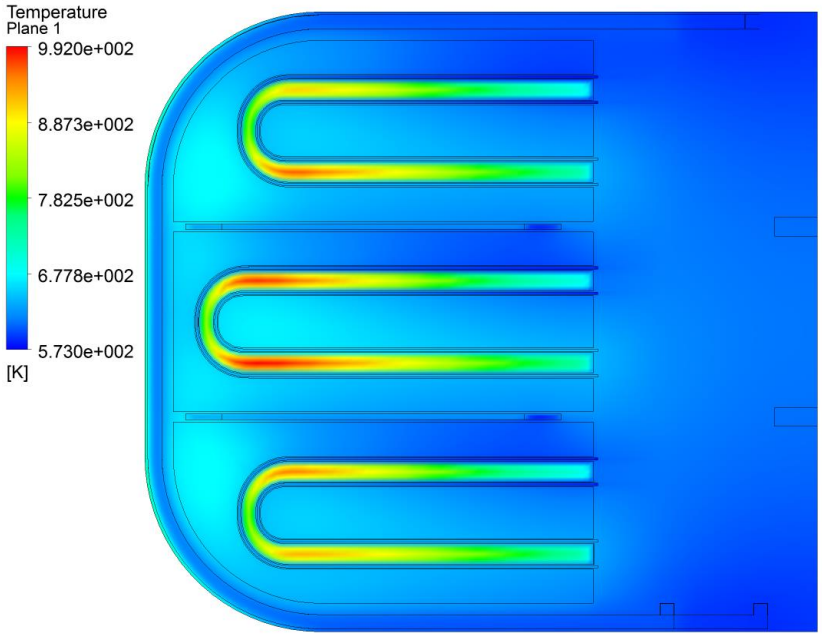

Figure 4: Temperature distribution in the middle of the slice model.

In Table 2 the main characteristics of the helium cooling circuits are presented. Most of the heat is removed by the helium cooling circuit in the first wall (~38 kW). The heat removal in the breeder units is also significant (~22 kW), whereas the cooling power of the horizontal grids is much lower (only ~3 kW each). If one considers that the plasma heating of the first wall is 23.0 kW (2x 5.83 kW curved part + 11.32 kW flat part), one obtains from the heat balance for the volumetric nuclear heating 43.3 kW. Thus the volumetric nuclear heating is about two times larger than the plasma heating.

Location	*Mass flow rate [kg/s]*	*Outlet average temperature [K]*	*Cooling power [kW]*
First wall	0.223	605.7	37.9
Horizontal grid 1	0.021	599.9	2.9
Horizontal grid 2	0.021	601.4	3.1
Breeder units	0.066	638.2	22.4
Total			66.3

Table 2: Main characteristics of helium cooling circuit.

2.2. Possibilities of Importing MCNP Output as Input to ANSYS

MCNP (version 5) has the ability to define a mesh, superimposed over the problem geometry for tallying purposes. These mesh tallies can have rectangular or cylindrical geometry. Within each cell of this three-dimensional mesh a value for the tallied quantity is calculated by MCNP. MCNP can, among other possibilities, tally gamma and neutron fluxes and neutron and gamma heating. In versions 5 and 6 it is possible to tally also the heating due to neutrons and gammas with a mesh tally. The use of the mesh tally makes it much easier to transform the heating data into ANSYS since the model geometry, which is most likely not rectangular, does not have to be modified.

Neutron and gamma heating are calculated by MCNP during the same run, but are output in two separate sets of data. They have later to be combined in order to obtain the needed input for ANSYS. It should be noted that MCNP, by default, covers only the transport of prompt gamma rays, but not delayed gammas. If it is, due to the choice of construction materials expected, that delayed gammas may have significant impact on material heating, special techniques have to be involved which make MCNP source code modification and recompilation necessary [3], [4]. These approaches are usually employed for shut down dose rate calculations. For most applications, using only neutron and prompt gamma heating would be sufficient.

It turns out, that photon heating can be for several factors higher than neutron heating, which means the photon heating can dominate in nuclear heating. During calculations for the ITER tokamak it turned out that for some components photon heating may significantly contribute to the total nuclear heating [5].

As an example of the capabilities of the transformation of heating data, obtained with MCNP into ANSYS, the nuclear heating calculations were performed for the MCNP model of the DEMO tokamak. The model was released by KIT in July 2012 in the frame of the WP12-DTM-03-T02 task – Provisional DEMO MCNP Model. The calculations were performed by JSI, imposing a cartesian mesh tally over the whole geometry; the resolution of the mesh was 117x28x174 points, corresponding to dimensions of the model. The obtained distribution of the neutron and gamma heating are presented in Figure 5; included is also the mesh tally resolution, presented by yellow dots.

For the calculations the MCNP5 mesh tally technique was applied for heating calculations by using the FMESH card with its FM tally multiplier card in which the material number “m” was set to zero, implying that the heating cross sections for the material in which the particle is traveling are used.

The largest difficulty in calculating the heating is to make the MCNP model and then to run it accordingly for the statistical errors in the regions of interest to be low enough. Several variance reduction techniques can be applied for this purpose, the most widely used being the application of weight windows.

Most likely the heating will not be calculated for the whole geometry, as was done in our example, but only for specific components. In this case the mesh is applied only over those components and the MCNP run optimized to give the lowest statistical error in the region of interest.

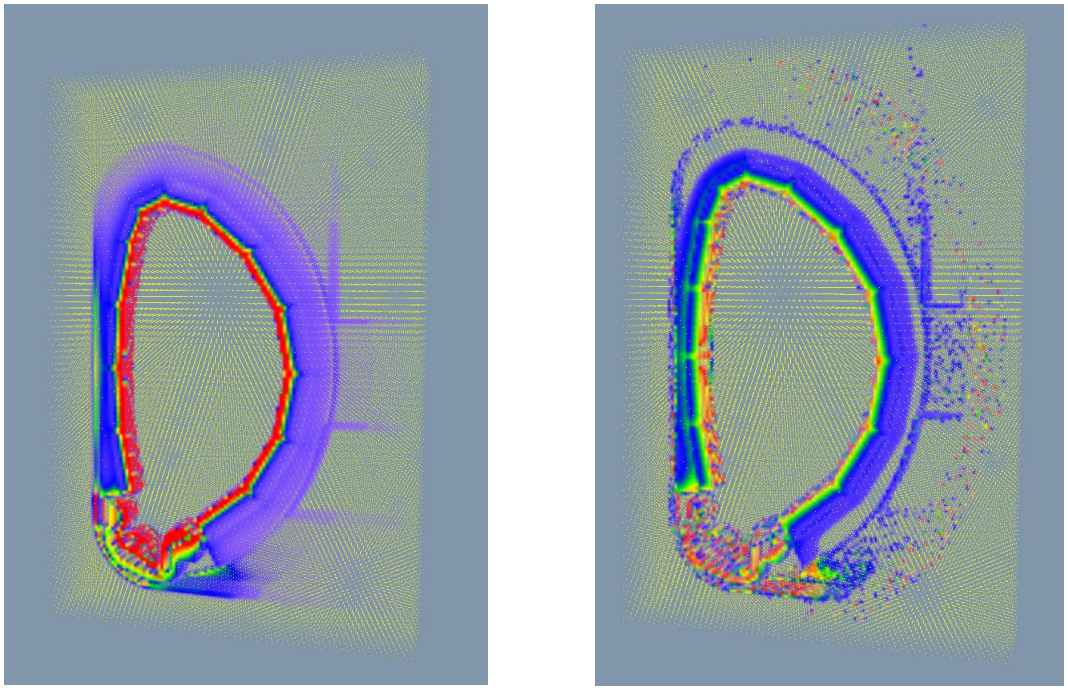

Gamma heating Neutron heating

Figure 5: Presentation of the heating distribution, obtained by using a mesh tally. Calculations were done for the provisional MCNP model for DEMO (supplied by KIT). The yellow dots represent the distribution of the mesh tally cells.

It should be also mentioned that the regular x-y-z rectangular cells of mesh-tally used for heating calculations does not necessarily coincide with the arbitrary oriented MCNP cells. Since the heating is averaged inside the mesh cells, along the border regions between two materials and especially between material and void, the material-to-void ratio inside the mesh-tally elements is changing substantially, causing quite visible difference in averaged mesh-tally heating for that mesh cell. This difference can be diminished by reducing the size of mesh-tally cells.

MCNP gives statistical errors for each mesh tally cell. They have to be kept within reasonable limits, which should in normal runs not exceed 0.10. Prior to export the mesh tallies into ANSYS, a check of the fulfilment of this restriction should be made. MCNP normalizes each run with respect to 1 source neutron. Care should be devoted to normalize the results to the determined fusion power.

3 CONCLUSIONS AND OUTLOOK FOR FURTHER WORK

The main objective of the performed task was to test the possibilities for data transfer from the MCNP neutronic analysis to the ANSYS CFX thermo-hydraulic analysis. The assessment was performed for the Blanket Test Case. The objectives of the task were fully achieved in 2012 and the continuation of these activities in the next year was not foreseen.

Based on the provided Test Blanket Module CAD model and the test specifications, the ANSYS CFX model was developed for the so called “slice” model, which considers a vertical slice of the blanket module. The modelled slice part of the blanket module was meshed using a fully hexahedral mesh. The inclusion of nuclear

heating in the CFX model is straightforward. Inside each domain (Beryllium, Eurofer, OSI) one has to define an additional subdomain, which serves as a heat source. The heat source can be defined by a user function, which can be a table of nuclear heating data provided for different locations in 3D. The table can be imported from a text file. In ANSYS Workbench it is possible to import data through the module called "External Data", but it seems that this option is not available for CFX. Also if it would be possible to import the data through the "External Data" module, this would not simplify the setup of the simulation, because similar steps would be required.

MCNP has the ability to define a mesh, superimposed over the problem geometry for tallying purposes. The mesh does not need to cover the whole geometry; it may be defined only in specific regions and it may be adequately refined where needed. Within each cell of this 3D mesh the nuclear heating may be calculated. The calculated nuclear heating data is given in form of a table in a text file, which may be directly imported into CFX after some basic editing.

The Blanket Test Case was simulated with ANSYS CFX, considering the provided 3D nuclear heating data. The loading time of the nuclear heating data significantly depends on the size of the data files, thus the density of the nuclear heating data points should be optimized. The simulation showed that the highest temperatures occur in the OSI region (996 K) due to its high volumetric heating and the low thermal conductivity. The volumetric nuclear heating (43 kW) is about two times larger than the plasma heating (23 kW). Most of the heat is removed by the helium cooling circuit in the first wall (38 kW). The heat removal in the breeder units is also significant (22 kW), whereas the cooling power of the horizontal grids is much lower (3 kW each).

4 REFERENCES

1 Blanket Test Case Definition, Karlsruhe Institute of Technology, 2012.
2 S. Keckes, L. Boccaccini, "Volumetric Heating Data for the Blanket Test Module Calculated by MCNP", personal communication, October 2012.
3 R. Villari at al., "Shutdown dose rate benchmark experiment at JET to validate the three-dimensional Advanced-D1S method", Fus. Eng. Des, Vol. 87, Issues 7–8, (2012).
4 Y. Chen, U. Fischer, "Rigorous mcnp based shutdown dose rate calculations: computational scheme, verification calculations and application to ITER", Fus. Eng. Des, Vol. 63–64, (2002).
5 A. Serikov, U. Fischer, D. Grosse, "High Performance Parallel Monte Carlo Transport Computations for ITER Fusion Neutronics Applications", Progr. Nucl. Sci. Tech., Vol. 2, (2011).

EVALUATION OF NUCLEAR DATA AND THEIR COVARIANCES FOR FUSION APPLICATIONS

Andrej Trkov

Jožef Stefan Institute, Jamova 39, 1000 Ljubljana
Andrej.trkov@ijs.si

1 INTRODUCTION

In the past, a common approach to new developments in nuclear technology was through mock-up experiments, which were representative in the general features of the full-scale device that was to be designed and constructed. Nowadays, experiments are relatively expensive. Furthermore, in the field of nuclear fusion the full scale devices are big and building of representative small mock-up experiments is not possible. For example, in the ITER device the temperature gradient has to be maintained between the superconducting magnets at near-zero temperature and the plasma core at hundred million degrees over a relatively short distance. Nuclear heating is the main mechanism for energy dissipation from the plasma; the system must provide adequate radiation shielding; it is also necessary to estimate the radiation damage that materials have to withstand for a safe operation of the device. Hence the neutronics properties of materials are highly important. Therefore, significant effort is placed into the development of techniques to propagate the uncertainties in nuclear data to the key parameters in the full-scale devices. This requires that in addition to the evaluation of the mean values of the nuclear data (i.e. cross sections, angular distributions, particle emission spectra, etc.), the covariances of these quantities must also be evaluated.

Tungsten is an important material that appears in the first wall of ITER and is currently tested in the JET device. In spite of several attempts to improve the evaluated cross section data for tungsten [1], the status of the nuclear data was unsatisfactory before the start of the project. Systematic discrepancies were observed in the benchmarks containing tungsten in the International Handbook of Evaluated Criticality Safety Benchmark Experiments [2], fusion neutronics benchmarks [3], and measured constants for neutron activation [4]. These discrepancies motivated the work on improving the evaluated nuclear data files for the tungsten isotopes.

Manganese is a dosimetry material and a component of steel alloys, which will be used extensively in the construction of ITER. There was a large discrepancy in the resonance integral calculated from the evaluated data files and the directly measured value. Some covariance information was available for the capture reaction, but it seemed to be very ad-hoc and unreliable. There was a clear requirement for a complete re-evaluation of the nuclear data for this material [4].

2 WORK PERFORMED IN 2007 - 2013

Initially, the focus of the work was in the development of methods for evaluating the covariance information in the fast neutron energy region, extending above 20 MeV. The work was extended to producing full evaluated data files for selected materials.

New evaluations for the tungsten isotopes ^{180,182,183,184,186}W in the neutron energy range up to 150 MeV were produced, including the covariance information. Minor adjustments to the existing resonance parameters were made. Evaluations in the fast energy region were based on nuclear model calculations using the EMPIRE-2.19 code; covariance data were generated with the Monte Carlo technique to produce a prior estimate for the covariance matrix. Experimental data were introduced through the GANDR system. An improved resonance parameter evaluation was contributed by L. Leal from the Oak Ridge National Laboratory. The evaluated files were tested on selected fusion neutronics benchmarks and fast reactor benchmarks, because they show high sensitivity to the data in the same energy range. Marked improvement in predicting measured integral parameters was observed, compared to the ENDF/B-VII.0 library, which is equivalent to FENDL-2.1 that was the adopted standard for ITER neutronics calculations at the time.

A new evaluation for ^{55}Mn was prepared in the energy range up to 150 MeV. The evaluation removed the long-standing discrepancy between the resonance integral calculated from the evaluated data files and the directly measured value. The methodology of evaluation was the same as for the tungsten isotopes. The resonance parameters with covariances were contributed by L. Leal from the Oak Ridge National Laboratory.

The basic evaluated nuclear data files, the same data in ACE format for Monte Carlo calculations and in MATXS format for deterministic calculations were made available. All of the above-mentioned evaluated data sets were adopted by the ENDF\B-VII.1 project [21] and are available from the main data centres. Likewise, the corresponding ACE files are included in the new release of the Monte Carlo code MCNP-6. The ^{55}Mn evaluation is also included in the IRDFF Dosimetry Library available from the IAEA [16].

The work was performed in collaboration with external partners, who were not funded from the contract from EFDA.

2.1. Nuclear Model Calculations

All calculations of the cross sections above the resonance range were fully based on nuclear model code EMPIRE [6]. Starting values for nuclear model parameters were taken from RIPL-2 [7]. A crucial point was the selection of the coupled-channel optical model potential (OMP). Direct interaction cross sections to low-lying levels and transmission coefficients for the incident channel were obtained from the isospin-dependent dispersive coupled-channel OMP [7, 8]. The same potential was used to calculate direct excitation of the collective levels in the continuum by the DWBA method. All the optical model calculations were performed with the ECIS code [9] that is incorporated into the EMPIRE system. The incident channel OMP was always used to calculate direct excitation of the collective levels in the continuum by the DWBA

method, which is important for a proper description of double differential cross sections and emission spectra above 5 MeV for all evaluated nuclei. Pre-equilibrium emission was considered using a one-component exciton model (PCROSS), which includes nucleon, gamma and cluster emission. Hauser-Feshbach [10] and Hofmann-Richert-Tepel-Weidenmueller [11] versions of the statistical model were used for the compound nucleus cross section calculations. Both approaches account for the multiple-particle emission and the full gamma-cascade. Level densities were described by the "EMPIRE specific" formalism (EGSM), which uses the superfluid model below the critical excitation energy and the Fermi gas model above [6]. Deformation-dependent collective effects on the level densities due to nuclear vibration and rotation and their temperature-dependent damping were also taken into account. Modified Lorenzian (MLO) radiative-strength function was taken as recommended by Plujko [7] and resulted in excellent agreement with the experimental neutron capture database. Total, capture, emission cross sections of neutrons and charged particles, average resonance parameters and angular distributions of neutron and proton scattering on all tungsten isotopes and manganese were in good agreement with the available experimental data.

The covariance matrix priors were generated by the Monte Carlo technique [12] using the EMPIRE code. The prior and selected experimental data from the EXFOR database were fed into the GANDR system [13] to produce the final covariance matrices. An example of the prior uncertainty generated by the MC method using nuclear model calculations for the (n,γ) cross-section on ^{182}W is shown in Fig. 1. In the same plot we can see the significant reduction of the prior uncertainty after we consider experimental data.

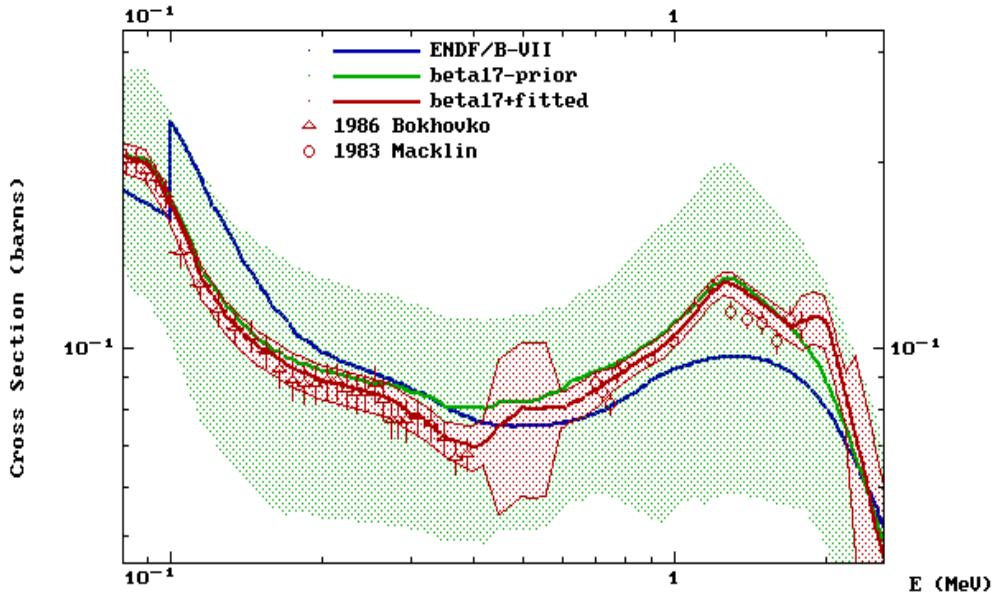

Figure 1: Uncertainties in the ^{182}W(n,γ) cross section of the prior and after entering the experimental data, in comparison with ENDF/B-VII.0 data.

For the ^{55}Mn evaluation there is excellent agreement with the experimental neutron capture database in the fast neutron range as shown in Fig. 2. The evaluated total inelastic cross section differs significantly from the ENDF/B-VII.0 evaluation, but

is in good agreement with Lashuk (n,n'γ) measurements of the excitation of first and second inelastic levels in ^{55}Mn nucleus as can be seen from Fig. 3.

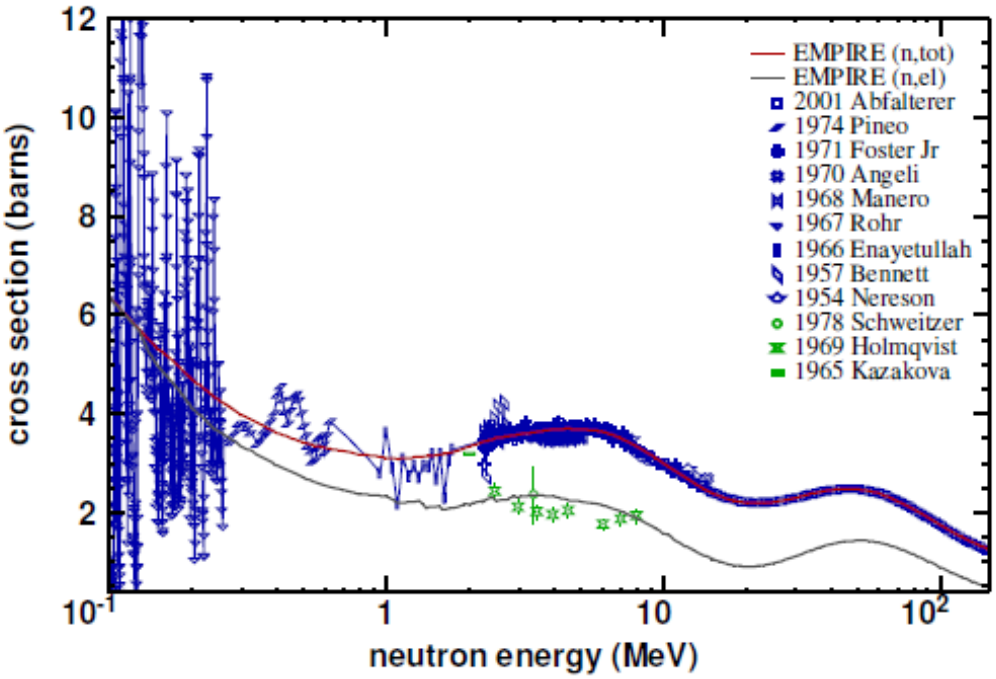

Figure 2: Experimental total and elastic cross sections on ^{55}Mn nucleus vs. EMPIRE=ENDF/B-VII.1 calculations with rigid-rotor dispersive coupled-channel neutron OMP (RIPL 1484). GANDR least-squares results are not shown.

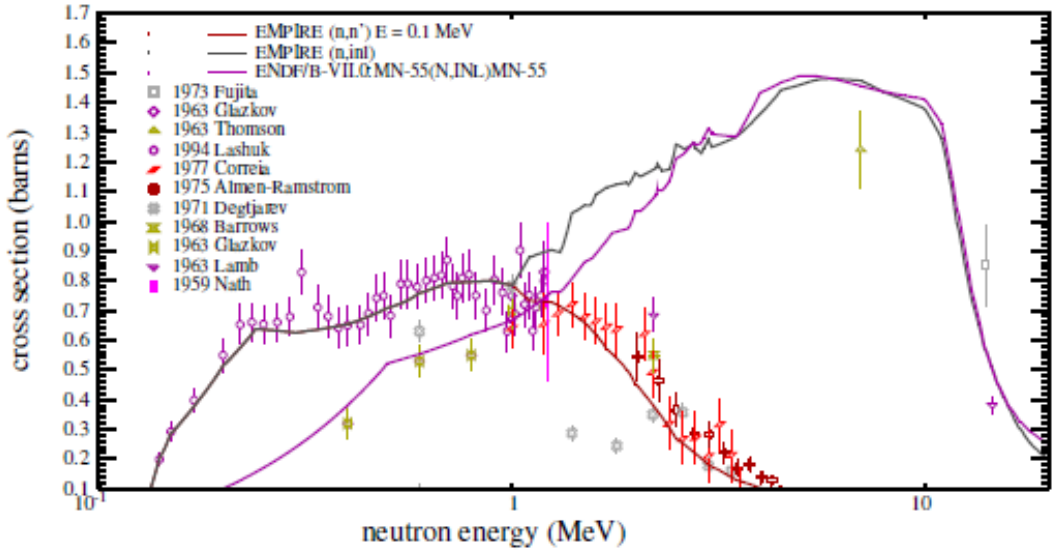

Figure 3: Experimental inelastic cross sections on 55Mn nucleus vs EMPIRE=VII.1 calculations (red,gray) and ENDF/B-VII.0 evaluation (magenta). GANDR least-squares results are not shown.

2.2. Nuclear Data File Validation

The files were checked for formal correctness with the ENDF utility codes CHECKR, FIZCON, PSYCHE and STANEF [18]. File processability was verified by running the suite of ENDF Pre-Processing codes [19] and preparing application libraries with the NJOY data processing system [20] for transport calculations using Monte Carlo and deterministic methods in ACE and MATXS format, respectively. Data validation was performed on test cases from international benchmark compilations:

- SINBAD: Fusion neutronics benchmarks with 14 MeV deuterium-tritium (D-T) sources, compiled at the OECD/NEA Data Bank [3], namely FNG-W, FNS and Oktavian (see details below).
- ICSBEP: Fast reactor assemblies from the Handbook of the International Critiality Safety Benchmark experiments [2].

An example of the excellent agreement between predicted and measured activities of monitor as a function of depth in the tungsten block irradiated with a D-T source (FNG-W benchmark from the SINBAD compilation) is shown in Fig. 4. The reactivity prediction of critical assemblies from the ICSBEP compilation containing tungstenis also greatly improved, as evident from Fig. 5.

The improvement in the simulation of the ^{55}Mn capture measurement in the Grenoble lead slowing-down-spectrometer [22] is shown in Fig. 6. The remarkable improvement removes the long-standing discrepancy between the resonance integral calculated from the evaluated data files and the directly measured value.

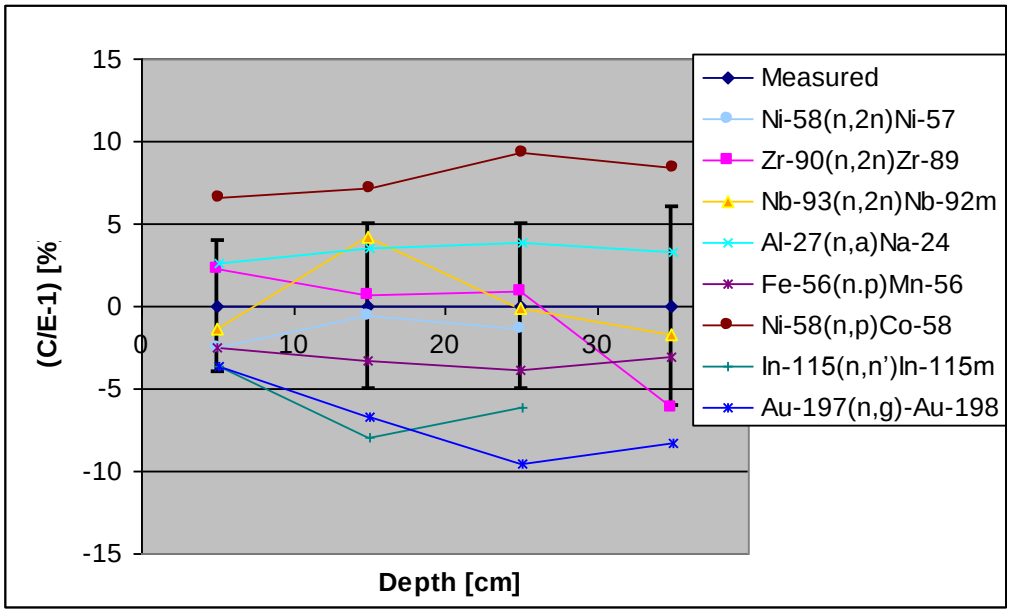

Figure 4: Comparison of calculated and measured reaction rates for the FNG-W benchmark

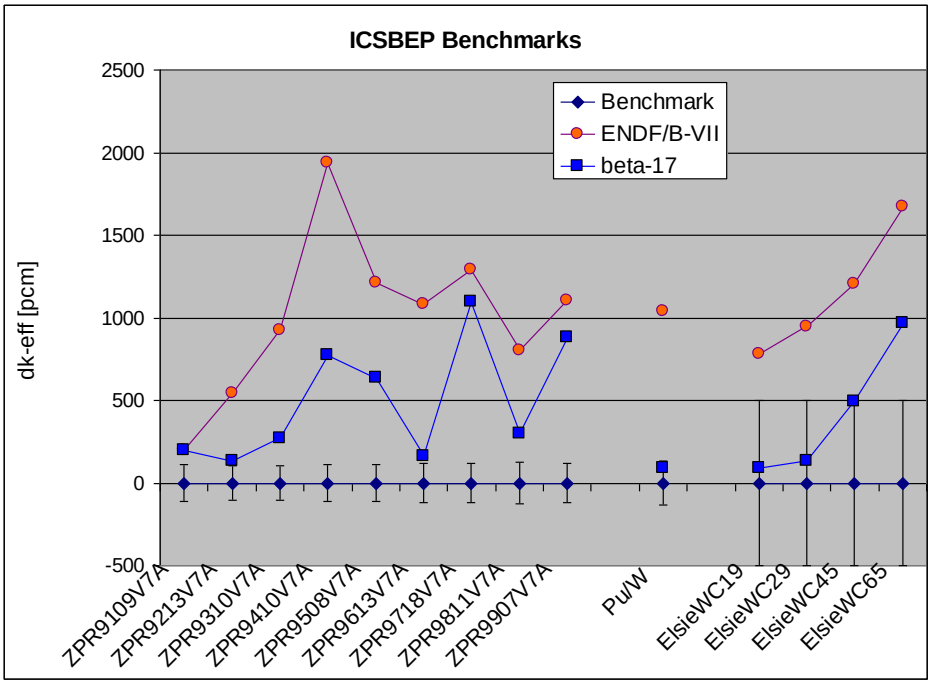

Figure 5: Differences between predicted and measured multiplication factors k_{eff} (in units pcm) using ENDF/B-VII.0 and the new data (labelled "beta-17").

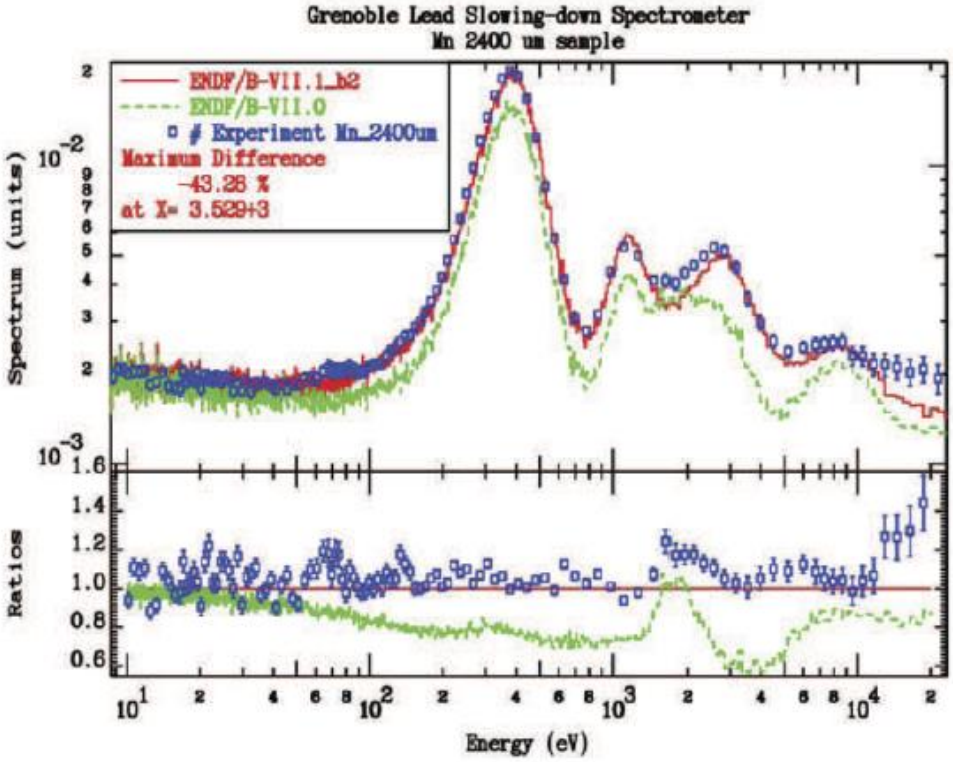

Figure 6: Simulation of the Grenoble lead-slowing-down experiment using ENDF/B-VII.0 and the newly evaluated data for ^{55}Mn (labelled "beta-17") compared to measured values.

3 CONCLUSIONS AND OUTLOOK FOR FURTHER WORK

The methodology for evaluating nuclear reaction data and their covariances was successfully applied to produce evaluated data files for the tungsten isotopes and manganese, which are relevant for fusion neutronics calculations. Benchmarking of the data was an integral part of the evaluation process, which proved to be crucial for producing high-quality evaluations. Furthermore it was shown, that it is necessary to consider as many benchmark types as possible. For example, the FNG-W benchmark from Frascatti and the criticality benchmarks from the ISBEP compilation are both sensitive to the tungsten capture data in approximately the same energy region, but with fine details in the sensitivity profile that made tuning of the data very difficult. The tungsten evaluations show good performance overall. There is still room for improvement, but this cannot be achieved without new measurements. A similar improvement in performance was also achieved with the ^{55}Mn evaluation. All evaluations extend to 150 MeV and include complete covariance information.

The work completed so far forms a solid basis for tackling even more demanding evaluation projects like the evaluation of nuclear reaction data for the isotopes of iron, which is the most abundant structural material in practically all fusion devices.

.

4 REFERENCES

1 Pereslavtsev, P., Fischer, U., 2007: Improved W data evaluation including benchmark tests, JEFF/EFF Meeting, NEA Data Bank, Paris, November 26-28, Technical report, EFFDOC 1032.

2 ICSBEP 2006, International Handbook of Evaluated Criticality Safety Benchmark Experiments, NEA Nuclear Science Committee, Nuclear Energy Agency, Organisation for Economic Co-operation and Development, Technical Report NEA/NSC/DOC(95)03.

3 SINBAD 2006, SINBAD FUSION, Neutronics Benchmark Experiments, Nuclear Energy Agency, Organisation for Economic Co-operation and Development, Package ID: NEA-1553.

4 Kodeli, I., Trkov, A., 2007: Validation of the IRDF-2002 Dosimetry Library, Nucl. Instr. Meth. A572, 664-681.

5 Capote, R., Trkov, A., Kodeli, I., Soukhovitskii, E., Leal, L.C., Herman, M., Muir, D.W., 2007: Evaluation of tungsten isotopes in the fast neutron range including cross-section covariance estimation, (Contribution #629) International Conference on Nuclear Data for Science and Technology, ND2007, 22-27 April 2007, Nice, France. Herman, M., Capote, R., Carlson, B., Obložinský, P., Sin, M., Trkov, A., Wienke, H., Zerkin, V., 2007: EMPIRE: Nuclear Reaction Model Code System for Data Evaluation. Nuclear Data Sheets 108, 2655-2715

6 Belgya, T., Bersillon, O., Capote R. Fukahori, T., Zhigang, G., Goriely, S., Herman, M., Ignatyuk, A.V., Kailas, S., Koning, A., Oblozinsky, P., Plujko, V. and Young, P., 2006: Handbook for calculations of nuclear reaction data: Reference Input Parameter Library-2, Technical Report IAEA-TECDOC-1506, IAEA, Vienna, Austria, 2006. Available online @ http://www-nds.iaea.org/RIPL-2/

7 Capote, R., Soukhovitski, E. Sh., Quesada, J. M. and Chiba, S. 2006: Isospin dependent dispersive coupled channel optical model potential for tungsten isotopes, Presented at the 11th International Conference on Nuclear Reaction Mechanisms, Varenna, Italy, June 12-16, 2006 (unpublished);

8 Capote, R., Sin, M., Trkov, A., 2007a. Modelling of nuclear data in the fast neutron region, in: Plompen, A.J.M. (Ed.), NEMEA-3: Neutron Measurements, Evaluations and Applications, EUR 22794 EN, European Commission, Luxembourg, pp.13-18.
9 J. Raynal, "Optical model and coupled-channel calculations in nuclear physics", in: computing as a language of physics, ICTP International Seminar Course, Trieste, Italy, 1971, International Atomic Energy Agency, Vienna, Austria, 281 (1972); "ECIS96", in: Proc. OECD/NEA Specialists Meeting on Nucleon-Nucleus Optical Model to 200 MeV, Bruy`eres-le-Chˆatel, France, 1997, 159–166 (Available from http://www.nea.fr/html/science/om200/).
10 W. Hauser and H. Feshbach, "The Inelastic Scattering of Neutrons", Phys. Rev. 87, 366 (1952).
11 H. M. Hofmann, J. Richert, J. W. Tepel, and H. A. Weidenm¨uller, "Direct reactions and Hauser-Feshbach theory", Ann. Phys. 90, 403 (1975).
12 Smith, D.L. 2005, Covariance Matrices for Nuclear Cross-Sections Derived from Nuclear Model Calculations, Technical Report ANL/NDM-159, Argonne National Laboratory, USA.
13 Muir, D.W., 2007. Global Assessment of Nuclear Data Requirements - the GANDR Project, an IAEA Nuclear Data Section Data Development Project. Available online @ www-nds.iaea.org/gandr/
14 Shibata, K., Kawano, T., Nakagawa, T., Iwamoto, O., Katakura, J., Fukahori, T., Chiba, S., Hasegawa, A., Murata, T., Matsunobu, H., Ohsawa, T., Nakajima, Y., Yoshida, T., Zukeran, A., Kawai, M., Baba, M., Ishikawa, M., Asami, T., Watanabe, T., Watanabe, Y., Igashira, M., Yamamuro, N., Kitazawa, H., Yamano, N. and Takano H., 2002: Japanese Evaluated Nuclear Data Library Version 3 Revision-3: JENDL-3.3, J. Nucl. Sci. Tech. 39, 1125.
15 Mughabghab 2006: Atlas of Neutron Resonances, Elsevier Science, April 17, 2006.
16 Bersillon, O., Greenwood, L.R., Griffin, P.J., Mannhart, W., Nolthenius, H.J., Paviotti-Corcuera, R., Zolotarev, K.I., Zsolnay, E.M., McLaughlin, P.K., Trkov, A., 2006: International Reactor Dosimetry File 2002 (IRDF-2002), International Atomic Energy Agency, Technical Report Series No. 452, Vienna, Austria.
17 Chadwick, M.B.. Obložinský, P., Herman, M., Greene, N.M., McKnight, R.D., Smith, D.L., Young, P.G., MacFarlane, R.E., Hale, G.M., Frankle, S.C., Kahler, A.C., Kawano, T., Little, R.C., Madland, D.G., Moller, P., Mosteller, R.D., Page, P.R., Talou, P., Trellue, H., White, M.C. et al. 2006: ENDF/B-VII.0: Next Generation Evaluated Nuclear Data Library for Nuclear Science and Technology, Nuclear Data Sheets 107, 2931-3118.
18 Dunford, C.L., 2005: ENDF Utility Codes Release 7.01/02, National Nuclear Data Center, Brookhaven National Laboratory, U.S.A., @ http://www.nndc.bnl.gov/nndcscr/endf/.
19 Cullen, D.E. 2007: PREPRO 2007 ENDF/B Pre-processing Codes, Nuclear Data Services, International Atomic Energy Agency, IAEA-NDS-39, Rev. 13.
20 MacFarlane, R.E., and Muir, D.W., 1997: The NJOY Nuclear Data Processing System, Radiation Safety Information Computational Center, Oak Ridge National Laboratory, USA, Package ID PSR-480.
21 M. Chadwick, et al. ENDF/B-VII.1 nuclear data for science and technology: cross sections, covariances, fission product yields and decay data. Nuclear data sheets, ISSN 0090-3752, 2011, no. 12, vol. 112, str. 2887-2996
22 L. Perrot, A. Billebaud,* R. Brissot, A. Giorni, D. Heuer, J.-M. Loiseaux, O. Méplan, and J.-B. Viano , "Precise Validation of Database (n,g) Cross Sections Using a Lead-Slowing-Down Spectrometer and Simulation from 0.1 eV to 30 keV: Methodology and Data for a Few Elements" , Nucl. Sci. Eng. 144, 142–156 (2003).

ANALYSIS OF TRITIUM PRODUCTION AND NEUTRON REACTION RATE MEASUREMENTS IN THE NEUTRONICS FNG-HCLL BENCHMARK USING THE DETERMINISTIC TRANSPORT, SENSITIVITY AND UNCERTAINTY CODES SUSD3D/DOORS

I. Kodeli

Jožef Stefan Institute, Jamova 39, 1000 Ljubljana
ivo.kodeli@ijs.si

1 INTRODUCTION

Fusion energy production will rely on fusion reactors such as ITER using deuterium and tritium fuel in the D-T reaction. Tritium is a radioactive isotope of hydrogen with a relatively short half-life and as such not available in nature therefore the future reactors should be capable of attaining tritium self-sufficiency by producing the tritium in a dedicated component – tritium breeding modules (TBM). Several such TBMs will be tested in ITER, using the tritium breeding blanket containing lithium, through the ^{6}Li(n,t)α and ^{7}Li(n,n't)α reactions.

A neutronics experiment was performed in 2009 at ENEA Frascati Neutron Generator (FNG) 14 MeV facility in the frame of European Fusion Technology Program on a mock-up of the EU Test Blanket Module (TBM), Helium Cooled Lithium Lead (HCLL) concept [1-7], with the objective to validate the capability of nuclear data to predict nuclear responses, such as the tritium production rate (TPR), with qualified uncertainties. This complemented the previous experiment completed in 2003 on the Helium Cooled Pebble Bed (HCPB) concept. The Tritium Production Rate (TPR) was measured using Li_2CO_3 pellets, containing both natural and ^{6}Li-enriched lithium, located at various depths, at two symmetrical lateral positions. The measurements of TPR were performed independently by three different teams at ENEA, TUD and JAEA.

This document presents the computational analysis of the benchmark using the deterministic transport, sensitivity and uncertainty code system. The analysis includes the calculation of the tritium production rate (TPR) in LiPb layers and the neutron reaction rates, which were measured in the benchmark. The SUSD3D cross-section sensitivity and uncertainty code package together with the 2D/3D deterministic transport codes DORT/TORT is used for the analysis of the experiment. Based on the sensitivity analyses the most important nuclear reactions and energy ranges in the particular reaction-rate measurements were identified. Furthermore the uncertainties of the calculated TPR were estimated and compared with the observed C/E (Calculated-to-

measured) ratios, providing in this way the information on the quality of the available nuclear cross-section data and the consistency of the corresponding covariance matrices.

2 FNG-HCLL BENCHMARK ANALYSIS

The cross section sensitivity and uncertainty calculations were performed using the SUSD3D [8] code, which requires as input quantities the direct and adjoint angular moment fluxes calculated by the Discrete ordinates codes (DORT or TORT [9]), as well as the transport cross sections and covariance matrices for the relevant materials and reactions. Both exact 3-dimensional (3D) and a simplified, but representative 2D geometrical models were developed for the sensitivity and uncertainty analysis in the scope of the previous tasks, based respectively on the TORT and DORT calculations. Good consistency between the 2D and 3D calculations was observed for several test cases [7], therefore the analyses presented here refer to the much less time consuming two-dimensional sensitivity and uncertainty analyses using the SUSD3D code with the neutron fluxes calculated by the DORT code. Nuclear cross-section data were taken from FENDL-2.1 [10] available in the 175 VITAMIN-J energy group structure and processed by the TRANSX code [11]. The response functions were taken from IRDF-2002 [12] (^{6}Li(n,t) reaction) and JEF-2.2 (^{7}Li(n,t) reaction).

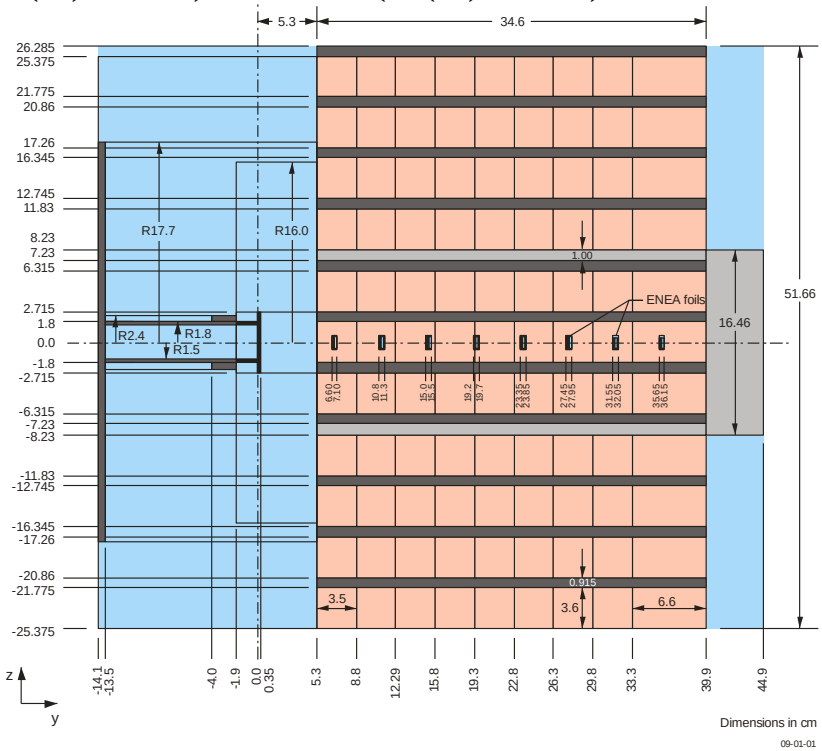

Figure 1: YZ side views of the final TBM-HCLL mock-up geometry showing the steel (dark gray), Polyethylene (light gray) and LiPb (pink) layers.

The HCLL mock-up (see Figure 1) consists of a block of 45 cm x 51.66 cm side-view and 34.6 cm long, placed 5.3 cm in front of the 14 MeV FNG neutron source. The block is composed of 11 alternating layers of LiPb bricks (3.6 cm high) and EUROFER-

97 plates (0.915 cm thick). Two additional thin layers and a back reflector of Polyethylene have been introduced.

In the first experimental set-up the fast and the thermal neutron flux was measured using the Al, Ni, Nb, In, Au an Mn activation foils up to the depth of about 30 cm. The second experiment was devoted to the measurement of the Tritium Production Rates (TPR) and TLD. The TPR responses were measured both with the natural (7.5 % ^{6}Li) and 95% enriched Li_2CO_3 pellets. Sets of 3 pellets with 1.3 cm diameter and thicknesses of 0.18/0.18/0.10 cm have been introduced at 7 radial positions starting from 3.65 cm to 28.55 cm in the mock-up.

As for the LiPb brick material composition, it has been revealed in the experiment that the actual lithium content is probably about half the nominal value of 15.7 at % [5, 6]. The lithium content used for the present sensitivity/uncertainty analyses was adjusted accordingly.

The C/E values for the fast neutron reaction rates measured at 8 detector locations in the FNG HCLL mock-up are presented in Figure 2, showing good agreement, within 5 to 10 %, between the measured and calculated results.

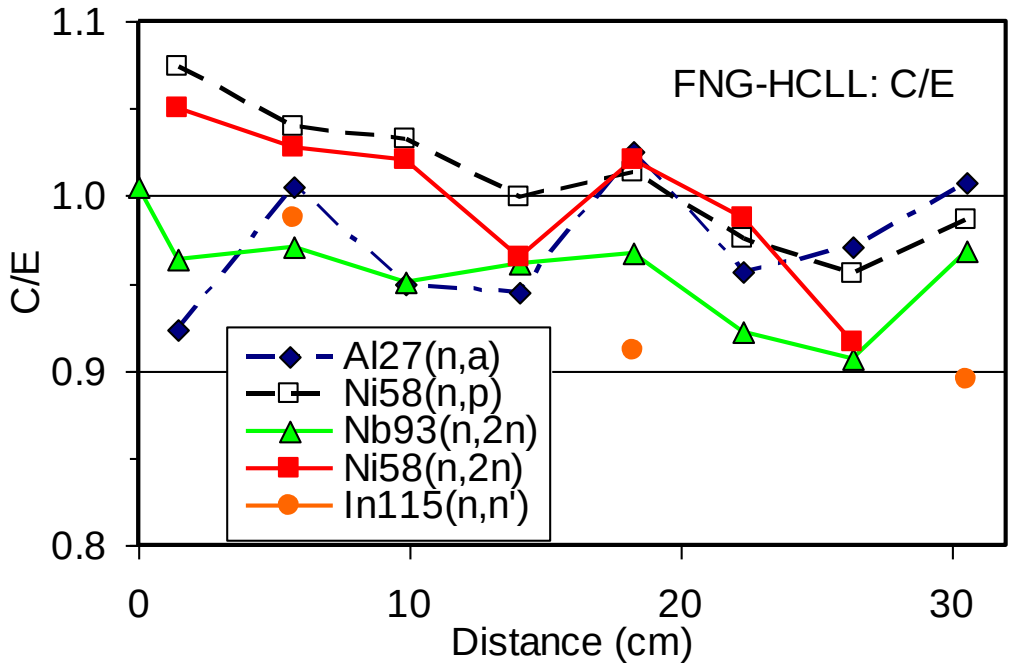

Figure 3: C/E values for the fast neutron reaction rates measured in the HCLL mock-up. The calculated values were obtained using the DOT calculations. The measurement uncertainty is between ±4% and ±5.2%, consisting of the statistical error (±0.9% - ±3.4%), the uncertainty of the FNG neutron source yield (±3%) and the HPGe efficiency (±2.5%).

For the uncertainty analysis several sets of cross section covariance matrices were used, i.e. from the ENDF/B-VI.8, ENDF/B-VII, JEFF-2.4 and the ZZ SCALE6.0/COVA-44G libraries [13-14]. The uncertainty estimations for the measured reaction rates and TPR are shown in Table 1.

We observed that the lead cross sections were the most important nuclear data parameter influencing the TPR, but even for these data the corresponding sensitivities

were found to be relatively low, below 1% of change in TPR per 1% of change in the cross sections. The most sensitive reaction was found to the elastic scattering on lead. Controversially, this is not the reaction causing the largest uncertainty, since the corresponding cross section uncertainty is relatively low. On the other hand, the precision in the (n,2n) and (n,3n) reactions of the lead isotopes is rather low, consequently most of the overall uncertainty in the calculated TPR is caused by the uncertainty in these cross section reactions.

Table 1: Total uncertainty in the calculated reaction rates based on various covariance matrix evaluations. Two sets of uncertainties are given, assuming either no- and complete correlation between the Pb isotopes. (SUSD3D results based on the DORT 2D neutron fluxes)

Covariance data	***Uncertainty –no/ full correlation (%)***							
	^{115}In(n,n') D8	^{27}Al(n,α) D8	^{58}Ni(n,p) D8	^{93}Nb(n,2n) D8	^{6}Li(n,t) D1	^{6}Li(n,t) D7	^{nat}Li(n,t) D1	^{nat}Li(n,t) D7
ENDF/B-VI	3.4/6.7	4.6/8.5	3.4/6.6	5.0/9.0	6.6/9.3	2.8/4.1	3.0/4.8	2.8/3.9
SCALE-6	2.8/5.2	7.1/12.2	4.9/8.8	7.2/12.3	2.2/4.1	1.4/2.5	1.2/1.8	1.2/2.1

* preliminary JEFF3.2 evaluation processed using an older version of NJOY

3 CONCLUSIONS

DORT and TORT/GRTUNCL-3D/SUSD3D computational schemes were used in the analysis of FNG-HCLL benchmark mock-up. The reaction rates and TPR were found weakly sensitive to the underlying nuclear cross sections. Using the ENDF/B-VI.8 and SCALE-6 covariance matrices, the uncertainties due to cross section uncertainties were estimated to be between 1 – 10 % (1σ), depending on the nuclear reaction and the covariance data used. In general, reasonable agreement is observed between the uncertainties based on different covariance matrices. According to these covariance data the reactions (n,2n) and, in the case of ENDF/B-VI.8 (n,3n), on lead were found to cause the highest uncertainty, although the corresponding sensitivities are not particularly high. Inelastic cross sections were also found to be important for some isotopes of lead.

The tritium production rate was found to be most sensitive to the cross sections of lead, hydrogen and the respective tritium generating reactions in lithium. However, according to the available cross section covariance data, the associated nuclear data related uncertainties are small, usually below 2 %, even for the deep positions of ~30 cm. Higher uncertainties were obtained using the ENDF/B-VI.8 covariance data, due to very high (possibly overestimated) uncertainties in the (n,3n) reactions in lead.

According to these results, the quality of the nuclear data seems to be sufficient for the reliable design of the HCLL TBM for the future fusion reactor, assuming that the actual reactor spectra would be reasonably similar to the one in the benchmark experiment. These conclusions are still to be verified and confirmed through the final comparison between the measured and calculated TPR, which is underway.

In some cases the quality of the available covariance data was found to be relatively poor. Matrices with small negative eigenvalues, and even unreal matrices (Li-7 in ENDF/B-VI.8) were detected. The need of a new evaluation of covariance data to cover some specific fusion related nuclear uncertainties was pointed out.

4 REFERENCES

1. P. Batistoni et al., Design optimisation and measuring techniques for the neutronics experiment on a HCLL - TBM mock-up, *Fus. Eng. Des.* ***84*** (2009) 430-434
2. P. Batistoni, M. Angelone, L. Bettinali, P. Carconi, U. Fischer, I. Kodeli, D. Leichtle, K. Ochiai, R. Perel, M. Pillon, I. Schäfer, K. Seidel, Y. Verzilov, R. Villari, G. Zappa, Neutronics Experiment on a HCPB Breeder Blanket Mock-up, *Fusion Engineering and Design*, ***82*** (15), p.2095-2104, (2007)
3. U. Fischer, P. Batistoni, A. Klix, I. Kodeli, D. Leichtle, R. L. Perel, Neutronics R&D efforts in support of the European breeder blanket development programme, Nucl. Fusion 49 (2009) 065009
4. I. Kodeli, Deterministic 3D Transport, Sensitivity and Uncertainty Analysis of TPR and Reaction Rate Measurements in HCPB Breeder Blanket Mock-up Benchmark, Proc. Int. Conf. Nuclear Energy for New Europe 2006, Portorož, Slovenia, Sept. 18-21, 2006
5. P. Batistoni, M. Angelone, P. Carconi, U. Fischer, K. Fleischer, K. Kondo, A. Klix, I. Kodeli, D. Leichtle, L. Petrizzi1, M. Pillon1, W. Pohorecki8, M. Sommer6, A. Trkov, R. Villari, Neutronics experiments on HCPB and HCLL TBM mock-ups in preparation of nuclear measurements in ITER, International Symposium on Fusion Nuclear Technology (ISFNT 9), 11. – 16.10.2009, Dalian, China
6. D. Leichtle, U. Fischer, I. Kodeli, R. L. Perel, A. Klix, P. Batistoni, R. Villari, Sensitivity and uncertainty analyses of the HCLL mock-up experiment, , International Symposium on Fusion Nuclear Technology (ISFNT 9), 11. – 16.10.2009, Dalian, China
7. Kodeli, Use of Nuclear Data Sensitivity and Uncertainty Analysis for the Design Preparation of the HCLL Breeder Blanket Mock-Up Experiment for ITER, International Conference "Nuclear Energy for New Europe 2008", 8 - 11. September, 2008, Portorož
8. Kodeli, "Multidimensional Deterministic Nuclear Data Sensitivity and Uncertainty Code System, Method and Application", *Nucl. Sci. Eng*., **138** (2001), pp. 45-66
9. W. A. Rhoades, et al., DOORS 3.2, One-, Two-, Three-Dimensional Discrete Ordinates Neutron/Photon Transport Code System, CCC-650, Radiation Safety Information Computational Center, Oak Ridge National Laboratory (1998).
10. D. L. Aldama, A.Trkov, FENDL-2.1: Update of an evaluated nuclear data library for fusion applications, Report INDC(NDS)-467 (Dec. 2004).
11. R.E. MacFarlane, TRANSX, Transport Cross Sections from MATXS Libraries, Vers. 2.15 (Nov. 94)
12. International Atomic Energy Agency: International Reactor Dosimetry File 2002 (IRDF-2002), Technical Reports Series No. 452, ISBN 92-0-105106-9, December 2006, "http://www-pub.iaea.org/MTCD/publications/PDF/TRS452_web.pdf".
13. ZZ SCALE6.0/COVA-44G, 44-group cross section covariance matrix library extracted from SCALE6.0, NEA Data Bank, USCD-1236/02 (May 2009)
14. I. Kodeli, VITAMIN-J/COVA/EFF-3 Cross-Section Covariance Matrix Library and its Use to Analyse Benchmark Experiments in SINBAD Database, Fus. Eng. Des. 75-79 (2005) 1021-1025

PUBLIC INFORMATION ACTIVITIES

Tomaž Skobe, Saša Novak, Luka Snoj

Jožef Stefan Institute, Jamova cesta 39, SI-1000 Ljubljana
tomaz.skobe@ijs.si

1 INTRODUCTION

The report summarizes various public information activities in the period 2007-2013. It involves basic information on the permanent exposition run by the Nuclear Training Centre and on other regular activities.

2 EDUCATIONAL PROGRAMME IN 2007 - 2013

Permanent fusion exhibition at the Nuclear training centre (http://www.icjt.org/an/) of the Jožef Stefan Institute was visited in the period 2007-2013 by 1.219 organized groups of 52.355 visitors altogether, mainly youngsters from primary, secondary and high schools. We were often visited also by graduate and postgraduate students and organized groups of adults.

	Number of groups	Visitors	Lectures on fusion technology	Lectures on radioactivity and radioactive waste	Lectures on electricity from nuclear energy
2007	187	7.904	25	35	127
2008	167	7.606	23	30	129
2009	180	7.507	22	19	135
2010	174	7.529	17	15	143
2011	185	7.445	19	19	140
2012	164	7.264	21	24	118
2013	162	7.100	20	23	117

Table 1: Visitors of the exhibition at the Nuclear Training Centre.

During the visit of ICJT, youngsters and other visitors can listen one of the three lectures on the following topics: Fusion technology and ITER project, Electricity from nuclear energy and Radioactivity and radioactive waste. After the lecture (which lasts approximately 45-60 min) all visitors attend the Radioactivity workshop, where visitors get acquainted with types and sources of ionizing radiation and how to protect against

different types of ionizing radiation. At the workshop we perform several experiments with alpha, beta and gamma emitters. We also "create" radioactive sources by filtering the radon and its daughters from the air.

Figure 1: Fusion exhibition.

2.1. Activities in 2007

In 2007 the word ”fusion“ appeared more frequently in popular articles than in previous years. Fusion was mentioned as a possible new source of energy in political speeches, at symposia (e.g., Symposium on the Environment: “Sustainable energy and economy of hydrogen” in Celje), as well as in everyday discussions, but it obviously attracted the attention of sociologists: In June 2007 Mrs. Hudej, a student of Social Sciences at the University in Ljubljana, defended her diploma work dealing with the sociological aspects of nuclear fusion (Nina Hudej, Družbene posledice jedrske fuzije, Diplomsko delo, Univerza v Ljubljani, Fakulteta za družbene vede, 2007).

It appears that the Slovenian Fusion Association is getting noticed by society, probably mostly due to the easily found SFA web site. The head of the research unit and the PI officer were contacted several times with different questions concerning fusion. In this way we also had an opportunity to discuss with a journalist who was writing a very negative article (he only asked for a little help in translating several professional terms from French).

In October 2007 at the Jožef Stefan Institute the national television station (SLO 1) filmed a programme about fusion. The contribution was part of a two-week series Alpe-Jadran-Donava aimed at showing fusion as a potential source of energy for the future and in particular to present the role of Slovenian scientists in the European fusion programme. Prof. Milan Čerček, the Head of the Slovenian Fusion Association, briefly described fusion basics, the concept of ITER and explained about the international fusion programme and the role of the Slovenian research groups in it. In the second part Ms. Sabina Markelj and dr. Saša Novak briefly presented some of the fusion-related research at the Department for Low and Medium Energy Physics and at the Department for Nanostructured Materials.

2.2. Activities in 2008

On April 9th 2008 Dr. Tomaž Gyergyek gave a lecture entitled "Fuzija – energija prihodnosti" (Fusion – Energy for the future) in the House of experiments in Ljubljana. The lecture has also been published at the web page: http://www.h-e.si/index.php?option=com_content&task=view&id=97&Itemid=1.

The speech of the European Commissioner Dr. Janez Potočnik about ITER has been translated to English, equipped with subtitles (H. Desmedt) and published at Youtube: http://www.youtube.com/watch?v=1YCRK5fOFIE .

The movie Starmakers synchronized in Slovenian language has been published at Youtube: http://www.youtube.com/watch?v=PWswTyYq0Q4. The script of the movie Fusion 2100 has been translated to be used for subtitles. The subtitled movie has been published at the SFA web pages. The Slovenian press agency STA has been provided with the official comment of the ITER project.

S. Novak attended the PIG meeting in Lisbon and presented the report on the SFA 4 activities in 2007. Based on the numerous ideas and activities resented by other associations, a tentative list of possible activities for the Y2008 was formed, such as:

1. Survey in primary schools about the issue of electrical energy and the knowledge about various sources including fusion,
2. Organization of the Science night in the Ljubljana city centre,
3. Organization of the second Fusion expo in Ljubljana,
4. Organization of PIG meeting 2009 in Ljubljana, etc.

The SFA applied for the project Fusion Expo and upon the acceptance, the action started in October 2008.

2.3. Activities in 2009

The Year 2009 was highly active for the PIs in the Slovenian Fusion association. Besides updating and correcting the brochures ("Cleaner Energy for the Future, "Fusion in Industry" and "Fusion Research, An Energy Option for Europe's Future"), communication with media, updating the web page, running the permanent fusion exhibition and giving fusion-related lectures, the most sound activities of the were surely taking over the travelling Fusion Expo (separate report), organisation the exhibition in Ljubljana and PIG meeting in Ljubljana.

Figure 2: Fusion Expo in Ljubljana.

Fusion Expo was organised as the first exhibition conducted by the SFA under the new contract. It was presented in Gallery Kresija in Ljubljana from 10th to 20th arch. A strong motivation to organise already the second Fusion expo in Ljubljana (first in 2005) was coupling both teams, i.e. the Fusion Expo team and the local organizer (host) in one place that gave us an opportunity to train the whole team and to collect precious information and suggestions for the next hosts.

The SFA has taken an organisation of the Public Information Group meeting 2009. It was held on 14th and 15th May at the Jožef Stefan Institute. On the first day the program was running at the headquarters of the JSI in Ljubljana, mostly at the Department for Nanostructured Materials. A part of the program was also a performance entitled "The power of experiments" presented by a group of young scientists. The main goal of the performance consisted of spectacular chemical experiments was to stress the importance of attracting the listeners by experiments instead of only theoretical presentations. As the first example the "teachers" wrote the equation $2H_2 + O_2 \rightarrow 2H_2O$ on the blackboard, supplementing it by data on enthalpy of the reaction and some additional chemical explanations, while in the next step they conducted several sound experiments accompanied by fire and laugh.

The second part of the meeting proceeded at the Nuclear Training Centre (ICJT) at the second site of the Jožef Stefan Institute. After the presentations and discussions, the participants visited the permanent exhibition on nuclear technologies, fusion and fission.

In May, Mr. Hugues Desmedt brought the camera and recorded a lot of material. A video clip about activities of the SFA in the laboratories involved in European Fusion Programme.

2.4. Activities in 2010

In the year 2010 we set up a new exhibit of JET Mark I diverter. Part of the JET Mark I divertor was a gift from JET to our exhibition. In 2010 we prepared a stylish stand for the exhibit and a started working on the poster explaining the function of divertor in tokamak.

Figure 3: JET Mark I divertor and Fusion Expo team.

In addition to the regular PI actions, the Slovenian version of brochures "Cleaner Energy for the Future (Bolj čista energija za prihodnost)" and "Fusion research" were corrected and SFA video clip was edited.

Another action was initiated at the PIG meeting 2010 at Riso, where the bottles served by the host gave us an idea for the new fusion communication tool "fusion water". By help of our graphic designer – a PhD student Aljaž Ivekovič, a label for the bottles was produced and for a trial used at the Fusion Expo in Brussels.

In April 2010 in the series "Ugriznimo znanost" (Let's bite science: Fusion, energy for the future) a broadcast on fusion (Fusion, energy for the future) was performed. In 20 minutes video a discussion with Slovenian scientists involved in fusion research was performed and the main features of the proposed fusion power plant presented. Beside the discussion in the studio, a part was recorded at the permanent fusion exhibition at ICJT and a part by the Nuclear power plant in Krško.

Figure 4: Label for Fusion Expo bottle.

One of the channels used to spread general as well as more detailed information on fusion technology, the latest achievements, the fusion related papers, etc., remains he "Unofficial ITER fan club" – the web page edited by David Jezeršek. From the statistics given below it is evident that the highest number of the visits comes from Germany, USA and UK. The number of the visits in 2010 was lower than in 2009, when Fusion expo took place in Ljubljana, which shows that the interest for fusion locally contributes significantly to the interest in fusion.

2.5. Activities in 2011

The PI officer S. Novak and the Fusion Expo leader T. Skobe attended the annual public information group meeting in Greifswald. Dr. Novak opened a discussion on the possible new fusion communication tool - "fusion water". The project "Only water?" that is supposed to illustrate the wide availability of deuterium in nature, as generally well accepted by the other PI officers, however, due to the missing part of the message – tritium, it was decided to further develop the idea before implementation.

In March 2011 the Head of research group prof. Milan Čerček was invited as a guest to the main evening news "Odmevi (Echoes)" at the national TV - SLO1. He explained the basic principle of fusion technology and the main advantages of nuclear fusion. Since this programme is among the most watched telecast, the fusion was well presented to the general public.

The regular public information activities involved editing the web page, translations, popular articles and lectures: In September, Dr. S. Novak was invited to

give a lecture on fusion energy at the regular meeting of Rotary Club Ljubljana Carniola.

At the occasion of the first plasma in JET after the installing the new ITER-like wall, Dr. Novak and Dr. Snoj wrote a paper describing the event and the pink plasma, and it was published in the main Slovenian newspaper DELO.

An interview with Prof. Tomaž Gyergyek was published in the gazette Vodice – Kopitarjev glas. The movie Fusia 3D, prepared by the Commission was translated from English to Slovenian language.

A new experiment for the House of experiments in Ljubljana has been under construction. The topic is repulsion force between equally charged particles that is supposed to be illustrated by aid of magnetic force.

Video clip of the Slovenian fusion association has been finished by help of Hugues Desmedt (EC). The texts and music were added (the music was voluntary composed by Vitalij Osmačko). The video has been published at the SFA web page (www.sfa-fusion.si).

2.6. Activities in 2012

In March, within the annual Open day at the Jožef Stefan Institute, we organized an exhibition of the activities performed within the project Fusion Expo and so we used this opportunity to increase the awareness of the fusion research.

The exhibition was at both sites of the JSI, in Ljubljana and at the Reactor Centre in Podgorica. The visitors could learn about the travelling exhibition and the guides were giving the explanation on the fusion-related questions.

In parallel, the Fusion Expo was presented in an article published in IJS Novice, the official quarterly J. Stefan Institute publication, which is distributed also to some public bodies, such as Ministries and Slovenian Agency for Science.

In the 239th edition of ITER Newsline an interview with dr. David Jezeršek was published (http://www.iter.org/newsline/239/1299). David is known to some of the PIs as the creator of the Unofficial ITER Fan Club website, which has been collected ITER-related news since even before ITER organisation itself created its own webpage.

In newspaper DELO an article »Step by step to fusion reactor« was published in October.

SFA MESCS video clip was subtitled in English and published at EFDA web page http://www.efda.org/2013/01/association-euratom-mescs-slovenia/.

SFA MESCS members were present at presentation of new book (Patent chasing, Lov na patent, http://www.bukla.si/?action=books&book_id=14699.

2.7. Activities in 2013

In March, within the annual Open day at the Jožef Stefan Institute, we organized an exhibition of the activities performed within the project Fusion.

In March, within the annual Jožef Stefan week and the open day at the Jožef Stefan Institute, Slovenian Fusion Association (SFA) contributed to the event with a lecture on fusion (it was presented by Dr. Luka Snoj) and an exhibition of the activities performed within the project Fusion Expo. We used this opportunity to increase the

awareness of the fusion research. During the lecture a live coverage from JET an ITER was restored.

In May Dr. Luka Snoj gave an interview about fusion for the Slovenian National Radio. In the same month an article about fusion, ITER and Slovenian contribution (Activities of SFA) to fusion project was published in daily newspaper DELO.

In spring a new action for promotion of science has been established by Dr. Saša Novak and run under umbrella of the Slovenian Academic Society for Science and Engineering (SATENA). Within the action "Science on the street, knowledge and ideas on the go" lectures for general public take place in the City centre. The first one was devoted to fusion (Making stars on earth), presented by Dr. Luka Snoj and moderated by journalist Uroš Škerl Kramberger. The event was also reported as a part of daily news on Slovenian national television - an interview with Dr. Luka Snoj and Dr. Saša Novak.

Figure 5: News on the Slovenian National television about the action "Science on the street, knowledge and ideas to go".

Journalist Uroš Škerl Kramberger published an interview with Dr. Luka Snoj in daily newspaper DNEVNIK. Interview was about fusion basics, fusion research, ITER and future fusion power plant.

On Slovenian National Televison there is a talk show about science each Thursday in the afternoon (Good hour, Bite a science). In December it was about research reactor TRIGA at Jožef Stefan Institute and about fusion (Dobra ura z Boštjanom).

3 CONCLUSIONS

Public Information (PI) is an important part of the Slovenian Fusion Association (SFA), whose main tasks is to disseminate the knowledge on fusion as a future energy source and to inform the general public on the ongoing and future fusion research activities in the European fusion programme. The activities from 2007 include running the permanent Fusion Expo at the Nuclear Training Centre (NTC) at the Jožef Stefan Institute (JSI), running the travelling exhibition "Fusion Expo", translation of brochures, posters and other information material published by European Fusion Development Agreement (EFDA), performing public lectures on fusion, on the ITER project and other fusion related topics, etc.

In the future we will continue with current activities and will certainly try to increase public awareness about fusion as a possible energy source for the future by improving current and performing additional activities.

In 2014 there could be a problem in implementing all activities, since there are no special financial resources for fusion PI activities. We strongly believe that PI on fusion should be a process which should never stop. Public acceptance of Energy of the future – fusion energy is important now and it will important in the near future. The PI

team is very dedicated to its work and will continue in the same way as described in the report - with a large number of different activities.

4 REFERENCES

1 Nina Hudej, Družbene posledice jedrske fuzije, Diplomsko delo, Univerza v Ljubljani, Fakulteta za družbene vede, 2007
2 Marijan Koželj, " Razlogov za optimizem (skoraj) ni, There is almost no reason for optimism", Delo, 23.8.2008
3 Tomaž Gyergyek, lecture "Fuzija – energija prihodnosti" (Fusion – Energy for the future), April 9th 2008 http://www.he.si/index.php?option=com_content&task=view&id=97&Itemid=1 Movie
4 Saša Novak, "Fuzijska elektrarna - znanstvena fantastika? ", Dnevnik, 11.08.2008
5 Primož Pelicon, " Otvoritev nove žarkovne linije (Opening the new beam line)" in Delo, 29.11.2008
6 Tomaž Gyergyek, Lecture "Fuzija", Svet Evrope, February 2009
7 Vest.Si, Interview with Tomaž Gyergyek, February 11, 2009
8 Radio Val 202, "Razlaga z razlogom - Fuzija", February 19, 2009
9 Ljubljana.si: "Fuzija, energija prihodnosti", March 9, 2009
10 Radio Slovenia 3 (ARS) (39:15), interview with a director of J. Stefan Institute prof. Jadran Lenarčič and dr. Saša Novak at the opening ceremony, March 10, 2009
11 Radio Si, interview with prof. Milan Čerček, March 10, 2009
12 Energetika.net, "Jedrska fuzija na ogled v Ljubljani", March 2009
13 Arhivo.com, "Fuzija, energija prihodnosti", March 11, 2009
14 Kvarkadabra.net, "Fuzija, energija prihodnosti - razstava", March 11, 2009
15 Siol.net, "Razstava Fuzija, energija prihodnosti, na ogled v Ljubljani", March 11, 2009
16 Planet.si, "Razstava Fuzija, energija prihodnosti, na ogled v Ljubljani", March 11, 2009
17 Indirekt.si, "Fuzija, energija prihodnosti v Kresiji", March 11, 2009
18 Energetika.net, Dr. Milan Čerček: "Fuzija bo predstavljala temeljni vir energije, a do porabe je še daleč", March 16, 2009
19 Matkurja.com, "V galeriji Kresija razstava z znanstvenim ozadjem", March 16, 2009
20 Burger.si, "Razstava, fuzija energija prihodnosti", March 17, 2009
21 RTV Slo.si, "Fuzija za čistejšo energijo prihodnosti", March 20, 2009
22 Dnevnik.si, "Plazemska krogla napoveduje fuzijsko prihodnost" • March 20, 2009
23 TV Pika, Sadovi znanja: "Fuzija", TV interview with prof. Milan Čerček, dr. Saša Novak and Dr. Luka Snoj , March 26, 2009
24 Radio KAOS,"Fuzija, energija prihodnosti": Interview with dr. Saša Novak, March 27, 2009
25 RTV SLO 1, evening news "Odmevi (Echoes), Interview with prof. Milan Čerček, March 2011
26 NOVAK, Saša, SNOJ, Luka. Dragocenih 15 sekund lososove rožnate svetlobe: nov korak v razvoju fuzijskih elektrarn. Znanost (Ljubl.), 15. Sept. 2011, 53, No. 127, p. 26.
27 NOVAK, Saša, Fuzija, energija prihodnosti, Rotary Club Ljubljana Carniola, Ljubljana, 26. Sept.2011.
28 http://www.iter.org/newsline/239/1299
29 http://www.delo.si/druzba/znanost/supervroca-pec-v-hladilniku.html
30 http://vimeo.com/67502564
31 http://ava.rtvslo.si/predvajaj/prvi-dnevnik/ava2.167891219/
32 http://www.dnevnik.si/ljudje/-dr-luka-snoj-
33 http://www.rtvslo.si/dobraura/epizoda/238
34 NOVAK, Saša (intervjuvanec), SNOJ, Luka (intervjuvanec), IVEKOVIĆ, Aljaž (intervjuvanec). Fuzija : RTV Slovenija 1, oddaja Dobra ura z Boštjanom : intervju. 5. dec. 2013. [COBISS.SI-ID 27416359]
35 SNOJ, Luka (intervjuvanec), NOVAK, Saša (intervjuvanec). Znanost na cesti, znanost in ideje na prepihu : Ni meja : prispevek v sklopu oddaje Prvi dnevnik RTV SLO 1, 30.5.2013. 2013. [COBISS.SI-ID 2682218

FUSION EXPO SUPPORT ACTION

Tomaž Skobe, Saša Bobič, Saša Novak, Melita Lenošek Kavčič, Mateja Južnik, Aljaž Ivekovič, Igor Jenčič, Borut Mavec, Bojan Žefran, Damijan Klep, Dušan Rudman, Jure Hribar, Luka Tavčar, Nina Udir, David Jezeršek, and others

Jožef Stefan Institute, Jamova cesta 39, SI-1000 Ljubljana
tomaz.skobe@ijs.si

1 INTRODUCTION

Slovenian Fusion Association (SFA) EURATOM – MESCS has taken over responsibility to run the Fusion Expo from 6th October 2008. The first Fusion Expo Support Action (WP08-PIN-FUSEX) has finished on 31st July 2010. The second support action under WP10-PIN-FUSEX started on 1st August 2010 and was extended until the end of year 2013. With notification letter the support for the Fusion Expo Task Agreement was extended to the end of June 2014. The main goal and intention of this project remain the same since beginning of our task agreement: to run the Fusion Expo in the most efficient way possible and to follow our tasks, which needs to be fulfilled:

1. Scheduling the exhibitions
2. Supervising the local organization
3. Graphical work and printing Fusion Expo panels
4. Moving the exhibits
5. Assembling/Disassembling Fusion Expo
6. Maintenance
7. Continuous report to EFDA
8. Organization of a supporting participation in international events for young generations
9. Providing the Fusion Expo with Fusion Show for larger events

2 WORK PERFORMED IN 2008 - 2013

Fusion Expo is an itinerant exhibition presenting various aspects of fusion research such as: fusion as a natural phenomenon and energy source science, fusion as a European research project, history of fusion research, European research facilities, ITER, future plans toward a power plant, technological, environmental and sociological aspects of this energy source etc.

The main target group of Fusion Expo is general public. It is specifically designed to address young students and it is also appropriate to addressing other audiences, such as decision makers or journalists. Being modular, it can easily be

adapted to different kind of events. All events in the period from 2008 to 2013 are presented in table 1.

Host / Event	Type of participation	Place	Date
2008			
European City of Science	Maxi Expo	Paris, France	14th- 16th November
2009			
Association Euratom MHEST	Mini Expo	Ljubljana, Slovenia	10th - 20th March
Research Connection 2009	Mini Expo	Prague, Czech Republic	7th - 8th May
Association Euratom IPPLM	Maxi Expo	Koszalin, Poland	27th May - 9th June
Association Euratom IPPLM	Maxi Expo	Szczecin, Poland	15th June - 15th July
Association Euratom IPPLM	Maxi Expo	Łodz, Poland	10th - 25th October
Association Euratom IPPLM	Maxi Expo	Katowice, Poland	3rd - 20th November
Irish Science Week	Mini Expo	Dublin, Ireland	10th - 13th November
Irish Science Week	Mini Expo	Cork, Ireland	17th - 21st November
2010			
Association EURATOM CIEMAT	Maxi Expo	Terrassa, Spain	4th March - 2nd May
Fusion for Energy - F4E	Mini Expo	Barcelona, Spain	17th - 21st March
ESOF 2010	Fusion Road Show	Torino, Italy	2nd – 7th July
Lowlands music festival 2010 - Association EURATOM FOM	Supporting participation in int. events, Fusion Road Show	Biddinghuizen, The Netherlands	20th -22nd August

Belgian Euratom Association & Iterbelgium	Academic Event, some parts of Expo	Brussels, Belgium	24th September
Belgian Euratom Association & Iterbelgium	Maxi Expo	Brussels, Belgium	25th October – 15th November
2011			
Association EURATOM CU	Maxi Expo	Bratislava, Slovakia	5th January – 18th February
ÖAW-EURATOM	Maxi Expo	Vienna, Austria	1st – 10th March
2011 EPS Conference, French Atomic Energy Agency	Maxi Expo	Strasbourg, France	26th June –2nd July
Lowlands music festival 2011	Fusion Road Show	Biddinghuizen, The Netherlands	19th – 21st August
Fusion show “Plasma’s. Fusie! Energie?”	Some parts of the Expo	Antwerp, Belgium	17th – 23rd November
2012			
Plasmas chauds	Maxi Expo	Nancy, France	26th January – 6th February
Science festival "Printemps des Sciences"	Maxi Expo	Charleroi, Belgium	16th March – 20th April
Jozef Stefan Institute open day	Hands on experiments	Ljubljana (two locations)	24th March
2nd European Energy Conference	Part of expo, Remote handling	Maastricht, The Nederlands	17th – 20th April
Visiatome	Maxi Expo	Marcoule, France	12th May – 8th July
Internal Event, PIN meeting	Hands on experiments	Culham, UK	14th – 15th June
Karlsruhe Institute of Technology (KIT), Fusion Programme	Some parts of Fusion Expo	Karlsruhe, Germany	3rd - 14th September
European Commission - SOFT 2012	Maxi Expo	Liege, Belgium	19th September – 7th October

Light12 event - European Night of Research	Some parts of Fusion Expo	Rome, Italy	28th September
Genoa Science Festival	Maxi Expo	Genova, Italy	25th October – 4th November
ITER Organization	Mini Expo	Aix-en-Provence, France	13th-28th November
2013			
CCFE, The Big Bang Fair	Hands on experiments	London, England	14th – 17th March
Science Centre AHHAA	Fusion Expo	Tartu, Estonia	17th May – 31th July
Business Bistro at ECSITE Annual Conference	Hands on experiments	Gothenburg, Sweden	6th June – 8th June
Sziget Festival	Support action	Sziget, Hungary	5th – 12th August
Science Days 2013	Hands on experiments	Rust, Germany	10th – 12th October
Scientific festival Week of Science and Technology 2013	Hands on experiments	Prague, Czech Republic	1st – 15th November
Fusion show “Plasma’s. Fusie! Energie?”	Some parts of the Expo	Antwerp, Belgium	21st – 22nd and 26th – 27th November

Table 1: List of realized exhibitions in 2008 – 2013.

2.1. Activities in 2008

The first exhibition that was shown under the EFDA Art 7 support action was hosted in Paris. The main coordinator of the event was EFDA with technical and worker support of our association. Because this was our first Fusion Expo exhibition and event without support of the local hosting association, our “on the field” team was a little bit expanded.

2.2. Activities in 2009

Slovenia has previously hosted Fusion Expo in 2005 and hence collected some experience that served as the main basis for the organizational plan for the exhibition. In 2009 we took a chance to show the redesigned exhibition in March. This offered a good opportunity to present the expo in a quite effective way. Within eleven days, close to

3.500 visitors visited the Fusion Expo and more than 90 % of them attended a guided tour or took a thorough look of the exhibition.

Figure 1: Fusion Expo in Ljubljana.

In Prague the Fusion Expo was hosted under the Research Connection 2009 conference, which was taking place in Prague under the Czech Presidency of the European Union.

In Koszalin was the first one of the planed four locations of the Fusion Expo in Poland in 2009. The location in Koszalin was the main campus of Koszalin University of Technology, new building near the city centre and very good accessibility. Second exhibition of the Fusion Expo in Poland was organized in Szczecin – the capital of the Westpomeranian Voivodship. In autumn 2009 we had continued with third exhibition in Poland, which was hosted in the third largest city in the country. Because of the faraway location from the city centre of the Łodz University which was hosted the Expo, the exhibition was visited by only announced groups of school children and students. The last one of the Fusion Expo in the series exhibitions in Poland was hosted at Katowice, supported by Institute of Physics, University of Silesia.

Till November 2009 the Fusion Expo had never been held in Ireland. The Fusion Expo was realised as a part of Science Week in Ireland, which is the biggest annual promotion of science to the general public. The Expo was held at the Dublin City University, where is also location of the Association EURATOM DCU Ireland. In connection with the Science Week in Ireland the Fusion Expo was hosted also in Cork, as a part of 'Discovery 2009 – Interactive Science Exhibition' event programme, a special feature catering for schools, students, teachers, local community and other adult audiences.

2.3. Activities in 2010

The Fusion Expo starts the 2010 tour with exhibition in Terrassa. With support of CIEMAT and Technical Museum of Catalonia (Museu De La Ciència I De La Tècnica De Catalunya) the Maxi Expo was hosted from 4th March until 2nd May. Most of the exhibitions at the Museum are permanent and from different technical areas, only small part of it is intended for temporary exhibitions. Second Expo, the Mini Fusion Expo, was hosted by F4E in Barcelona. The Expo was presented as a part of School Graduates Education Exhibition, taking place at Fira de Barcelona. F4E has putted great impact to make the Fusion Expo even more interesting, visible and hearable. By the expectations of the host there were more than 80.000 students in opened days.

Euro Science Open Forum 2010 (ESOF2010) was a unique way to stimulate the diffusion of science with many areas dedicated to industry, research and technology centres. Main locations were Torino squares, which has symbolised the relationship among science, industry and design. The Fusion Expo was presented with some interactive models and with the Danish Fusion Road Show as a part of our support action.

The Lowlands music festival 2010 was held in August 2010 at Biddinghuizen. Lowlands music festival attracts visitors from all over the Europe, with about 25-30% non-Dutch visitors every year. In 2010 it was attend by approximately 55.000 visitors, the Fusion Road show drew over 2.500 visitors during three days.

In Brussels were two events: academic event (one day) and Maxi Fusion Expo. The event was held in the Palace of the Academies, next to the Royal Palace, in Brussels. The Academic Event took place in the main building of the Palace refurbished auditorium, while the Expo was housed in the Atrium of the Palace. The academic event was focused on fusion and ITER device with invited guests on the highest level with His Royal Highness Prince Philippe of Belgium and other very important decision makers, researchers and journalists.

2.4. Activities in 2011

First Maxi Fusion Expo in 2011 was in Bratislava (Slovakia) – in the Avion Shopping Park. Visit rate was very high – 21.040 visitors that interacted with guides or exhibits and additional visitors that only read texts or have a look at exhibits, but did not interact with them. The total number was very impressive.

Second exhibition (Maxi Fusion Expo) was hosted at the Technical University in Vienna. Approximately 2.000 visitors came to the exhibition and also a large number of students and teachers of the University walked through the exhibition, many of them returned to study the exhibition more closely or to watch the Fusia 3D movie.

In summer Fusion Expo (also maxi) was hosted by Association Euratom CEA in the “Palais de la musique et des congrès Pierre-Pflimlin” in Strasbourg. Exhibition in Strasbourg was connected to 2011 EPS Conference.

EFDA's support action (Fusion Road Show with the mellator) was in Biddinghuizen in the Nederlands (3 days event). The festival visitors stayed at the fusion stand for 10 minutes on average, and the entire exhibit drew 10.000 people during the three day festival.

Some parts of expo (mellator, repulsive target, bicycle power plant, plasma ball and JET poster) were presented on the show “Plasma’s. Fusie! Energie?” in November 2011 at the Antwerp University. The mellator, the repulsive target, the bicycle power plant and the JET poster were received by the schools with great enthousiasm.

2.5. Activities in 2012

Year 2012 started with Maxi Fusion Expo in Nancy (Faculty of Sciences & Technologies Vandoeuvre). According to host report the action was a success regarding main objectives which were above all to disseminate knowledge among students and persons interested in energy topics and to try to encourage high school students for physics.

Second exhibition in 2012 (Maxi Fusion Expo) was hosted by Centre de Culture Scientifique (CCS) de l'Université libre de Bruxelles" in Charleroi. Science festival "Printemps des Sciences" was also very interesting for youngsters – especially 3D movie - Fusia.

On March 24 all departments of Jozef Stefan Institute were opened for general public. Fusion Expo was present on two locations of the Institute.

In April 2012 the new Remote Handling Experience exhibit, which simulates the maintenance operation at JET, was a central attraction at the European Energy Conference in Maastricht. Visitors were challenged to manipulate "tiles" – wooden blocks – into their allotted spaces using only the on-screen camera view.

Third Maxi Fusion Expo was organized in exhibition centre Visiatome - CEA Marcoule. Fusion Expo exhibition was placed in Visiatome - a centre for discovery and learning proposed by the Atomic Energy and Alternative Energies Commission (CEA), a French public research organization.

In June 2012 was an internal event – Public Information Network yearly meeting, which was organized in Culham from 14 to 15 June. Fusion Expo team sent hands on experiments, which were presented to PIN members and other visitors of Culham centre.

The 6th "Karlsruhe International School on Fusion Technology" took place in Karlsruhe at the beginning of September 2012. This summer school, annually organized by the Karlsruhe Institute of Technology (KIT) was focused on the development of the fusion components as well as the associated processes like cooling and fuel cycle.

Liege in Belgium hosted 27th Symposium on Fusion Technology (SOFT) and within the framework of the SOFT, EFDA and Fusion Expo presented exhibition on Nuclear Fusion.

Turn on the light on science was European project in Rome (already since 2008) as the "European Researchers Night." In November Fusion Expo has been hosted in the prestigious new University Library, in Genoa City Center. It has been part of the official program of the tenth edition of the Genoa Science Festival and has been included in the web-site, as one of the "high-lights" of the 2012.

In November Fusion Expo has been hosted in the prestigious location of the Aix en Provence Tourist Office in a very centre of the city. Host of the event was ITER organization.

2.6. Activities in 2013

The Big Bang is the largest celebration of science, technology, engineering and maths for young people in the UK. The event is aimed at showing young people (primarily aged 7-19) just how many exciting and rewarding opportunities there are out there for them with the right experience and qualifications. The main attraction at CCFE's stall was the Remote Handling Demo provided by Fusion Expo.

Second Fusion Expo exhibition in 2013 was in the AHHAA Science Centre in Tartu in Estonia where since 1997 interactive science exhibitions let the visitors discover and experience science.

ECSITE is the European network of science centres and museums, linking science communication professionals in more than 400 institutions in 50 countries. As a

member of Ecsite EFDA presented a newly developed (Beta version) fusion game at the Business Bistro in the booth no. 41.

In 2013 Fusion Expo also contributed with a financial support to the Hungarian fusion association at Sziget festival.

Fusion Expo exhibition was presented at Science Days in Rust organized by the Science und Technologie e.V. The aims of Science Days are to encourage the acceptance of science and technology among people in general, to focus more attention on science as a school subject, and to help teenagers orient themselves towards a future profession.

In November Fusion Expo exhibition was presented at Science and Technology Week of the Academy of Sciences which is the largest science festival in the Czech Republic organized by the Academy of Sciences of the Czech Republic along with partner organizations.

On 21, 22 and 26 November 2013 the University of Antwerp welcomed more than 3500 17- and 18-year-old pupils and teachers in an interactive show about nuclear fusion. This interactive show combines science and theatre techniques to illustrate the ongoing research about nuclear fusion.

3 CONCLUSIONS

We could conclude that Slovenian Fusion Expo team organized a large number of very successful exhibitions in whole Europe. Feedbacks from all events were very positive.

There was a lot of additional work at the beginning: the Fusion Expo inventory was continuously supplemented with missing parts of tool kit (e.g. screwdrivers, screws, stretch belts, protection foil, electrical cables, etc.) and broken or damaged items (transport boxes, electric bulbs, reflectors, DVD players, etc.). After fitting wheels to the biggest and heaviest transport boxes at the first stage of our support action we had gradually equipped most of the rest of transport boxes with wheels. This makes movement at the host location significantly easier. During the support action and after many transport cycles to or from the Fusion Expo locations, several of transport boxes were damaged. Our Expo Team has taken care to renew and replace the damaged parts.

The main two problems at the beginning and also later were to make the whole setting up of the exhibition easier, with less manual work and physical power. With enthusiastic approach we tried to do everything to reach the planned results and to make the Fusion Expo visible in the best possible light. In 2013 we added hands-on experiments to the exhibition and they were very well accepted by visitors. But after several exhibitions we could conclude that certain experiments (like remote handling, mellator) are not suitable for frequent transports.

The Fusion Expo teams strongly support all fusion public information activities in the future. It is important to work on the refreshment of the exhibition; the new Fusion Expo should be able to present fusion in a very attractive way.